Universidad de Huelva

Departamento de Ingeniería Química, Química Física y Ciencias de los Materiales

3D printing of hydrogels and thickened fluids for dysphagia management : in situ mixing and gelling

Memoria para optar al grado de doctora
presentada por:

Isabel Diañez Amores

Fecha de lectura: 5 de mayo de 2021

Bajo la dirección de los doctores:

Inmaculada Martínez García

Críspulo Gallegos Montes

Huelva, 2021

Universidad de Huelva

3D printing of hydrogels and thickened fluids for dysphagia management:

IN SITU MIXING AND GELLING

Huelva, 2021

Isabel Diañez Amores

Supervisors:

Dr. Inmaculada Martínez García

Prof. Dr. Críspulo Gallegos Montes

Acknowledgements

This PhD thesis has been carried out in the framework of several collaborative projects funded by Fresenius Kabi Deutschland GmbH (Germany).

First of all, I would like to thank my thesis supervisor, Dr. Inmaculada Martínez García, for accompanying and guiding me throughout this long journey. It may sound cliché to say that this thesis would not have been possible without her, but I don't think it has ever been so true. Thank you very much for always teaching me and helping me with infinite patience, for stopping many of the blows I would have received over the years and always seeking the best for me. I think that, in addition to a wonderful director and co-worker, I also take a friend with me. And here's another one for you.

I would also like to thank my supervisor, Dr. Críspulo Gallegos Montes, for the trust he has placed in me and for always being available despite the distance and the difficulties. It has been a real honour and a real good fortune to have your supervision. I would also like to thank him and Fresenius Kabi for giving me the opportunity to work on something I am passionate about. It is these 'coincidences' that change a life.

My sincere thanks to Dr. José María Franco Gómez for also having trusted me during all this time and for having given me a priceless freedom to work, even when it seemed that nothing was going well. I sincerely hope that the result does justice to that trust. It has also been a pleasure to work with the rest of the 'Fresenius Team', Dr. M.ª Carmen Sánchez Carrillo and Dr. Concepción Valencia Barragán, whom I would also like to thank for their work at the head of the PhD Programme. All of us doctoral students would be lost without you.

I consider myself privileged to have met all of you professionally, but also personally. Thanks to all the members of the Research Centre in Chemical Products and Processes Technology (Pro^{2}TecS) and the Complex Fluids Engineering Group for welcoming me and for creating a good atmosphere in which work becomes less hard. And, especially, to my colleagues in the lab (or rather, to my friends in the lab). Adri, Espe, Clara, Rocío, Ortega, Esteban, Juanky,

Belén, Antonio, Trini, Mauricio... And so many others who are, have been (Cris and Rubens, it all started with you) and will be. I take unforgettable moments with you. I hope that soon we will be able to have those departmental meals that I miss so much.

Finally, I would like to give special thanks to my family.

To my parents. I am what I am thanks to you. You have been, are and will always be my reference points in life. Infinite thanks for your love and protection throughout my life, for giving me the best example to follow and for supporting me exactly the same when I have chosen not to. You are the best parents one can have. Truly, thank you.

To Elena, for tightening the screws that were falling out along the way. It has been incredible to live through the good times with you and much easier to deal with the bad times. Thank you for bearing my anguish, my worries and my bad moods. Thank you for making me so happy.

To my brothers, my grandparents and all my family and friends. I am sorry I have not been more present. You are much more important to me than I make you out to be.

This thesis is part of me and part of all of you. Thank you all very much.

Isabel

Agradecimientos

Esta Tesis ha sido realizada en el marco de diversos proyectos de colaboración financiados por Fresenius Kabi Deutschland GmbH (Germany).

En primer lugar, quería dar las gracias a mi directora de tesis, la Dra. Inmaculada Martínez García, por acompañarme y guiarme durante todo este largo viaje. Puede sonar a tópico decir que esta tesis no habría sido posible sin ella, pero no creo que nunca haya sido tan cierto. Muchas gracias por enseñarme y ayudarme siempre con una paciencia infinita, por frenar muchos de los golpes que habría recibido en estos años y buscar siempre lo mejor para mí. Creo que, además de una maravillosa directora y compañera de trabajo, me llevo también una amiga. Y aquí tienes otra.

Quería dar las gracias también a mi director, el Dr. Críspulo Gallegos Montes, por la confianza que ha depositado en mí y por estar siempre disponible a pesar de la distancia y las dificultades. Ha sido un auténtico honor y una verdadera suerte contar con su supervisión. Además, quiero agradecerle a él y a Fresenius Kabi que me hayan dado la oportunidad de trabajar en algo que me apasiona. Estas "casualidades" son las que cambian una vida.

Mi más sincero agradecimiento al Dr. José María Franco Gómez por haber confiado también en mí durante todo este tiempo y haberme dado una libertad para trabajar que no tiene precio, incluso cuando parecía que nada iba bien. Espero sinceramente que el resultado haga justicia a esa confianza. Ha sido un placer también trabajar junto al resto del "Fresenius Team", la Dra. M.ª Carmen Sánchez Carrillo y la Dra. Concepción Valencia Barragán, a quien también quiero agradecer su labor al frente del Programa de Doctorado. Todos los doctorandos estaríamos perdidos sin ti.

Me considero una privilegiada por haberme encontrado con todos vosotros en lo profesional, pero también en lo personal. Gracias a todos los miembros del Centro de Investigación en Tecnología de Productos y Procesos Químicos (Pro^2TecS) y al Grupo de Ingeniería de Fluidos Complejos por acogerme y por crear ese buen ambiente en el que el trabajo se hace menos duro. Y, especialmente, a los compañeros del laboratorio (bueno, a los amigos del

laboratorio, mejor dicho). Adri, Espe, Clara, Rocío, Ortega, Esteban, Juanky, Belén, Antonio, Trini, Mauricio... Y tantos otros que están, han estado (Cris y Rubens, con vosotros empezó todo) y estarán. Me llevo momentos inolvidables con vosotros. Ojalá que pronto podamos hacer esas comidas departamentales que se tanto se echan de menos.

Por último, quería dar las gracias de forma especial a mi familia.

A mis padres. Soy lo que soy gracias a vosotros. Habéis sido, sois y seréis mis referentes en la vida. Infinitas gracias por vuestro cariño y protección durante toda mi vida, por darme el mejor ejemplo a seguir y por apoyarme exactamente igual cuando he elegido no hacerlo. Sois los mejores padres que se puede tener. De verdad, gracias.

A Elena, por apretar los tornillos que se me iban cayendo por el camino. Ha sido increíble vivir contigo los buenos momentos y mucho más fácil sobrellevar los malos. Gracias por aguantar mis angustias, mis preocupaciones y mi mal humor. Gracias por hacerme tan feliz.

A mis hermanos, a mis abuelos y a toda mi familia y amigos. Siento no haber estado más presente. Sois mucho más importantes para mí de lo que hago ver.

Esta tesis tiene parte de mí y también de todos vosotros. Muchas gracias a todos.

Isabel

Contents

CONTENTS

Introduction

Chapter 1
Introduction

Resumen

Esta tesis se centra en el desarrollo de nuevas tecnologías para la impresión 3D de alimentos y, más específicamente, para alimentos con propiedades reológicas controladas para su uso como productos orientados a la disfagia.

La primera parte de este trabajo tiene como objetivo desarrollar un sistema novedoso de impresión 3D para la obtención de hidrogeles. Se describe un procedimiento de gelificación in situ inducida por un cambio de temperatura para la impresión en 3D de dispersiones acuosas de κ-carragenato. La impresora 3D fue modificada para permitir la alimentación de fluidos de baja viscosidad y enfriar la capa impresa de forma más eficiente empleando un sistema de convección forzada. Las muestras de gel así obtenidas mostraron capacidad de sustentación de las capas impresas y una respuesta reológica comparable a la de un gel de referencia preparado convencionalmente. Además, se analizó el efecto de las principales variables de impresión, como la temperatura del hotend, la velocidad de impresión y la altura de la capa, en la respuesta viscoelástica lineal de los geles mediante la aplicación de la metodología de las superficies de respuesta (RSM). En general, la estructuración del gel aumenta linealmente al disminuir la velocidad de impresión y la altura de la capa. El aumento de la temperatura del hotend, hasta un valor máximo, también favorece la estructura de la red del gel. Sobre la base de los resultados obtenidos en este análisis, se propone un método de optimización para reducir al mínimo la temperatura y el tiempo necesarios para imprimir en 3D un gel con propiedades reológicas preestablecidas. En general, este estudio demuestra que es posible generar in situ materiales de gel impresos en 3D con posibles usos en alimentación y fármaco-nutrición, sin la ayuda de aditivos o iniciadores.

Se ha diseñado y fabricado un dispositivo único adaptado a una impresora 3D que permite alimentar en continuo y mezclar in situ sólidos y líquidos para la producción de geles y fluidos espesados. En particular, se estudió la capacidad de este accesorio para mezclar correctamente un espesante en polvo comercial orientado a la disfagia con varios fluidos convencionales (agua, zumo y leche). Se

definieron las concentraciones objetivo del espesante para lograr mezclas con viscosidades correspondientes a las texturas establecidas por el National Dysphagia Diet Task Force (NDD) —tipo néctar, miel y pudding— para los fluidos espesados. Se evaluó tanto la exactitud del contenido de sólidos como la respuesta reológica de las mezclas obtenidas. Aunque se observaron fluctuaciones en las concentraciones de las mezclas obtenidas por mezcla continua con respecto a los valores objetivo, las viscosidades obtenidas estaban dentro de los límites establecidos para cada una de las texturas deseadas. Los fluidos espesados procesados con el accesorio de mezcla para impresión en 3D mostraron viscosidades muy similares a las de sus homólogos mezclados a mano y un mayor grado de estructuración, especialmente cuando se imprimían a bajas velocidades, así como una menor cantidad de aire atrapado.

En base a los resultados obtenidos, se pretende y se espera que estos métodos alternativos de preparación permitan la producción de geles y fluidos espesados con formas y colores más atractivos para el tratamiento de la disfagia a largo plazo, mejorando la calidad de vida de los pacientes con disfagia y promoviendo el cumplimiento del tratamiento.

1.1. Summary

This thesis focuses on the development of new technologies for 3D food printing. Specifically, for foods with controlled rheological properties for use as dysphagia-oriented products.

The first part of this work aims to develop a 3D printing system with gelification. It reports a successful 3D printing-based in situ temperature-induced gelification procedure of κ-carrageenan aqueous dispersions. 3D printer was modified to handle low viscosity fluid feeding and more efficiently distribute ambient air at room temperature causing forced convection to accelerate the cooling of the printed layer. Thus obtained gel samples showed self-sustaining capability and a rheological response comparable with a reference conventionally prepared gel. Moreover, the effect of main printing variables, such as temperature of the hotend, printing speed and layer height, on the linear viscoelastic response of the gels was analysed by application of the response surface methodology (RSM). In general, gel strength linearly increases by decreasing printing speed and layer height. A rise in the temperature of the hotend also increases the strength of

the gel network, but only to a certain extent, above which not noticeable improvement in this regard was achieved. Based on the results obtained from this analysis, an optimisation method is proposed to minimise the temperature and time needed to 3D print a gel with pre-set rheological properties. Overall, this study demonstrates that it is possible to generate in situ 3D printed gel materials with potential uses in food and pharmaco-nutrition, without the aid of reactive additives or initiators, and using a facile protocol.

After that, the design, implementation and evaluation of an accessory designed and manufactured to be adapted to a 3D printer to allow the in situ and continuous mixing of solid and liquid feeds is also described. In particular, the capacity of this accessory to correctly mix a dysphagia-oriented commercial powder thickener with several conventional fluids (i.e. water, juice, and milk) was studied. Target thickener concentrations were defined in order to achieve mixtures with viscosities corresponding to the textures established by the National Dysphagia Diet Task Force (NDD) —nectar-like, honey-like, and spoon-thick— for thickened fluids. Both the accuracy of the solid content and the rheological response of the obtained mixtures were evaluated. Although fluctuations were observed in the concentrations of the mixtures obtained by continuous mixing with respect to the target values, the viscosities obtained were within the limits established for each of the desired textures. The thickened fluids processed using the 3D printing mixing accessory showed viscosities very similar to their hand-mixed counterparts and a higher degree of structuration, especially when printed at low mass flow rates, as well as a lower amount of entrapped air.

It is therefore intended and expected that these alternative methods of preparation allow the personalised production of gels and thickened fluids with more appealing shapes and colours for the long-term dysphagia management, improving the quality of life of patients with dysphagia, and promoting treatment compliance.

1.2. Justification

Swallowing difficulty or dysphagia is a symptom derived from a multitude of pathologies and can have serious consequences for people who suffer from it, especially in the form of respiratory conditions caused by the aspiration of

beverages or food into the airways. There are many different phenotypes of patients with dysphagia, each with its specific characteristics and needs. However, it is common for low-viscosity fluids to be the most susceptible to aspiration and, therefore, the riskiest for these patients. For this reason, one of the most common approaches in dysphagia management is to modify the diet to avoid low-viscous fluids. To replace them, it is possible to increase the viscosity of liquid drinks and foods by adding powdered thickening agents. This method makes it possible to obtain a wide variety of foods suitable for dysphagia, but it entails some problems, especially with regard to their preparation. As an alternative, the market offers ready-to-use dysphagia-oriented products, but these have limited ranges of presentations and flavours. This can lead to patients becoming tired or bored and ultimately abandoning treatment.

It is in this context that 3D food printing (3DFP) emerges as a tool for producing dysphagia-friendly meals with different shapes, colours and flavours, which are more attractive and less repetitive for patients in long-term treatments. However, most of the progress made so far has focused only on " shaping " by 3D printing of pre-prepared pastes or dough-like materials. While this is already an advance in the nutritional management of dysphagia, it does not address the problems of manual preparation of thickened fluids and the limited range of ready-to-use products. For this purpose, the development of new technologies for 3D printing of foods is necessary, allowing the automatic preparation of these formulations with the correct thickener content, as well as the incorporation of additional components to provide pleasant flavours and odours or the incorporation of nutrients or drugs.

On the other hand, 3D printing is a process that involves a large number of variables (temperatures, flows, etc.), which can be modified to obtain products with different final properties from the same raw materials. Unfortunately, studies evaluating the influence of these printing variables on the rheological properties of 3D printed foods for application in the manufacture of dysphagia-oriented products are not yet sufficient.

This thesis therefore focuses on the evaluation of the influence of printing variables on the rheological behaviour of printed products and on the development of 3D food printing technology with mixing, for the preparation of dysphagia-oriented products.

1.3. OBJECTIVES

This thesis focuses on the development of new 3D food printing (3DFP) technologies for their application in the preparation of products for dysphagia, with customisable rheological and nutritional properties to meet the specific needs of each patient. To this end, the more specific subobjectives detailed below will be attempted:

- Development of a gelling 3D food printing (G3DFP) system. A setup for the continuous feeding of low viscosity fluids and their subsequent gelling in situ during the printing process will be implemented.
- Evaluation of the influence of printing variables on the gelling process and, consequently, on the rheological properties of the gels produced by this method.
- Development of a mixing 3D food printing (M3DFP) system. Design and manufacture of a solid/liquid mixing device adaptable to a 3D printer for the automatic thickening of fluids by the addition in controlled proportions of a thickening agent in powder form.
- Evaluation of the accuracy of the thickener concentration in the mixtures obtained by means of M3DFP and of their flow properties.

1.4. THESIS STRUCTURE

This Ph.D. dissertation has been divided into five chapters. A short summary of their contents is presented below.

This introductory **Chapter 1** outlines the summary, justification and objectives of this research work.

The state of the art is presented in **Chapter 2**. It aims, first of all, to provide the reader with an overview of dysphagia, its main problems and its management through dietary modification. Then, some fundamental concepts about thickening and gelling are also included, with a special emphasis on the materials used throughout this work. Finally, some basic notions of conventional 3D printing and 3D printing of foods are provided, as well as the advances made in this field which are most relevant to this study.

Chapter 3 sets out the general experimental details of this research work, looking at materials, methods of preparation and equipment used to conduct it.

Chapter 4 sets out the main results obtained throughout this research work. It is in turn divided into subsections, the first of which corresponds to the development of gelling 3D printing (G3DFP) and the evaluation of the effect of the main printing variables on the rheological behaviour of the gels obtained. In the second subsection, the design of the solid/liquid mixing device is presented in detail. Its performance will be evaluated later in the last subsection of this chapter.

Chapter 5 summarises the main conclusions of this research work.

Finally, the **Annexes** include copies of articles already published or submitted to publication in peer-reviewed journals.

State of the art

CHAPTER 2
State of the art

2.1. DYSPHAGIA AND ITS NUTRITIONAL MANAGEMENT

Dysphagia refers to a disorder in the functions of clearing substances —such as food, drink or saliva— through the oral cavity, pharynx and oesophagus into the stomach at an appropriate rate and speed (i.e. a disorder in swallowing). It is a symptom (and not a disease itself) of upper gastrointestinal tract-related conditions and can be divided into two different types, based on the anatomical location of the impairment: oropharyngeal dysphagia and oesophageal dysphagia[1,2].

In oropharyngeal dysphagia (or 'high' dysphagia), abnormal processes affect the mouth, pharynx and proximal oesophagus, making patients have difficulty initiating the swallow and transferring liquids or food boluses to the oesophagus. On the other hand, causes of oesophageal dysphagia ('low' dysphagia) mostly affect the oesophageal body and oesophagogastric junction (FIGURE 1), and is often indicated by a sensation of solid food and/or liquids moving slowly or getting stuck a few seconds after swallowing. It is important to identify what type of dysphagia a patient is suffering from, as this can be helpful in diagnosing an underlying pathology and in choosing the most appropriate actions to take in order to minimise the consequences of both the primary disease and the dysphagia itself[3–6].

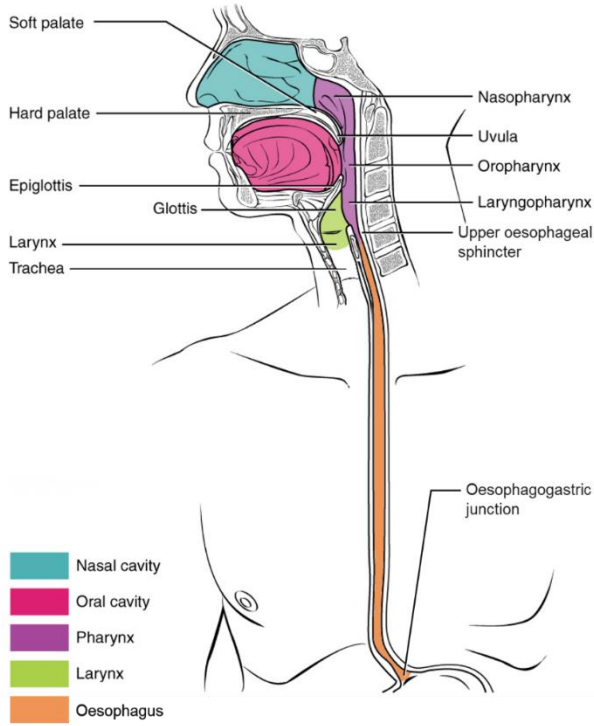

FIGURE 1. Anatomy of the mouth, pharynx and oesophagus. Adapted from OpenStax College - Anatomy & Physiology, Connexions Web site. Available at https://openstax.org/books/anatomy-and-physiology/pages/1-introduction

The main concern regarding oesophageal dysphagia is a potential malignant origin, but it rarely presents severe complications and can, in general, be effectively clinically managed[7–9]. On the contrary, oropharyngeal dysphagia (OD) can lead to variety of adverse health outcomes, including malnutrition, dehydration, pneumonia and increased hospital readmissions, morbidity and mortality, especially (yet not exclusively) for elderly people[10,11]. OD is, moreover, frequently unrecognised and therefore untreated[12–15].

2.1.1. Prevalence and main causes of oropharyngeal dysphagia

The prevalence data on OD in the general population are very scarce. Reported prevalence of dysphagia usually ranges from 4 to 20% amongst general

population[16–19]. However, most studies did not discriminate between oropharyngeal and oesophageal dysphagia. A telephone survey conducted by Kertscher et al. to determine the incidence of OD in a random selection of 2600 Dutch people yielded a result of 12.1% prevalence[20].

The possible causes of OD are many and varied, including neurological, structural, myopathic, iatrogenic, infectious and metabolic[21]. OD mainly develops in elderly people, patients with neurological and neurodegenerative diseases and patients with head and neck diseases[22]. Stroke is the most common cause[23,24], and the incidence of OD amongst these patients ranges between 33 and 45%[25–28]. OD is also a common consequence of traumatic brain injuries, though the clinical heterogeneity of this kind of patients makes it very difficult to provide common data on its scope[29,30]. Prevalence of OD related to neurological or neurodegenerative diseases is extremely high. For instance, it ranges between 58 and 95% in Parkinson's disease[31–33], between 75 and 93% in Alzheimer's disease[34–36], between 82 and 85% in infant cerebral palsy[37,38], between 32 and 83% in multiple sclerosis[39–42] and between 29 and 100% in motor neuron diseases (such as amyotrophic lateral sclerosis, progressive bulbar palsy and progressive muscular atrophy)[43–45]. In cases of head and neck cancer, swallowing disorders caused by the disease are added to those resulting from surgery and treatments with radio or chemotherapy[46,47], giving prevalence data of between 45 and 79%[48–51]. And these are not the only cases where treatment is the cause of swallowing disorders, being OD of iatrogenic origin a well-known issue[5,52].

The elderly are also especially prone to dysphagia (the European Society for Swallowing Disorders and European Union Geriatric Medicine Society propose OD to be considered as a geriatric syndrome[10]), although it is difficult to determine to what extent this is due to a higher incidence of the aforementioned and other pathologies or to the age-related alterations in oropharyngeal morphology and function[53]. The prevalence of OD in elderly people who are able to live independently ranges between 11 and 34%[54–56]. Nevertheless, these rates rise dramatically in institutionalised elders to between 12 and 70%[13,57–59].

While it is clear that the risk of OD increases with age, cases have often been reported in children, usually associated with other diseases such as cerebral palsy, but also in otherwise healthy children, sometimes with concerning consequences[60–62]. For the latter, these disorders are usually due to swallowing

immaturity and disappear during the first years of life, so they should only be assessed and treated if swallowing problems are abnormally frequent or severe, or if they lead to recurrent respiratory infections[63–65].

Despite epidemiological data of OD are strongly influenced by the method of assessment, the time frame, the severity of the primary disease and the age or even the origin of the participants considered in the different studies, the impact of dysphagia is undeniable, not only for individuals but also for institutions and health system.

2.1.2. Consequences of dysphagia

In the hospital setting, OD predicts a poor prognosis and is associated with longer hospital stays, higher costs and increased risk of mortality[66]. Nutrition, hydration and quality of life issues, as well as social isolation may arise. Nonetheless, aspiration (especially if not immediately recognised) may be the key factor that precipitates the decline in a patient's outcome by leading to life-threatening pulmonary complications such as aspiration pneumonia[67]. Early identification of these and other comorbid conditions is essential in the proper management of dysphagia to achieve better patient outcomes.

2.1.2.1. Aspiration and aspiration pneumonia

The pathways for breathing and swallowing cross in the pharynx, which makes perfect timing of these processes essential for them to occur safely. If there is a dissociation between respiration and oral/pharyngeal stages of swallowing, this results in food bolus reaching the pharynx when the larynx is still open, allowing swallowed material to enter the airways. Thus, aspiration can be defined as passage of foreign material below the level of the vocal folds[68–71] and it is one of the main causes of complications in OD, as it can eventually lead to the development of aspiration pneumonia or even to fatal choking episodes[71]. For this reason, predicting patients' aspiration risk is one of the main goals in the clinical assessment of OD and many evaluation tools have been developed for this purpose. In general, severity of aspiration is determined by its frequency, the amount of aspirated material and the possibility of evacuating it by coughing, either reflexively or voluntarily[72]. When the aspiration occurs without a coughing reflex or other overt signs, it is referred to as ‘silent aspiration’. In a study conducted by Garon et al. on 2000 patients at risk of aspiration, it was detected in 50.6% of the cases and, of these, more than half (54.5%) were silent

aspirators, with the highest prevalence amongst patients with head and neck cancer and neurological patients[73]. Particularly high rates of silent aspiration have also been observed in children with neurologically-based OD (81-94%)[74–76]. The lack of awareness by patient, family members and hospital staff that the aspiration is taking place may lead to a longer period of unattended aspiration and can increase the risk of developing complications such as aspiration pneumonia[77,78].

Aspiration pneumonia is the acute inflammation of lung tissue caused by the passage into the airways of large amounts of material contaminated with pathogenic bacteria[1,79]. The existence of aspiration does not necessarily imply the development of aspiration pneumonia. In fact, small aspirations are very common and occur without sequelae in healthy people[80]. Since the presence of pathogenic bacteria in the oropharyngeal cavity is a sine qua non, conditions that favour their proliferation can be considered as risk factors for aspiration pneumonia. In this sense, age is again influential (the elderly present a greater oropharyngeal colonisation of pathogenic bacteria[81]) as well as a poor oral hygiene[82]. Diseases, malnutrition and dehydration, smoking, weakened immune system and certain medications, among other factors, also increases the risk of aspiration pneumonia[79,80,83,84].

Patients suffering from aspiration pneumonia present more comorbidities, longer hospital lengths of stay, poorer outcomes and higher mortality rates than patients with other types of community-acquired and healthcare-associated pneumonia, in addition to increased recurrence and hospital readmissions[85–88]. Hence, early identification of patients at risk of aspiration and other aggravating conditions is of paramount importance, so that intervention can take place as soon as possible. Proper feeding management can be key in preventing aspiration and consequent aspiration pneumonia[89,90], as will be discussed in detail below.

2.1.2.2. Malnutrition and dehydration

The impairment in the efficacy of deglutition, present in 25–75% patients with dysphagia, often results in malnutrition and/or dehydration in OD patients[91].

The World Health Organization (WHO) defines malnutrition as deficiencies, excesses, or imbalances in a person's intake of energy and/or nutrients[92]. Malnutrition is the most obvious consequence when thinking about the complications associated with swallowing disorders. What is perhaps less

obvious is the true magnitude of this problem and its influence on the outcome of OD patients, especially when it appears in conjunction with chronic or acute diseases or aging. Malnutrition (or risk of malnutrition) has been reported in about the 20% of the patients with neurogenic OD[93], in more than half of the older patients with OD associated with chronic neurological diseases and in almost 70% of those admitted to the hospital with acute diseases[94].

Malnutrition has many adverse health effects, especially when associated with other diseases or disorders. It is known that a poor nutritional status leads to increased length of hospital stay, poorer physical function, weakened immunity, impaired wound healing and a worse quality of life in general[95–98]. As a result, malnourished patients suffer more complications, have longer hospital stays and, ultimately, higher mortality rates[99].

In children, early detection and treatment of malnutrition is essential, in addition to the above, to ensure that they reach their full potential for growth and development[60,63].

On the other hand, dehydration can be even more problematic than malnutrition in patients with OD, due to the fluid intake restrictions they are forced to endure. In a study conducted by Leibovitz et al., about 75% of orally fed patients with swallowing difficulties showed signs of dehydration, as did 18% of those who were fed by nasogastric tube[100]. Maintaining an adequate fluid-electrolyte balance is essential for the proper functioning of the organism. Complications derived from dehydration include hypotension (and the consequent risk of falls), perfusion of organs and tissues, decreased cardiac output and, finally, hypovolemic shock. Besides, if it is left chronically untreated, dehydration increases chronic kidney disease, morbidity, and mortality[101].

Fluid thickening is a usual practice to avoid dehydration in OD patients with unsafe swallowing. However, the dissatisfaction of patients to diets composed of only thickened fluids can also lead to reduced fluid intake[102].

2.1.2.3. Psychosocial issues in dysphagia

Dysphagia also have a great effect on the psychological state and social relationships of patients who suffer from them. Many studies have detected more symptoms of anxiety and/or depression in patients with OD than in other

patients, although the degree of psychological distress does not always match the severity of the swallowing disorder[103].

The fear of choking, the dependence on others and the consequent concern about being a burden, the belief that their condition cannot be treated and the profound lifestyle changes that OD can bring (such as the inability to enjoy meals) are some of the most common handicaps for these patients. In addition, it is common for these problems to result in lack of appetite, isolation, reduced self-esteem or even non-compliance with assigned treatments[103–106].

Pulmonary and nutritional issues —as direct threats to patient survival— are commonly the main concern of clinicians and caregivers, while the psychological and emotional aspect is more of a priority for patients, in part because they feel more protected from biomedical complications by their health care providers[107]. Furthermore, the latter also experience the situation differently depending on whether their condition is acute or chronic. Fear and a sense of vulnerability are the feelings that prevail amongst acute patients, turning into depression, frustration, worry and even embarrassment in chronic patients[108].

2.1.2.4. Economic burden

The management of dysphagia and its associated complications also entails an increased economic cost derived from the diagnosis, hospital care, medication, rehabilitation or the need for nutritional support[66]. One of the most influential factors in this cost increase is the length of stay. A meta-analysis by Attril et al. of eighteen previous studies concluded that OD increased length of stay by approximately four days. In another analysis, based on eleven previous studies, they estimated an increase in costs caused by OD of 40.36% when compared with non-OD patients[109]. Moreover, this extra cost is not only incurred on the hospital stay. Westmark et al. also found an increase in hospital costs of almost 40% but, in addition, studied the increase in costs in the municipality (nursing, home care and training) of about 33%[110]. It is difficult to estimate how much of these and other costs are borne by the patient, given the heterogeneity of health systems around the world and the economic impact OD in the form, for instance, of low productivity or lost work days, in addition to travel or out-of-pocket costs, which may be an unmanageable economic burden for some people[10,111].

From all these data , it can be seen how important it is to employ cost-effective specialised swallowing assessment and strategies aimed at avoiding complications such as aspiration pneumonia or malnutrition, or treating them in their early stages[112–116].

2.1.3. Nutritional management of dysphagia

Whether breathing and swallowing are successfully coordinated depends not only on the individual, but also on the properties of the ingested substances and those of the bolus formed after processing in the oral stage[117,118]. Thus, texture modified foods and thickened fluids are a widely accepted strategy to make the swallowing process safer for people with OD, recognised and recommended by the European Society for Swallowing Disorders (ESSD), the World Gastroenterology Organisation (WGO) and the European Society for Clinical Nutrition and Metabolism (ESPEN), among many other official bodies and professionals all around the world[3,10,119–123].

Texture modification of solid foods is mainly aimed at reducing the need for chewing and facilitating food preparation in the oral stage, as well as reducing the consequences of accidental swallowing of unchewed food (e.g., choking). Special emphasis is therefore placed on food particle sizes[124,125]. Other properties such as adhesiveness, cohesiveness, firmness, fracturability, hardness, springiness, viscosity, slipperiness, and yield stress are other significant properties evaluated in the characterisation of solid and semi-solid foods for patients with dysphagia[22,126].

On the other hand, the use of thickened fluids is basically intended to reduce the risk of aspiration associated with thin liquids. The improvement in swallowing safety by increasing bolus viscosity is widely reported in the literature, evidenced by the reduction of both material penetration into the laryngeal vestibule and aspiration below vocal cord level.[93,122,127–136]. In fact, the relationship between viscosity and correct or incorrect oropharyngeal function is so consistent that Clavé et al. developed and validated a test —the Volume-Viscosity Swallow Test (V-VST)— for bedside screening of OD[137,138].

2.1.3.1. The role of viscosity in nutritional management of OD

Many mechanisms have been proposed and studied to explain the effect of viscosity on swallowing, most of them based on the timing of physiological events

in relation to bolus flow. Longer oropharyngeal swallow responses have been reported in OD patients, with delayed temporal events of swallowing (e.g. airway closure and upper oesophageal sphincter opening), whose duration varies depending on the degree of impairment and phenotype of the patient[64,93,117,135]. Since the increased viscosity of the bolus slows down its transit speed, thickened fluids increase the chance of airway closure in time to avoid aspiration[139–142]. Not only this, but there are indications that viscosity directly influences the human physiological response[122,126,143], promoting changes that could compensate for impaired swallowing mechanisms, which could be another explanation for the observed reduction in thick fluid aspiration in patients with OD[128].

Although the reduction of the risk of aspiration with increasing viscosity is the most widespread trend, this also depends on the specific type of impairment of each patient. In a study of 70 patients with dysphagia caused by different primary diseases, Choi et al. identified swallowing parameters that predicted the aspiration of thin or thick fluids, concluding that those who had difficulty with the movement of the bolus through the first part of the swallow were more likely to aspirate only thick fluids[144]. In addition, thickened fluids also have other drawbacks, such as the low acceptance they have from some patients[102,122,132] or the increased post-swallow residue left by higher consistencies[126,130,131], so it is essential to assess and determine the exact viscosity that is most appropriate for each patient, and not to consider that thicker is always better[145,146].

In this respect, standardisation is also a key factor, since lack of uniformity between the different texture definitions used in different countries or even in different care centres can cause the delivery of inappropriate food and fluid textures to patients with dysphagia. Furthermore, it also hinders efficient communication among professionals and researchers, hindering progress in the field of nutritional management of dysphagia as well as industrial development of commercial dysphagia-oriented products[22,124,125].

Several organisations and national bodies in different countries (and even independent researchers[147]) have developed their own guidelines and definitions on dietary modifications for dysphagia management, resulting in a whole range of classifications and terminologies, many of which have no clear limits or objective way of assessment.[125,148,149]. Of these, the most common and accepted in recent years has probably been the one developed by the American

Dietetic Association. The National Dysphagia Diet Task Force (2002) difference between four viscosity levels for fluids: thin liquid (1-50 mPa·s), nectar-like (51-350 mPa·s), honey-like (351-1750 mPa·s) and spoon-thick (<1750 mPa·s), according to their viscosity values at a shear rate of 50 s^{-1} and a temperature of 25 °C[150]. The American standard is also the only one (together with the Japanese standard) that provides a specific condition for the measurement of viscosity such as the shear rate value of 50 s^{-1}. This is of great importance because most fluid and semi-solid boluses show a non-Newtonian shear-thinning behaviour —i.e., viscosity decreases when increasing shear rate— and it is therefore essential for comparison that the given viscosity value is measured at the same shear rate[22,151]. In fact, it is not unusual that viscosity values differ even by several orders of magnitude for two different shear rates in dysphagia-oriented thickened fluids[152–156]. However, the choice of this and not another shear rate and temperature values are not free of controversy, as there is no scientific evidence that these conditions are representative of the conditions to which the bolus is subjected during the swallowing process.

In the case of temperature, it is clear that the value of 25 °C is not in line with body temperature and that the temperature range in which food and drinks can be served is quite wide. Therefore, and considering that the effect of temperature on viscosity can change significantly from one material to another, it would be advisable to be aware of this factor when evaluating dysphagia-oriented products[157–159].

On the other hand, shear rate values occurring during pharyngeal stage of the swallowing were estimated to vary between about 260 and 930 s^{-1} for barium liquid, while values between 13 and 209 s^{-1} were obtained for thickened fluids with viscosities between 0.5 and 2 Pa·s (at 50 s^{-1}), in a device designed for that purpose[142,156,160]. These data show the wide variation of the shear rate during swallowing since it depends on both the flow properties of the bolus and the geometry of the different zones it passes through[146]. As previously mentioned, the transit speed of the bolus decreases as its viscosity increases, so the effect of thickening is 'amplified': the shear rate is lower and, therefore, the drop in viscosity induced by the shear is also lower. In fact, this can be the reason why Nishinari et al. found that their patients were more prone to aspiration when they swallowed polysaccharide solutions that were less viscous at low shear rates, even though their viscosities were the same at 50 s^{-1}[161]. They used in their

study solutions with spoon-thick consistency (almost 2 Pa·s at 50 s^{-1}) that probably flowed slowly when swallowed and therefore their behaviour was more in line with that observed at low shear rate values. Thus, in order to properly classify and select dysphagia-oriented products, it would be recommendable to consider a wider range of shear rates and not a single value as has usually been done.

In addition, when measuring the viscosity of a shear-thinning fluid against the shear rate, this relationship can often be fitted to a power-law model with the expression:

$$\eta = k\dot{\gamma}^{n-1} \quad (1)$$

where η is the apparent viscosity, $\dot{\gamma}$ is the shear rate, k is the consistency index and n is the flow index[151]. The consistency index and, even more so, the flow index can help to easily compare shear-thinning fluids with each other and also to extract more information from this type of measurement. For instance, Vickers et al. found a link between these indices and various swallowing-related properties. Specifically, they determined that the consistency index was negatively related to swallowing pressure in the anterior oral cavity and that fluids with a lower flow index (more shear-thinning) were perceived as less sticky, less mouth coating and required fewer swallows to clear the palate[162].

2.1.3.2. Other swallowing-related rheological properties

Despite viscosity is actually considered as the key parameter in assessing the flow of liquids and semi-solids, most of them require a more comprehensive characterisation to have all the information regarding their behaviour during swallowing. Many materials show a rheological response that is the combination of a viscous component and an elastic component, i.e. they behave partly as a solid and partly as a liquid (viscoelastic materials)[151]. Furthermore, viscoelastic behaviour does not necessarily have to be associated with a certain viscosity profile, since materials whose flow curves overlap can nevertheless have different viscoelastic responses, an effect that has been observed precisely in dysphagia-oriented products[163,164]. In addition, it has also been observed that viscoelastic properties influence the swallowing profile of the food bolus[165], so its characterisation provides complementary information to the flow properties that can be of great interest in the development and assessment of this type of products[152,166].

The forms of characterisation seen so far are aimed at evaluating the response of the materials to the shear. However, during the swallowing process not only shear deformations occur, as the bolus is also subjected to extensional flow[156,167,168]. Although the assessment of the bolus extensional properties and its effect on swallowing safety is still not widespread, there is evidence that its role is likely to be important[169–172]. Thus, several studies have already been carried out to evaluate the response under extensional flow of dysphagia-oriented products[171,173–176].

Although it is actually outside the bounds of rheology, tribology is worth mentioning in this section, as the assessment of the lubricating properties of the bolus and other swallowing elements is attracting increasing interest in the field of dysphagia. Both oral processing and swallowing involve the interaction of a large number of surfaces with very different properties, creating a friction that influences mouth feeling and ease of swallowing[177–180].

What is clear is that swallowing is a complex process to be assessed and that products aimed at OD patients should be thoroughly characterised to predict their behaviour with complete certainty. Moreover, in most cases, the equipment —and expertise— needed to perform this characterisation is not available for clinicians and even less so for OD caregivers[181]. In order to solve this problem, in addition to the lack of standardisation of dysphagia-oriented products that was previously discussed, the International Dysphagia Diet Standardisation Initiative (IDDSI) has recently been launched. The IDDSI framework has been developed through the collaboration of health professionals, caregivers, patients, organisations, researchers, food service providers and industries from around the world, who have agreed on a new classification for modified foods and thickened liquids (see **FIGURE 2**), as well as methods for testing them.

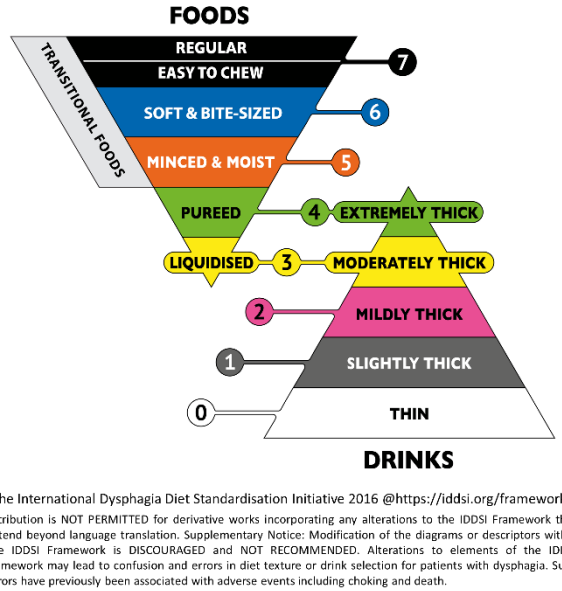

FIGURE 2. IDDSI classification of modified diets[182]

Following IDDSI guidelines, food hardness is evaluated by applying a fork to the sample and observing its behaviour while, for assessing of cohesiveness and adhesiveness, a spoon tilt test is recommended. On the other hand, thickened fluids are categorised depending on the results obtained from gravity flow tests performed with a 10 mL syringe[183]. The gravity flow test is designed to evaluate flow properties as a whole, rather than focusing on a specific parameter, so that the result is more representative of the actual behaviour of the thickened fluids[184]. This also makes it difficult to compare it with other methods and thus to check its reliability[181,185,186]. Nevertheless, there are already studies in which this new classification has been successfully applied[187,188]. The characterisation techniques proposed by this initiative can be very useful in those cases where more accurate characterization techniques are not available. However, it must also be accompanied by a correspondence with more rigorous methods of analysis, with a solid and proven scientific basis, allowing the industrial production of standardised products in a repeatable manner[189].

2.1.3.3. Nutritional intake in modified diets

As discussed above, texture-modified foods and thickened fluids are the most widespread and accepted strategy to ensure safe swallowing while trying to avoid malnutrition and/or dehydration as common complications in patients with OD[190]. However, modified diets are sometimes counterproductive in the pursuit of the second objective[15].

Several studies point to the prescription of thickened fluids as a cause of impaired hydration status[159,191]. Sharpe et al. found no significant difference between the rate of intestinal absorption of water from thickened fluids and from pure water for common types of thickeners[192], so this increased risk of dehydration seems to be due to reduced fluid intake[102,193] (see recommended and real fluid intakes in Table 1), either caused by the refusal of thickened fluids by some patients or by any impediment to easy and continuous access to fluids[194–200]. Patients' dislike of thickened fluids is a matter of concern, since it can lead not only to reduced fluid intake, but also to the complete abandonment of treatment[105,201], with the consequent risk of complications and adverse outcomes[202]. Not less importantly, being forced to maintain a dissatisfying diet for prolonged periods of time has a major impact on patients' quality of life[105,203]. Furthermore, in a study carried out by Vivanti et al., it was concluded that the greatest contribution to daily liquid intake came from food and not from thickened beverages, suggesting that it could be very productive to encourage the consumption of fluid dense foods[195]. Since the level of satisfaction and the ability of the thickened fluids to reduce patients' thirst decreases as the degree of thickening increases[159,203], it may be more pleasant for patients to have the more consistent textures presented as food and to have beverages reserved for cases where lower levels of thickening are required. Additionally, allowing pure water intake could be considered, as there are studies that indicate that pure water (as opposed to other clear liquids) does not increase the risk of developing aspiration pneumonia —under certain conditions— and could be a way to help quench patients' thirst, while maintaining fluid meals as the main source of fluid intake[204–206].

Apart from hydration status, dietary intake also tends to be affected when modified diets are followed. It has been observed that the modified diets provided to patients in hospitals and other care facilities are sometimes below the recommended nutritional requirements. In addition, modified diets tend to

be less rich than regular diets, so it is not uncommon for the dietary intakes of patients on modified diets to fall far short of the required values, both in macro and micronutrients[196,207–211]. TABLE 1 shows the dietary intakes of patients following modified diets in hospitals and other care facilities, compared to Dietary Reference Values (DRV) recommended by the European Food Safety Authority (EFSA) for healthy adults.

TABLE 1. Fluid and nutrient intakes of patients on modified diets and comparison with Dietary Reference Values

	†Dietary Reference Values (DRV)[212]	‡Nutrient Intake	% of DRV
Fluids (mL)	2250[a]	612-1454[193,195,196,200,213]	27-65
Energy (kcal)	2078[a,b]	927-1909[196,207,211,213–215]	45-92
Protein (g)	61[c,d]	40-56[196,207,211,214,215]	66-92
Potassium (mg)	3500	2208-2885[207,211]	63-82
Magnesium (mg)	325[a]	127-256[207,208,211]	39-79
Calcium (mg)	950[e]	732-757[207,208,211]	77-80
Vitamin B6 (mg)	1.65[a]	1.10-1.13[208,211]	67-69
Vitamin B12 (µg)	4.0	1.9-3.5[207,208,211]	48-88
Vitamin C (mg)	102.5[a]	92.0-155.0[207,208,211]	90-151
Vitamin D (µg)	15.0	2.6-5.8[207,208,211]	17-38
Vitamin E (mg)	12.0[a]	0.9-4.8[208,211]	8-40

†All DRVs refer to adults ≥ 18 years, unless otherwise indicated. Regular text represents Adequate Intake (AI), text in italics represent Average Requirement (AR) and text in bold represents Population Reference Intake (PRI)

‡Intakes of patients who were not receiving support by non-oral routes. Oral nutritional supplements (ONS) are included.

[a]Average of the values for men and women

[b]For adults between 60 and 69 years (moderately active)

[c]For a body weight of 73.5 kg (EU average for men and women between 60 and 69 years[216])

[d]For adults ≥ 60 years

[e]For adults ≥ 25 years

Of course, the reference values shown are very general, since the nutritional needs of each individual depend on many factors such as age, gender, lifestyle and the existence of diseases, among others[123,212]. However, changes in the reference values are not radical in most cases and, considering how far the intake values of many of the nutrients are from those that would be recommended, the nutritional deficit of patients following modified diets is undeniable. This deficit is especially significant in the case of some vitamins such as E and D, whose

intake in the best cases is not even half of that recommended. Although vitamin E deficiency is not common, it can occur in cases of malnutrition or in people with malabsorption conditions and can even cause neurological symptoms[217]. Some studies also suggest that diets rich in vitamin E and other antioxidants may be beneficial in preventing and reducing the severity of dysphagia and some of its major causes such as Parkinson's or Alzheimer's disease[218–221]. Unlike vitamin E deficiency, hypovitaminosis D is a widespread problem worldwide, especially among the elderly, and is associated with an increased risk of diseases such as osteoporosis and musculoskeletal pain, heart disease, certain types of cancer and immune and metabolic disorders, as well as neurological and neurodegenerative diseases. The major source of vitamin D is supposed to be skin synthesis, but limited exposure to sunlight, use of sunscreens, and other factors that affect vitamin D photoproduction (such as age or ethnicity, among others) mean that in many cases this is not enough. On the other hand, there are few foods that contain significant amounts of this fat-soluble vitamin, so the use of supplements and dietary fortification becomes essential in many situations[217,222–224].

Both menu fortification and the use of oral nutritional supplements (ONS) are good strategies for trying to improve the dietary intakes of patients on modified diets[208,225,226]. However, these measures also have their drawbacks, one of which is the increase in costs, especially in view of the enormous waste that results from patients not consuming all the menus or supplements provided to them[214,215,227]. Based on this, it may be crucial to improve the acceptance of modified diets, as it is of no use to increase the amount of nutrients provided if patients do not consume them. To this end, it is emphasised that modified diets should only be used when clinically indicated and with the minimum possible restrictions depending on the condition of each patient[228,229]. On the other hand, it is clear that acceptance is totally linked to the different sensorial stimuli obtained from food. Since there are elements of the eating experience that are irretrievably lost through changes in texture, this loss must be compensated for as far as possible in other respects, such as smells, tastes or visual appearance of the modified food[201,229,230]. The possibility of choosing between several menu options or that the different foods on the menu can be differentiated from each other also seems to have a positive influence on the degree of acceptance of modified diets[207,231].

2.2. MODIFYING FLOW PROPERTIES OF FOODS AND BEVERAGES

The quality of any food product can be evaluated based on several key factors such as appearance, flavour (comprising taste and odour), texture and nutritional content[232] (FIGURE 3). As seen in the previous section, none of these aspects can be neglected when developing dysphagia-oriented foods and beverages, although texture —and flow properties, more specifically— obviously requires special attention and careful control in these products.

Texture can be defined as the way in which the different constituents combine into micro and macro structures that externally manifest in terms of flow and deformation[233]. The texture of foods is derived from their structure at the molecular, microscopic and macroscopic level which, in turn, depends on both their ingredients and the way they are processed to obtain the final product[163,232].

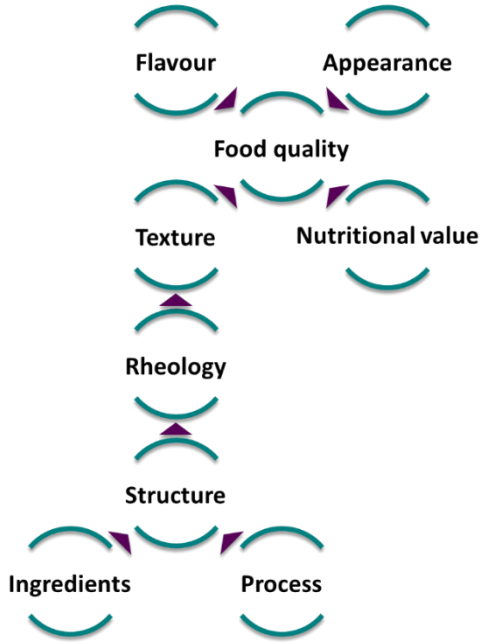

FIGURE 3. Key factors affecting food quality

Polysaccharides, proteins and fats are key ingredients for the development of structure in food, as well as the formation of colloidal-type microstructures such as emulsions and foams[234].

When the aim is, in particular, to control the rheology of aqueous foods and beverages in order to modify their ability to flow, the most common practice is the use of hydrocolloids as thickening or gelling agents[235].

2.2.1. Thickening and gelling in aqueous media

Hydrocolloids can be defined in a simplified way as water-soluble polymers which provide viscosity and gelation in solution[236]. For this reason, it is not surprising that hydrocolloids —especially polysaccharides such as starches and gums— are often major components in foods formulated for dysphagia management[237–239]. Most of hydrocolloids are non-digestible and flavourless polysaccharides with multitude of functional properties and structure-forming capabilities (apart of those already mentioned of thickening and gelling) such as stabilisation, emulsification, encapsulation and the ability to form films and membranes, among others. Being natural polymers from renewable sources, they are also biocompatible, biodegradable and non-toxic, in addition to being widely available and therefore low in price in most cases. All these valuable features make them probably the most important group of functional ingredients for food applications[239,240].

Most hydrocolloids are used in aqueous solution and a proper solubilisation is the first step to achieve their maximum functionality. Solubilisation involves a continuous process of hydration, in which the intermolecular binding of the hydrocolloid is gradually replaced by polymer-solvent binding, so effective dispersion is crucial for hydration to occur as correctly and efficiently as possible[241]. Polysaccharides in solution can form networks and gels which can be classified into different groups from a rheological point of view[242]:

- Entanglement networks (entangled and non-entangled)
- Weak gels (or structured liquids)
- Strong gels

In entanglement networks, no enthalpic polymer-polymer interactions are present and flow restriction depends mainly on size and number of molecules in solution. Gelling, on the contrary, implies the creation of specific physical or

chemical bonds (usually physical, in the case of natural hydrocolloids) to form a three-dimensional network, also exhibiting a net transition between the liquid and solid-like behaviour, normally induced by changes in temperature, the presence of certain ions or variations in pH[240]. Thickeners generally belong to the first group, although the boundaries between them are sometimes unclear and materials can be found that share characteristics with more than one. An example is the weak gel behaviour characteristic of xanthan gum[242].

The general mechanisms of thickening and gelling, as well as the typical rheological properties resulting in each case, are described below.

2.2.1.1. Thickening

The increase in viscosity (thickening) produced by hydrocolloids in solution is due to non-specific physical entanglement of disordered polymer chains[235]. In diluted solutions, conformationally disordered random polymer coils constitute individual 'islands' with little or no influence on each other, distributed in space in a heterogeneous way and without interpenetration among them. As the concentration increases, the collisions between chains increase, reaching a point where more chains can only be accommodated by overlapping and interpenetrating each other and the concentration of the solution equals that within the domain of each of the single chains. This critical concentration is called the overlap concentration (C*) and can be regarded as the boundary between the diluted and concentrated (or semi-diluted) solutions, indicated by a sudden increase in viscosity[240,243]. In fact, when the zero-shear viscosity (η_0, see **FIGURE 6**) —or the specific viscosity, $\eta_{sp}=(\eta-\eta_0)/\eta_0$, to remove the contribution of solvent viscosity— is plotted against the polymer concentration on a log-log scale (**FIGURE 4**), a linear dependence is obtained in which the overlap concentration can be identified by a marked change in tendency[243,244]:

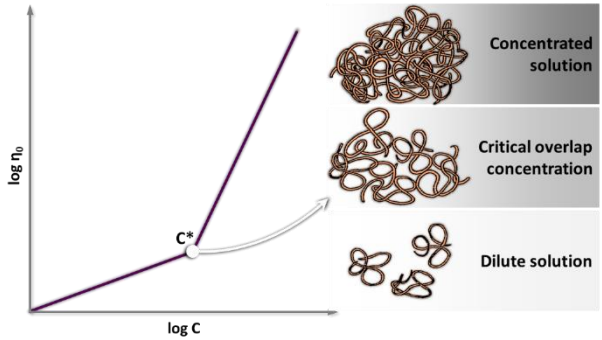

FIGURE 4. Generalised viscosity-concentration dependence for random coil polysaccharides (Adapted from Robinson, 1982[245], and Sworn, 2004[244])

Actually, the polymer chains cease to behave as isolated entities as soon as the infinite dilution regime is exceeded, so it would be more correct to consider C* as a relatively narrow concentration range in which the distribution of the polymer chain segments becomes uniform throughout the entire solution[240]. At higher concentrations (up to three or four decades above the overlap concentration[246]) another critical concentration, the entanglement concentration (C_e, see FIGURE 5), above which the degree of entanglement of the polymer chains becomes significant, this state being known as entangled semi-dilute regime[247,248].

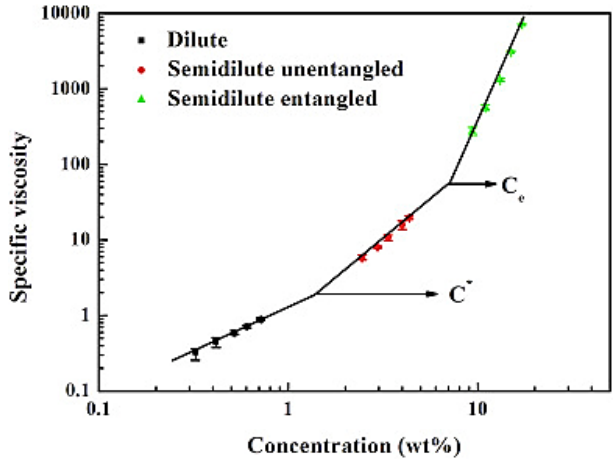

FIGURE 5. Typical concentration regimes in solutions of entangled polymers

Beyond determining the amount of thickener needed to obtain a given increase in viscosity, these concentration regimes also affect the hydrodynamic properties of the polymer solutions[249] and therefore also their performance during processing. The degree of entanglement is essential in polymer solutions used, for instance, in electrospinning[247,250] and electrospraying[251,252] or 3D printing[253]. On the other hand, around the overlap concentration there is usually a significant change in flow properties of hydrocolloid solutions. In the diluted state, the polymer chains have the capability to move freely, whereby the rheological response remains Newtonian as for pure solvent. Above C*, a non-Newtonian behaviour is usually observed and, in particular, the shear-thinning behaviour characteristic of fluids with a complex microstructure ('structured' fluids), with Newtonian regions at low and high shear rates as illustrated in FIGURE 6[243,244].

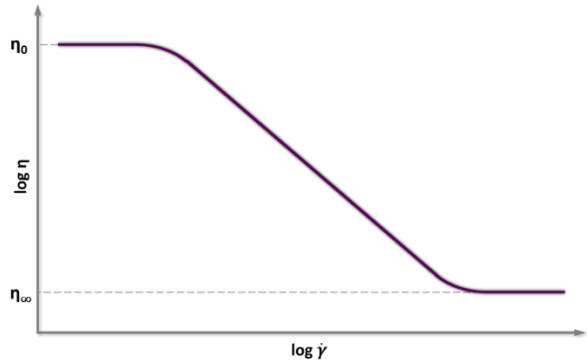

*FIGURE 6. Typical dependence of apparent viscosity (η) with shear rate ($\dot{\gamma}$) for polymer solutions above C**

At low shear rates, the disruption of entanglements due to shear is slower than or equal to the formation of new entanglements and therefore viscosity does not change with shear rate. This constant value is known as the zero-shear viscosity (η_0). When the shear rate exceeds a critical value, disentanglement predominates over re-entanglement, resulting in a sharp drop in apparent viscosity. Finally, when no further disruption is possible, the viscosity becomes again constant in what is referred to as the infinite-shear viscosity (η_∞)[243,244]. These curves can be approximated by different models, according to the regions considered, whose representative parameters are usually used as a way to characterise and compare the rheological behaviour of entangled polymer solutions and other structured fluids. TABLE 2 summarises some of the most relevant models used to this end[151].

TABLE 2. Rheological models used to approximate viscosity-shear rate dependence in structured fluids

Model	Expression	Shear rate range
Ostwald-de Waele Model	$\eta = k\dot{\gamma}^{n-1}$	Power-law shear-thinning region
Sisko Model	$\eta = \eta_\infty + k\dot{\gamma}^{n-1}$	Power-law shear-thinning and high shear rate constant viscosity regions
Ellis Model	$\frac{\eta}{\eta_0} = \frac{1}{1 + \left(\sigma/\sigma_{1/2}\right)^{\alpha-1}}$	Low shear rate constant viscosity and power-law shear-thinning regions

Carreau Model	$\frac{\eta - \eta_0}{\eta_0 - \eta_\infty} = \frac{1}{[1 + (\lambda\dot{\gamma})^2]^s}$	Low shear rate constant viscosity, power-law shear-thinning and high shear rate constant viscosity regions

The power-law (Ostwald-de Waele) model is often sufficient to characterise these structured fluids in the usual shear rate range, but more complex models, such as Sisko's or Carreau's, are useful when it is interesting to compare also Newtonian zones at low and high rates. Ellis' model uses stress, rather than shear rate, as the independent variable[254].

It has been previously seen how the degree of entanglement of the polymer solutions increases with concentration and, since their shear-thinning behaviour is derived from the processes of formation and disruption of these entanglements, the effect of concentration on the rheological response of these fluids is generally significant[242]. For instance, it can be seen in FIGURE 7 how an increment from 0.6 to 2% in concentration translates into a several-decade increase in η_0 and a considerably earlier critical shear rate (that from which the drop in viscosity begins) in guar gum solutions:

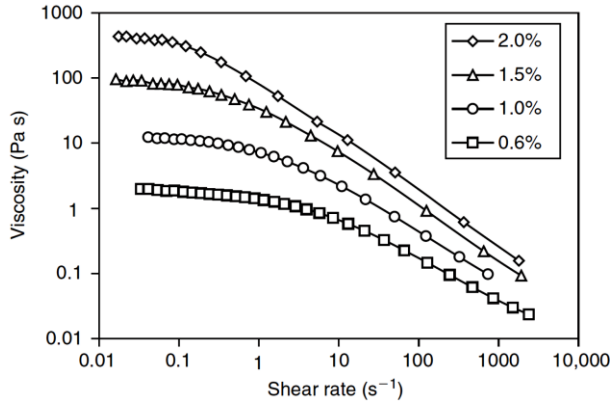

FIGURE 7. Effect of concentration on viscosity-shear rate dependence of guar gum solutions[242]

Apart from concentration, many other factors such as time, temperature, molecular weight, solvent affinity or electrostatic interactions among chains and with the environment affect the flow properties of entangled polymer

solutions[240,241,255,256]. However, one of the most decisive is the structure of the polymer chains. The stiffness, branching and conformation of the chains have a strong influence on the response in viscous flow, with large differences between polymers being observed[243], as shown in FIGURE 8.

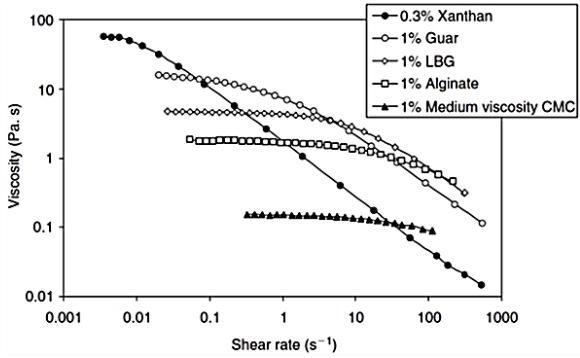

FIGURE 8. Shear-thinning behaviour of different polysaccharides[242]

Nevertheless, Morris et al. found that a large variety of commercial flexible random coil polysaccharides with broad polydispersity had a common dependence on viscosity with concentration and shear rate. Below and above C*, specific viscosity varied according to $C^{1.4}$ for dilute solutions and according to $C^{3.3}$ for concentrates. In addition, all concentrated solutions collapsed into a master curve when viscosity is expressed as a fraction of zero-shear viscosity and shear rate as a fraction of a critical shear rate ($\dot{\gamma}_{0.1}$) defined as the one at which the apparent viscosity drops to 90% of the zero-shear viscosity value ($\eta=\eta_0/10$), as shown in FIGURE 9[257]:

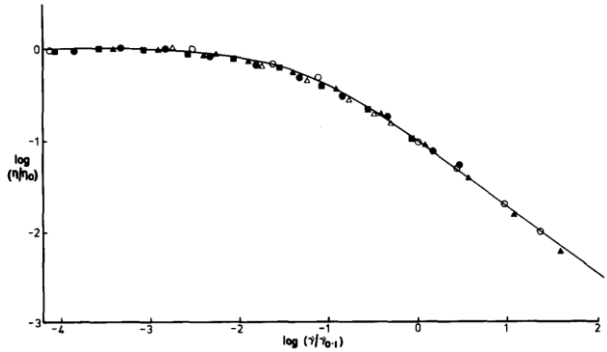

FIGURE 9. Generalised shear-thinning behaviour of concentrated solutions of random coil polysaccharides (guar gum, λ-carrageenan, locust bean gum, 'high mannuronate' alginate and hyaluronate[257]

Although this generalisation of the shear-thinning behaviour of entangled random coils solutions is applicable to most polysaccharides, even at different concentrations and temperatures[258,259], it is not however able to adequately reflect the rheological behaviour of some polysaccharides essential to the food industry, such as starch or xanthan gum, to which the globular structure and stiffness of their chains, respectively, confer particular flow properties[260].

It is not only the viscosity that changes as the concentration in entangled polymer solutions increases. Entangled polymer solutions, like most if not all materials, have a response to deformation that lies somewhere between elastic and viscous behaviour (i.e. they are viscoelastic) and this response is also affected by the degree of interaction between the polymer chains and, therefore, by the concentration regime of the solution. FIGURE 10 shows schematically the typical evolution of storage (G', elastic component) and loss (G'', viscous component) moduli with frequency for aqueous polysaccharide entangled solutions below and above the overlap concentration C*:

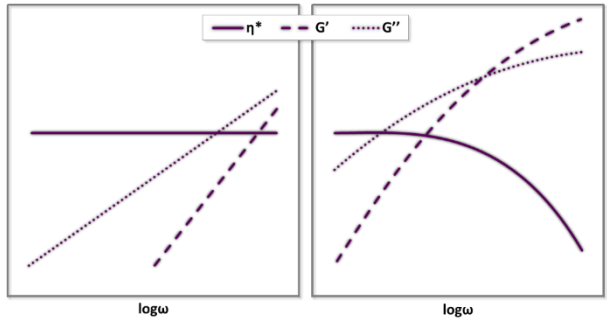

FIGURE 10. Typical viscoelastic response for aqueous polysaccharide solutions below (left) and above (right) overlap concentration (Adapted from Sworn, 2007[242])

Below C*, both modules are highly frequency dependent and G'' has higher values than G' over a wide range of frequencies. At concentrations above the overlap, entanglement formation causes that, if frequency is high enough to make the time scale of the measurement shorter than the molecular rearrangement rate, the elastic response becomes higher than the viscous one and both depend less on frequency, resulting in a gel-like behaviour (see section 2.2.1.2: Hydrogelation). However, as there is no interaction among the polymer chains other than entanglement, the complex viscosity resulting from non-destructive tests —such as oscillatory tests carried out within the linear viscoelastic range— of the entangled solutions matches the apparent viscosity obtained in flow destructive tests (this is, they obey the Cox-Merz rule). Thus, the complex viscosity does not depend on the frequency at concentrations below C*, but it does above it[242].

Also in this sense, both starch and xanthan gum show peculiarities, as they are capable of creating interactions beyond pure entanglement. Starch is capable of acting both as a thickener and a gelling agent, while xanthan gum exhibits weak gel properties (see section 2.2.1.1.2: Xanthan gum) and high viscosity at very low concentrations.

2.2.1.1.1. Starch

Starch is the most widely used food thickener, because of its great versatility and its abundance in nature, which makes it a low-priced raw material. In addition, its taste is not perceptible at low concentrations (up to around 5%), so it can be

found in a wide variety of foods to provide texture, extend shelf life or reduce costs[235,243]. There are many types of starches derived from different plants such as corn, wheat, potato, tapioca or rice, among many others, but they are all composed of two types of polysaccharides: amylose and amylopectin. Amylose is a predominantly linear polymer, whose content in most native starches ranges from 15 to 30%. Amylopectin, on the other hand, is a very high molecular weight and highly branched polymer which is the major component in most starches[261]. Starch occur naturally as small granules, whose exact size and morphology vary depending on the amylose/amylopectin ratio, locations and structures [262]. The most common representation of the starch granule is as a radial organisation of alternating shells of amorphous and crystalline regions, as shown in FIGURE 11, where amylopectin is responsible for the crystalline structure and amylose is mainly located in the amorphous region of starch granules[261,263].

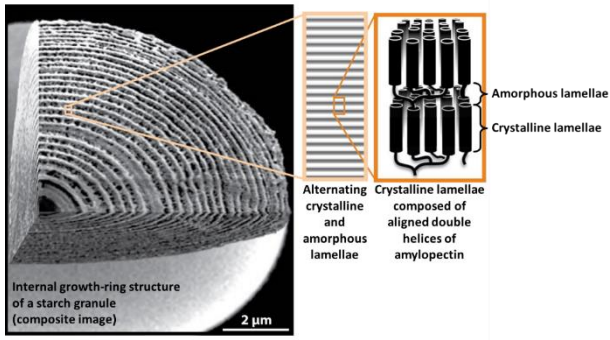

FIGURE 11. Internal configuration of the starch granule (Adapted from Zeeman, 2010[264], and Streb, 2012[265])

Many of the physical properties of starch are directly linked to this granular structure which gives it certain features that are different from those of other hydrocolloids. One of the advantages of this granular structure is related to flavour perception. Thickening of foods with hydrocolloids often results in flavour suppression that increases with the concentration of thickener, especially above C* (when, as previously discussed, a rapid increase in viscosity occurs). Flavour and mouthfeel perception of viscous solutions depends on their effective mixing with water (or saliva) and this is much less efficient in solutions of entangled polymers than in solutions with granular structure. For this reason,

flavour suppression is much less for starches capable of maintaining their granular integrity than for other hydrocolloids[261,266].

Another characteristic of starch is that it is capable of acting both as a thickener and as a gelling agent depending on how it is processed. Native starch is insoluble in cold water and only forms suspensions with tendency to sediment. When these suspensions are heated (Figure 12), the starch granules begin to absorb water, swelling to a maximum size at which point the starch produces maximum thickening. Further heating will then cause the starch granules to begin to break down and the viscosity decreases. If the temperature is maintained long enough, the granules break down completely and amylose and amylopectin are released into the solution while the viscosity drops to a minimum. When this solution cools down, amylose and amylopectin associate to give a gel-like structure[261,263,267].

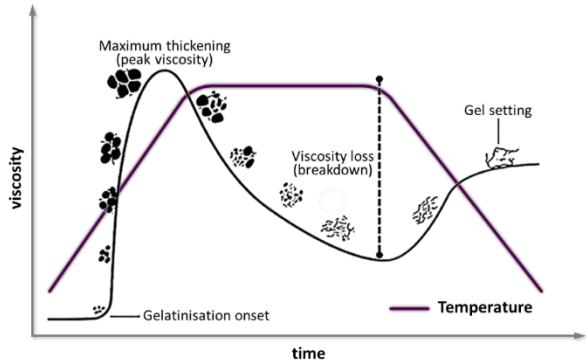

Figure 12. Typical gelatinisation process for starch in excess water (Adapted from Schirmer, 2015[268])

The temperatures at which these processes take place, as well as the specific physical properties of starch in each of these states, are determined by the content of amylose, amylopectin and also by the presence of lipids, phosphates or electrolytes (among other factors, such as cooling speed), so that large differences can be found between starches from different plant sources[261,267]. However, if the variety of properties offered by traditional native starches are not enough to meet the needs for a given application, it is also possible to control their thickening and gelling behaviour by different methods. Modification of the

source crops, chemical and physical modification or enzymatic treatments are the main ways to obtain starches with specific functional properties[267]. One of the most interesting features for food thickening is the ability to hydrate and increase viscosity in cold water, without the need for heating, thus being able to be applied to the thickening of foods that cannot —or do not need— to be subjected to high temperatures or as an instant thickener to be used directly by consumers without cooking. This can be achieved by pre-gelatinisation of starch, a physical modification carried out by the simultaneous heating and drying of a starch slurry, usually carried out by drum drying. During this process, the starch granules gelatinise, absorbing water and losing their crystalline structure, a state that is 'captured' by rapid drying. If water is added later, it will interact more easily with starch, resulting in an increase in viscosity without the need for heating[261,269]. However, pre-gelatinisation causes the damage or even the total breakdown of the starch granules, and therefore these starches have a lower thickening capacity than their native starch, as well as a granular texture. For this reason, granular cold water swelling starches (GCWS) have emerged, in which the typical pre-gelatinisation process is modified by the presence of different chemicals to maintain the integrity of the starch granules, resulting in greater thickening capacity, more homogeneous texture, greater clarity and better tolerance to processing than in pre-gelatinised starches[269].

Gelatinised starch granules, however, become susceptible to hydrolysis by the action of α-amylase, an enzyme present in the saliva of humans and other animals, which can cause significant viscosity reduction in starch-thickened fluids[270,271]. This effect, which on the one hand seems to favour the perception of flavours[272], can, on the other hand, have very negative consequences in some applications of starch, such as fluid thickening in the management of dysphagia, and must be taken into account when developing this type of product[273].

2.2.1.1.2. Xanthan gum

Xanthan gum is a high-molecular weight branched polysaccharide produced at the cell wall surface of the several bacteria of the *Xanthomonas* strains. It is soluble in cold water, provides very high viscosities at low concentrations and has a highly shear-thinning behaviour, which results in good mouthfeel (almost perfect flavour release at concentrations well above C*) and pouring qualities. All these properties make it an extremely useful additive in the food industry

and it has a wide range of applications as a thickener, stabiliser and suspending agent[274–276].

The primary structure of xanthan gum consists of a substituted cellulose column with trisaccharide side chains that align around the main chain to form a fivefold helix. Although the most widespread idea is that this conformation consists of a single helix, there are also authors who claim that these helices associate to form a double helix dimer, as shown in FIGURE 13[277,278].

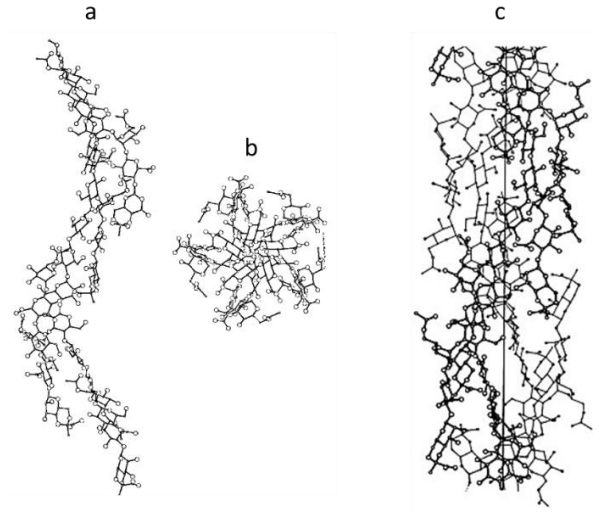

FIGURE 13. Molecular conformation of xanthan gum as (a) single helix, perpendicular to helix axis; (b) single helix, view down helix axis; (c) double helix[277,278]

Whether as single or double helix, xanthan gum is characterised by the formation of ordered networks of rigid rod-like molecules, which cause xanthan solutions to exhibit high viscosity values at low concentrations compared to other polysaccharides, as well as a highly shear-thinning behaviour caused by shear-induced disruption of these networks, as schematised in FIGURE 14.

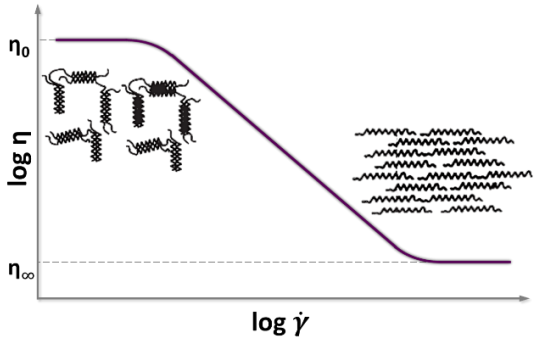

FIGURE 14. Molecular origin of xanthan gum shear-thinning behaviour (Adapted from Sworn, 2009[275])

Xanthan gum is an anionic polysaccharide, so the presence of salts in the solution medium has a decisive influence on its rheological response. On the one hand, its viscosity decreases significantly with the presence of salts in solution (see FIGURE 15) due to the shielding effect of the ions on the charges of the polymer chains, so that these can acquire a more compact structure and more chains are needed to achieve the same degree of interaction and the consequent increase in viscosity as for a salt-free solution[246].

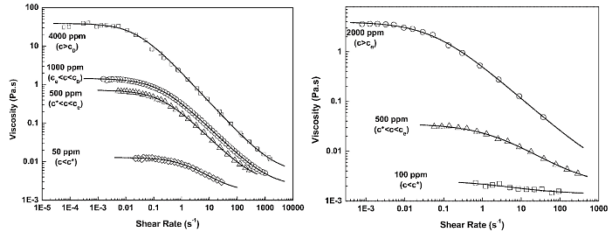

FIGURE 15. Evolution of viscosity with shear rate of xanthan gum solutions at different concentrations in a salt-free medium (left) and in 50 mM NaCl (right)[246]

In FIGURE 15, it can be seen how, below C*, xanthan shows a nearly Newtonian behaviour in the presence of salts, while shear-thinning is already observed in a solution with half the concentration in a salt-free medium. In addition, viscosities at zero shear decrease by up to an order of magnitude in the 50 mM NaCl solution. If looking at the graph on the left, an additional curve can also be seen with respect to the one on the right. This is because, in a salt-free medium,

xanthan gum has a third critical concentration (C_D), which marks the point where the electrostatic blobs (the zone of influence of the charged monomers) begin to overlap and the viscosity increases with concentration to the same extent as it would for an uncharged polymer[246,279]. FIGURE 16 shows this and other critical concentrations (C* and Ce) for xanthan without the presence of salts.

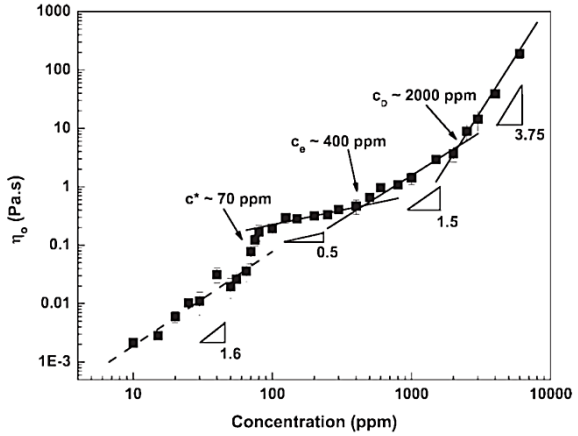

FIGURE 16. Critical concentrations for xanthan gum in salt-free solution[246]

On the other hand, the presence of salts delays the change in conformation of xanthan gum, from the rigid ordered state to a more flexible and disordered one, caused by heating. The presence of ions stabilises the ordered helical conformation and this transition, which occurs at around 40 °C in a salt-free medium, can be delayed by low salt concentrations to temperatures above 90 °C[275].

However, the greatest peculiarity of xanthan gum, also consequence of the rigidity and the tendency of its chains to form ordered networks, is maybe its weak gel behaviour. FIGURE 17 clearly shows the difference in the viscoelastic behaviour of the xanthan compared to guar gum, which does not form this type of ordered structure.

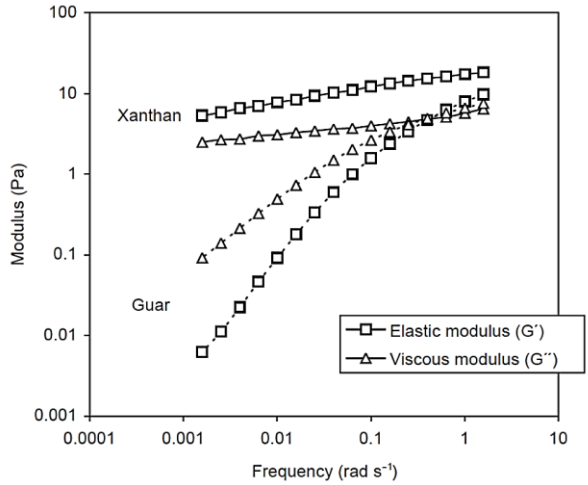

FIGURE 17. Viscoelastic behaviour of xanthan and guar gums at 0.6% in tap water[275]

It can be seen how the response of xanthan gum, contrary to guar, is eminently elastic and only slightly dependent on frequency, denoting a considerable degree of structuration.

2.2.1.1.3. Commercial thickeners for dysphagia management

Commercial thickening powders are a simple and cost-effective way to obtain fluids or semi-solids with the required texture for safe swallowing by dysphagic patients. There are thickening powders in the market based on different ingredients (mainly starches and gums) that show different rheological behaviours when they are used for thickening fluids for dysphagia management. FIGURE 18 shows how the increase in viscosity produced by different commercial thickeners can greatly vary, depending on the composition of the thickener.

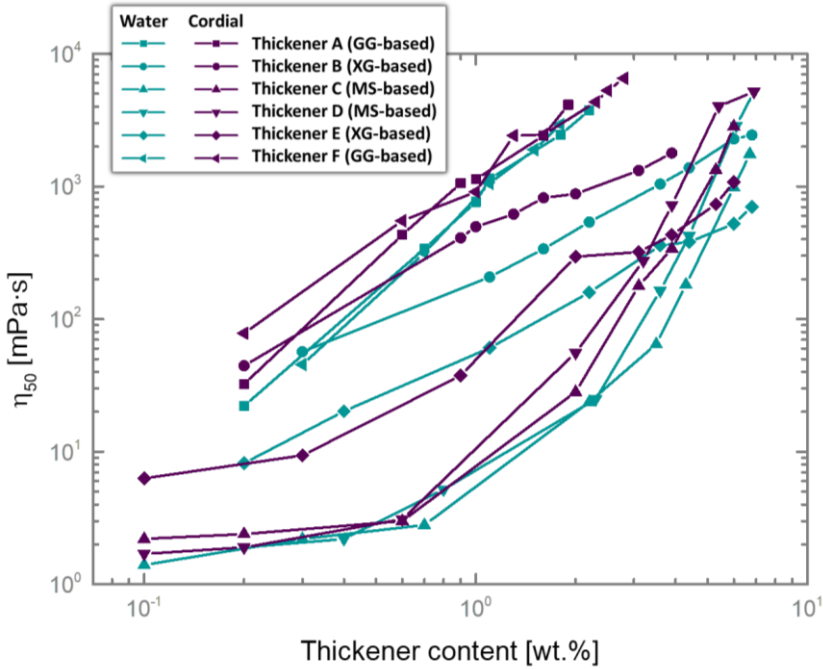

FIGURE 18. Evolution of η_{50} (viscosity at 25 °C and 50 s^{-1}) with concentration for different commercial thickeners. GG=guar gum, XG=xanthan gum, MS=maize starch (Data from Sopade, 2007[280])

As can be seen in Figure 18, gum-based thickeners provide higher viscosities than starch-based thickeners at same concentrations. The latter, moreover, seem to undergo up to two regime changes in a range of concentrations in which the dependence of viscosity on the thickener concentration does not seem to change in the case of gums. The different rheological behaviours of gum and starch-based thickeners is not surprising, especially considering the disparity in their microstructures, as can be seen in FIGURE 19.

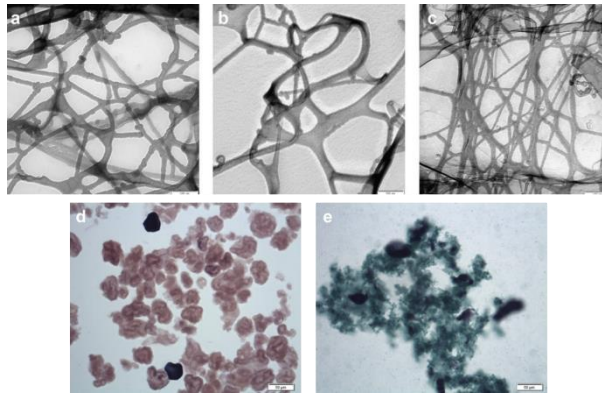

FIGURE 19. TEM (Transmission electron Microscopy) micrographs of xanthan gum-based (a, b and c) and Light Microscopic images of starch-based thickeners (d and e)[174]

These differences in viscosity, however, are not only observed when changing the main component. In Figure 18, it can be seen how the viscosity of xanthan-based thickeners also differs from each other. This is because, as seen in previous sections, the exact viscosity of polysaccharide solutions depends on many factors, such as the molecular weight of the polymer or the presence of other components. Commercial thickening formulations may contain only one type of thickener, and very different behaviours can be observed depending on the characteristics of the raw materials and the proportions in which they are found. Gums show very interesting properties for the elaboration of dysphagia-oriented thickeners, such as the weak gel behaviour of xanthan gum —which makes it flow like a coherent bolus during swallowing[165]— or its resistance to α-amylase, which causes viscosity to be reduced in starches. In contrast, gums add a 'slimy' mouthfeel that can be objectionable for some consumers and are less digestible than starches[273,281–283], so mixtures of both types of polysaccharides are sometimes used. The combination of both gives rise to morphologies in which the swollen starch granules are surrounded by a continuous phase containing the gum molecules[284]. In these cases, the nature of the components, their relative content and the total concentration determine whether the contribution of each component to the viscosity and viscoelastic properties of the solution is purely additive, whether there is synergy between them or whether, as is often the case in starch/xanthan mixtures, the gum reduces the interactions of the granules, thereby easing their flow[284–286].

The use of two or more thickeners and other additives makes some commercial formulations quite complex (as well as unknown, at least in detail). Furthermore, not only the thickener is responsible for the rheological behaviour of thickened fluids, being the dispersing medium, temperature or even processing conditions decisive factors in their final performance. Figure 18 shows how viscosities differ for the same thickener content when thickening a cordial (a sweet fruit-flavoured drink) instead of water. In fact, the data represented in Figure 18 belong to the first of a series of three articles in which Sopade et al. analyse the rheological behaviour of various commercial thickeners in water, cordial, fruit juice and milk, finding that the resulting viscosity depends on the solids content of the dispersing medium[280,287,288]. Other authors have also thickened different beverages and the effect of pH, density, fat content and temperature of the dispersing medium on final performance of thickened fluids has been characterised[22,281,286,289–291].

Other products for dysphagia are sold ready-to-use (RTU) and do not present these drawbacks. These products, however, have the problem that the range of flavours and formats available is obviously limited. As a result, their consumption over long periods of time often leads to patient fatigue and abandonment of treatment, with the consequent risk to their health[22,105,202]. The wide variety of rheological responses and organoleptic properties that can be obtained by combining different formulations of powdered thickeners and dispersing mediums can undoubtedly be a great advantage in responding to the needs of different phenotypes of dysphagic patients while avoiding diet fatigue. However, in order to take advantage of its full potential, it would be necessary to develop an information system that would relate the different types of dysphagia with the best rheological properties to manage them and the thickener-medium combinations that could provide those properties.

2.2.1.2. Hydrogelation

Hydrogels are three-dimensional networks formed by hydrophilic polymers dispersed in an aqueous medium, which maintain their structure thanks to chemical or physical bonds —unlike what happens in thickened fluids, where the restriction of molecular freedom of movement is merely topological—[240,292,293]. Nevertheless, defining clearly and concisely what constitutes a gel is not an easy task. Ever since Lloyd stated, in 1926, that 'The colloidal condition, the "gel", is one which it is easier to recognize than to define'[294], various definitions and ways of classifying gels have been proposed in search of a consensus that did

not seem to be reached. The continuous appearance of new materials and ways of considering the already known ones, made it necessary to revise again and again the conditions that a material had to fulfil to be considered a gel, to the point that, already in 1997, Nijenhuis came to claim that 'A gel is a gel, as long as one cannot prove that it is not a gel'[295]. However, a gel can be generally described as a soft, solid or solid-like material consisting of a fluid —present in a substantial amount— and polymer chains, smaller molecules or particles that connect to each other to form a three-dimensional network, where this connectivity results in loss of fluidity[296]. A gel network consisting of polymers with segments or hydrophilic groups —such as hydroxyl (-OH), carboxyl (-COOH), amide (-CONH-, $-CONH_2$) and sulfonic ($-SO_3H$) groups— that give it the ability to retain large amounts of water is called hydrogel[292,297–299].

Hydrogelation can occur by crosslinking of polymer chains either through physical interactions or covalent bonds (chemical crosslinking), as illustrated in FIGURE 20. However, chemical crosslinking is practically the exclusive domain of synthetic polymers, whilst the gels formed from polysaccharides and other hydrocolloids are usually non-covalently crosslinked physical gels, in which the gel structure is maintained by interactions, such as hydrogen bonds, hydrophobic association or cation-mediated crosslinking[240,243,300].

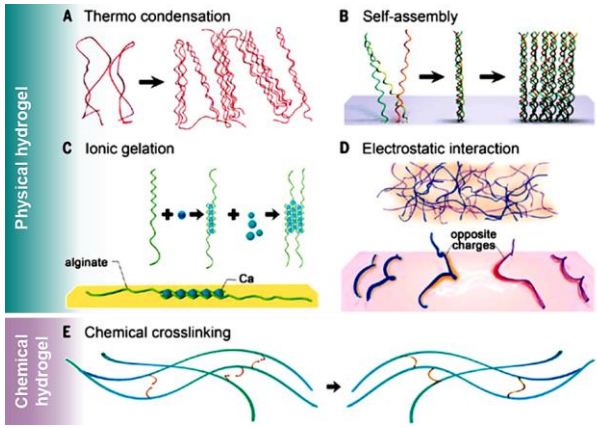

FIGURE 20. Hydrogels formation through (a to d) physical and (e) chemical crosslinking (Adapted from Zhang, 2017[293])

As already mentioned at the beginning of section 2.2.1 (Thickening and gelling in aqueous media), gelling agents undergo a well-defined transition from the sol state (a colloidal suspension of solid particles in a liquid, in which the size of the dispersed phase is so small that gravitational forces are negligible and short-range forces predominate) to the gel state: the so-called sol-gel transition[301], which can be induced by different environmental changes. Many natural polymers undergo temperature-induced disorder-to-order conformational transitions, being the formation and association of this ordered structures the origin of the gel network formation (**FIGURE 20A**). Usually, lowering the temperature of a hot polysaccharide solution —in which the polymer chains are disordered and can move freely— causes this transition to occur, and the gel sets on cooling. However, some temperature-driven hydrogels can also set during heating[240,302]. The affinity (e.g. opposite charges) between different segments of a polymer (**FIGURE 20B**) or between different polymers (**FIGURE 20D**) can also be the driving force for molecular arrangement. The same effect can also sometimes be achieved by the addition of ions —divalent cations— to the medium (**FIGURE 20C**), which stabilise and shield the repulsive forces between chains, allowing them to organise themselves in a more compact way, eventually leading to the development of the gel network[243,293]. The presence of ions in the medium is also necessary in many cases (for all polysaccharide polyelectrolytes) to promote gelling through other mechanisms, such as temperature gelling[240]. The nature of each polymer, as well as the different gelling mechanisms and conditions, will determine the structure (see **FIGURE 52**) and strength of intermolecular regions of association in the gel network (junction zones) and, consequently, the properties of the resulting gel and its behaviour from a rheological point of view.

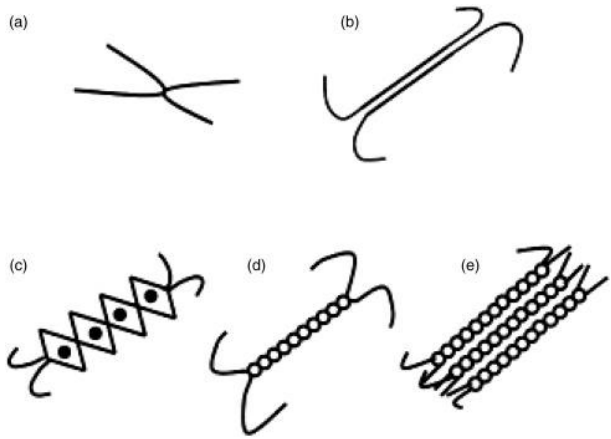

FIGURE 21. Idealised junction zones in polysaccharide gels: (a) point crosslink, (b) extended block-like junction zone, (c) egg-box model, (d) double-helical junction zone and (e) junction zone formed by aggregation of helical segments of the polysaccharide chains

It is possible to differentiate between weak and strong gels concerning the respective viscoelastic behaviours. In both cases, as schematised in FIGURE 22, the viscoelastic response is predominantly elastic, with the storage module, G', higher than the loss module, G'', over the whole typical frequency range (between 10^{-2} and 10^{2} s^{-1}). In other words, these materials behave more like a solid than a liquid, contrary to what happens in the case of entangled polymer solutions[242,296].

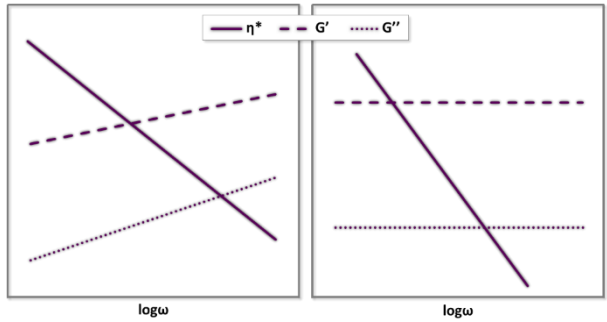

FIGURE 22. Typical viscoelastic response for weak (left) and strong (right) gels (Adapted from Sworn, 2007[242])

Thus, the main difference between weak and strong gels is the evolution of the linear viscoelastic functions with frequency. The moduli in strong gels are independent of frequency, while, in the case of weak gels, a slight drop can be observed as frequency decreases, with the viscous and elastic moduli being further apart from each other in the case of strong gels than in the case of weak ones[242,296]. As already mentioned when discussing the weak gel behaviour of xanthan gum, these systems do not comply with the Cox-Merz superposition principle, since the gel network interactions contribute to the complex viscosity obtained in non-destructive oscillatory tests, but not to that obtained in destructive flow tests[240,242].

It is also possible to differentiate between weak and strong gels in terms of viscosity. In steady shear, a strong gel will rupture completely whereas a weak gel will flow[242]. This difference is especially relevant for the application of these materials in dysphagia-oriented nutrition, since strong gels can fracture when subjected to the high deformations that occur during swallowing, while weak gels tend to flow more like a single 'coherent bolus' that can be ingested more easily and safely by dysphagic patients[165,303,304]. Weak gel behaviour is quite common, not only in the field of dysphagia, but also in the food industry in general, since semi-solid foods are normally physical gels that flow after a certain time. Thus, it is not surprising that the model developed by Gabriele et al.[305] to describe the viscoelastic behaviour of this type of material has been widely used[306]. This 'weak gel model' assumes that these materials are composed of a cooperative arrangement of flow units that interact with each other to some extent, the complex modulus, G^*, being related to the frequency according to the expression:

$$G^* = \sqrt{(G')^2 + (G'')^2} = A\omega^{1/z}$$

being A the 'strength' of the interactions between flow units and z the number of rheological units correlated with one another in the three-dimensional structure. This model has proved to be very useful in the characterisation of foods with this type of behaviour, as it allows to characterise and compare them on the basis of only two parameters with physical meaning[306].

The rheological behaviour of polysaccharide-based gels can be tuned by controlling their processing conditions, and their strength will increase with polymer concentration[243]. Indeed, analogous to the overlap concentration, C*,

described for entangled polymer solutions, there is also a critical gelling concentration, C_0, below which the gel will not form under typical conditions, being this concentration characteristic of each polysaccharide[240].

2.2.1.2.1. Carrageenan

Carrageenans are a family of polysaccharides extracted from red algae, with no nutritional value but with a variety of functional properties that make them widely used in the food industry (especially in the manufacture of dairy products). They are also finding some applications in the fields of dysphagia-oriented foods[304,307] and dosage forms[308,309].

There are three basic types of carrageenan: kappa, iota and lambda (FIGURE 23), which can be obtained in a relatively pure form or being part of a mixture of carrageenans[310].

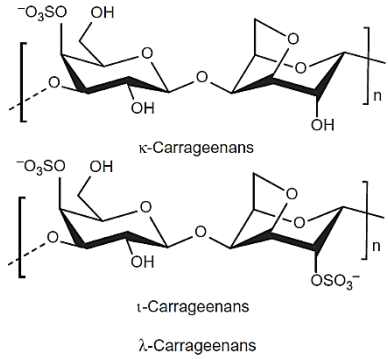

FIGURE 23. Repeating units in carrageenans[310]

However, only κ and ι-types have gelling properties, as can be seen in TABLE 3.

TABLE 3. Some key properties of carrageenans [307,310]

Property	κ-Types	ι-Types	λ-Types
Solubility			
In hot water	Soluble above 60°C	Soluble above 60°C	Soluble
In cold water	Na^+ salt soluble. Limited swelling of K^+, Ca^{2+} salts	Na^+ salt soluble. Ca^{2+} salt gives thixotropic swollen particles	Soluble

Gelation			
Effects of cations on	Strongest gels with K^+	Strongest gels with Ca^{2+}	Nongelling
Types of gel formed	Firm, brittle	Soft, elastic	Nongelling. Viscous solutions formed

The different types of carrageenans, either individually or mixed, combined with different contents and species of cations under specific conditions, give rise to a wide spectrum of textures, making them of proven utility in the stabilisation, thickening and gelling of food systems[307,311].

Carrageenan gelation is the result of the transition from coil (disordered) to a double helix (ordered) conformation[312]. When a carrageenan dispersion is heated up to a temperature that exceeds 40-60 °C, it begins to hydrate, producing an increase in viscosity due to the greater resistance of the swollen particles to flow[311] (FIGURE 24).

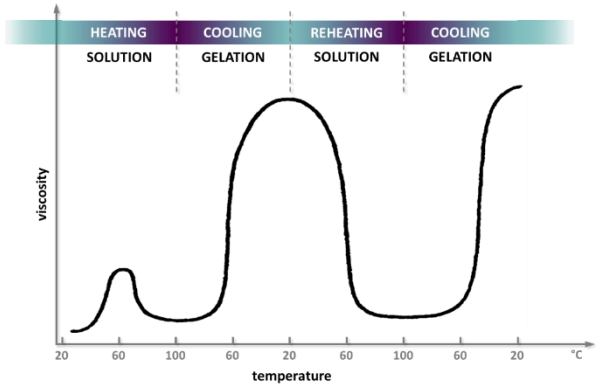

FIGURE 24. Schematic representation of changes in viscosity with temperature for carrageenan gelling solutions

All carrageenans hydrate at high temperatures, and kappa and iota carrageenans exhibit a low fluid viscosity when the solution is further heated up to 75-80 °C[307]. Subsequent cooling of this solution will cause the random coils (FIGURE 25A) of the carrageenan to adopt the double helix conformation (FIGURE 25B), first causing an increase in viscosity and, finally, the formation of a gel when the temperature drops below 40-50 °C[310]. This conformational transition is sufficient for carrageenan to exhibit an elastic response and a weak gel

rheological behaviour. Nevertheless, as happens with many other gelling biopolymers, carrageenan helices have the ability to associate in the presence of certain ions to form rigid rods (FIGURE 25C)[313].

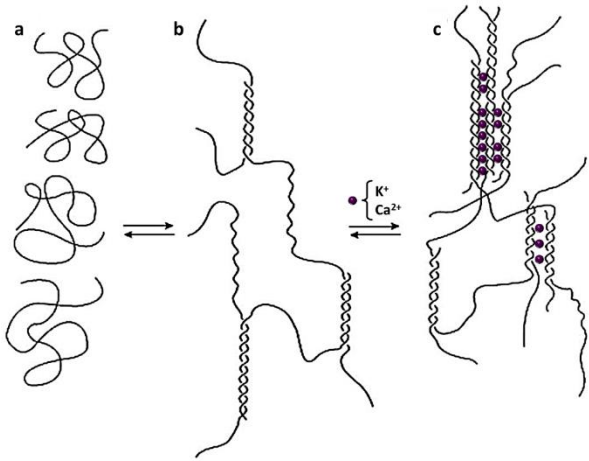

FIGURE 25. Hypothesised mechanism of gelation of κ- and ι-carrageenans (Adapted from Zhang, 2019[310])

Aggregation of carrageenan helices is promoted by the presence of these cations. Although it is not imperative for the gelation to take place, this leads to the formation of stronger gels than those obtained in non-aggregating conditions[313]. FIGURE 26 is an example of the effect of ions on the viscoelastic response of κ-carrageenan gels obtained in aggregating or non-aggregating media.

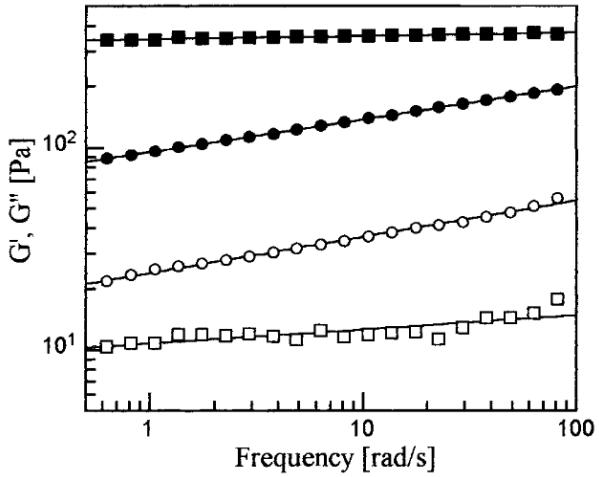

FIGURE 26. Frequency dependence of G' (filled symbols) and G" (unfilled symbols) of κ-carrageenan in aggregating (squares) and non-aggregating (circles) conditions. Aggregating conditions: 0.15% w/w κ-carrageenan in 0.2 mol/dm³ KCl. Non-aggregating conditions: 1.5% w/w κ-carrageenan in 0.2 mol/dm³ NaI[313]

In FIGURE 26, it can be seen how the gel obtained in the presence of K^+ show linear viscoelastic moduli that can be assumed to be independent of frequency and can therefore be considered a strong gel. The iodide ion, on the other hand, prevents the aggregation of the helices[313], giving rise to a gel in which the viscoelastic functions do show a certain dependence on frequency. That is, it is a weak gel. This difference in behaviour is even more significant given that the concentration of carrageenan is ten times higher in the case of the gel obtained in the non-aggregating medium than in that prepared in the presence of the gelling-promoting potassium ion. The important role of cations in the gelification of carrageenan is well known. In fact, in one of their works, Piculell et al.[314] even constructed a schematic 'state diagram', in which they represent the conditions required to obtain strong or weak gels, depending on the concentration of carrageenan and a specific mixture of salts (FIGURE 27).

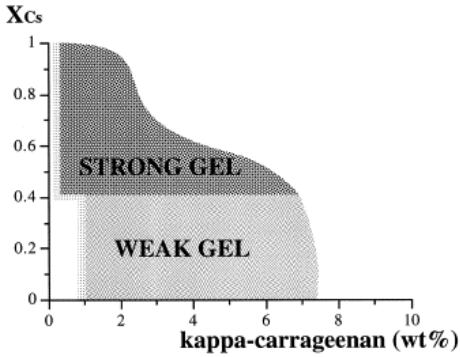

FIGURE 27. Schematic `state diagram' showing states displayed by κ-carrageenan in 0.1 M mixed salt solutions of NaI and CsI[314]

Based on this scheme, we can see that the presence of ions can be even more decisive for the rheology of the gel than the concentration of carrageenan. In fact, the gelling temperature is also strongly influenced by the ion content, so that it may be the cause of the gel forming or not under certain thermal conditions. FIGURE 28 shows the wide range of gelling temperatures of a carrageenan as a function of KCl concentration, as well as its hysteresis (the difference between the gelling temperature when cooling a hot solution and the melting temperature of the gel), which also increases with the ionic content.

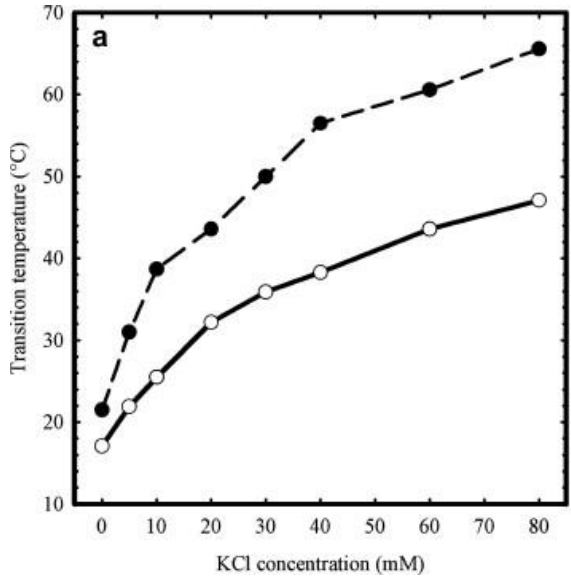

FIGURE 28. Gelling (white points) and melting (black points) temperatures of 0.5% κ-carrageenan as a function of KCl content[315]

2.3. 3D PRINTING IN DYSPHAGIA MANAGEMENT

'3D printing' is a term that comprises several manufacturing techniques with a common denominator: the creation of objects by the progressive addition of material, layer by layer or bit by bit[316]. In fact, 'additive manufacturing' is the formal name for these techniques, differentiating them from subtractive-based ones, such as turning or drilling, and formative techniques based on pressure and/or temperature moulding, such as injection moulding, casting, stamping or forging[317]. Since its first steps around 1980[316], additive manufacturing (AM) has been growing with the emergence of new technologies, printable materials and applications, to become what has come to be seen as the third industrial revolution[318] and the key to a change in current production models[319].

One of the strongest points of 3D printing is the possibility of creating objects from a three-dimensional computer model, without the need to plan and implement a complex and costly manufacturing process. In fact, the first name this technology received was 'Rapid Prototyping' and, although today it has

become much more than that, it is clear that the versatility of this form of manufacturing makes it a very powerful tool in innovation and the development of new products[317,320]. Moreover, these advantages are not only useful at an industrial level. The RepRap project and the 'maker movement' have made 3D printing an affordable technology for researchers and individual users, who share ideas and information in what has become a large global R&D community[316,321].

Today, 3D printing finds applications in fields as diverse as mechanical engineering and has even appeared as a maybe unexpected ally in the fight against the COVID-19 pandemic[322,323]. This chapter will review some basic principles of 3D printing, as well as the current and possible future contributions of this powerful technology to the field of dysphagia management.

2.3.1. Basics of additive manufacturing

The process of converting a digital model into a real object by means of additive manufacturing (AM) involves a series of steps that are usually common to all techniques and applications, as shown in FIGURE 29.

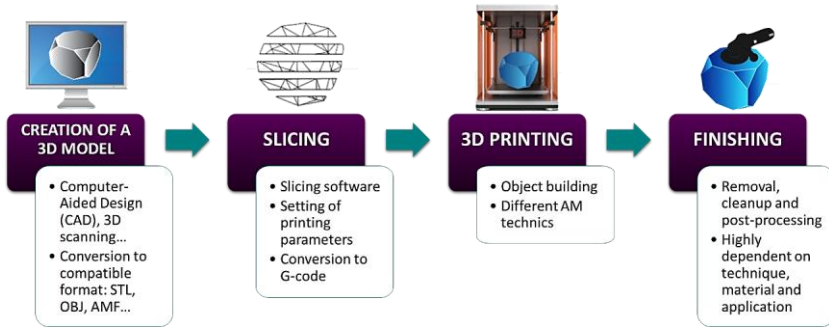

FIGURE 29. Generalised additive manufacturing workflow (Images from Deloitte.com[324])

The first step in this process is the creation of the digital model, which is usually carried out via computer-aided design (CAD) software, although it can also be obtained by other means, such as 3D scanning. The CAD model must then be converted to STL format (AMF, OBJ or 3DP are other possibilities, although STL is by far the most common, and can be considered almost a standard), a type of file that describes the object only in geometric terms, simplifying the usually more complex CAD model. The next step would be slicing the object. Previously, 3D printing was defined as a way of creating objects layer by layer. In fact, the

lamination software digitally divides the original STL model into those layers, defining the coordinates to be followed by the print head to print each layer. It also allows to make minor modifications to the object and to define its position, as well as to configure the printing parameters. The lamination software converts all this information into a G-code file that the 3D printer is now able to 'understand'. At this point, it is time to move on to what has become the 3D printing process itself, which, as will be seen below, can greatly vary depending on the additive manufacturing technique chosen. This, together with other factors, such as the printing material and the purpose to which the object is dedicated, will greatly determine how the removal of the object, its cleaning and post-processing will be carried out, as these procedures, which may be trivial or even unnecessary in some cases, can become very complicated in others[317,325].

As mentioned above, additive manufacturing comprises different manufacturing processes and techniques. **FIGURE 30** summarises those that could be considered 'conventional', although it is not easy to distinguish what is conventional from what is not in a field such as this, which is relatively young and constantly innovating.

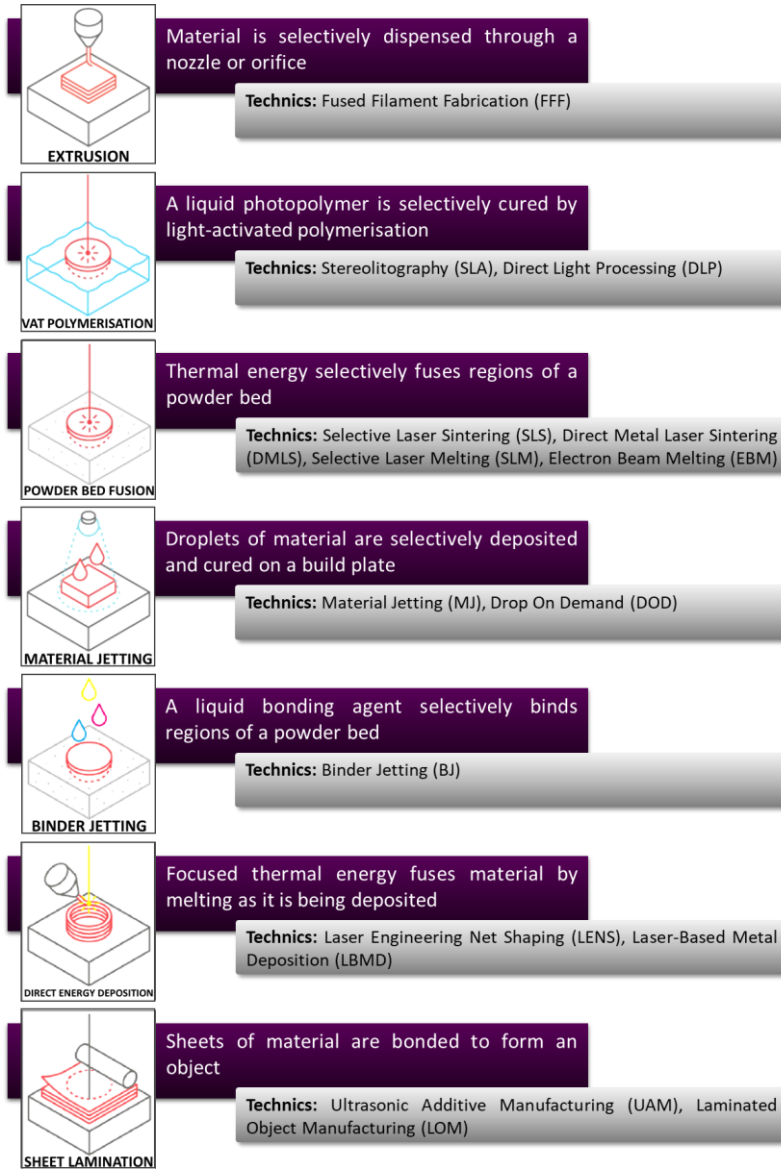

FIGURE 30. Additive manufacturing processes and technics (Adapted from Redwood, 2017[317])

Today, energy-based technologies (SLA, SLS, DLM…) are probably the most widespread on an industrial level, due to the good dimensional accuracy and surface finish of parts printed in this way, which can more closely resemble injection moulded parts. However, material extrusion-based techniques are the most popular among private users and researchers, mainly because of their enormous adaptation possibilities, which make them compatible with countless applications[316,317,322].

Fused Filament Fabrication (FFF) is the leading exponent of 3D printing technologies based on extrusion. It was the first of these to be developed —in 1989, by Stratasys, under the trade name of Fused Deposition Modeling (FDM)[316]— and can be considered the basis of all the extrusion-based techniques that have been developed since then, with which it shares key elements and parameters[326]:

1. Material feeding, either from a limited amount of preloaded material or from continuous feeding.
2. Liquification, if necessary. The material must be in a liquid or semisolid state to be extruded.
3. Extrusion. The material is moved through a nozzle of a certain shape and size by the action of pressure, being assimilable to conventional polymer extrusion processes.
4. Positional control of the extrusion head for plotting according to a predefined path and in a controlled manner.
5. Solidification and bonding of new material to adjacent regions that had been previously deposited[326].

Given this common process, it is not surprising that most extrusion-based 3D printing machines consist of many of the same fundamental parts. **FIGURE 31** shows these parts for an FFF 3D printer.

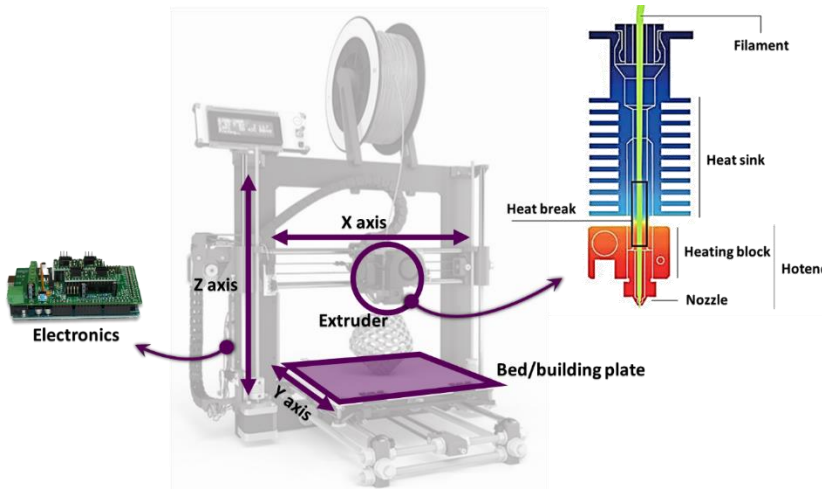

FIGURE 31. Main parts of a cartesian FFF 3D printer (Images from RepRap.org[327] and filament2print.com[328])

As previously pointed, same applies to printing parameters. In any 3D printing process, there are hundreds of modifiable parameters that will affect the result to a greater or lesser extent, although some will become more relevant than others depending on the specific configuration of the 3D printer, the characteristics of the printing material, and the requirements of the final print. A description of some of the most critical factors in most extrusion-based 3D printing techniques[329] is given below:

- Printing temperature. It is the temperature of the hotend while printing. It must be selected according to the printing material.
- Printing speed. This is the linear motion speed of the print head. It can be defined and configured independently for different parts of the object (e.g. surface or infill) and also for non-extruding displacements (travel speed).
- Extrusion rate. It is the volumetric flow of deposited material and depends directly on the printing speed and other parameters, such as the layer height or the nozzle diameter. It is normally calculated automatically based on these factors and not determined by the operator.

- Layer height. It is the 'thickness' of each of the layers that are deposited to create the object. It can also be seen as the increase in the Z-axis of the nozzle position between two consecutive layers.
- Nozzle diameter. This is the diameter of the hole through which the material is extruded. Most 3D printing systems have interchangeable nozzles of different diameters. Increasing the diameter of the nozzle reduces the printing time, but also the ability to print small details.
- Cooling. 3D printers can, and usually do, have a fan attached to the print head, which may or may not be activated (also adjustable) depending on the characteristics of the material and the geometry of the object. It may not be considered as a printing parameter itself, but it can certainly be a key factor for the final result.

Broadly speaking, it can be considered that temperature, speed and cooling determine the consistency of the extruded material, while the layer height and the nozzle diameter define the resolution of a printed FFF part[317].

2.3.2. 3D food printing: personalised products for specific population groups

The food sector, like so many others, has not remained indifferent to the great explosion of 3D printing. However, the particularities of the food sector mean that not all additive manufacturing techniques are compatible with these applications. **TABLE 4** summarises general features of different 3D food printing (3DFP) techniques, comparing the strengths, limitations and applicability of each[330].

TABLE 4. Comparison of different 3DFP technologies[330]

		Extrusion-Based	Selective Laser Sintering	Binder Jetting	Inkjet Printing
Available material		Chocolate, soft material such as dough, cheese, meat puree	Powdered materials such as sugar, chocolate, fat	Liquid binder and powdered materials such as starch, sugar, protein	Low-viscosity material such as pizza sauce
Factors affecting printing precision	**Material properties**	Rheological properties, mechanical strength, T_g	Melting temperature, flowability, particle size, wettability, T_g	Flowability, particle size, wettability and binder's viscosity and surface tension	Compatibility, ink rheological properties, surface properties
	Processing factors	Printing height, nozzle diameter, printing rate, nozzle movement rate	Laser types, laser power, laser energy density, scanning speed, laser spot diameter, laser thickness	Head types, printing rate, nozzle diameter, layer thickness	Temperature, printing rate, nozzle diameter, printing height
	Post-processing	Additive, recipe control	Removal of excess parts	Heating, baking, surface coating, removal of excess parts	No
Advantages		More material choices, simple device	Complex 3D food fabrication, varying textures	Complex 3D food fabrication, full colour potential, varying flavours and textures	More material choices, better printing quality, fast fabrication
Limitations		Incapable of fabricating complex food designs, difficult to hold 3D structures in postprocessing	Limited materials, less nutritious products	Limited material, less nutritious products	Simple food design, only for surface filling or image decoration
Products					

The selection of the 3DFP technique will be determined primarily by the material to be printed, so the versatility of extrusion-based techniques is undoubtedly one of the main reasons why these are the most popular in food printing[322].

The most basic requirement for a material to be able to be printed by extrusion is that it must be in a fluid/semisolid state or that it can become so, for example, through changes in temperature. In this respect, different branches or subcategories can be distinguished within the extrusion-based 3DFP: non-phase-change extrusion, melting extrusion and gel-forming extrusion.[331].

Non-phase-change extrusion is carried out without temperature control and is applied to pastes and doughs, whose printability depends solely on their rheological properties[332]. Melting extrusion, on the other hand, would be the most similar variant to a conventional non-food FFF process, in which the material is melted for deposition and hardened when cooled, although it is usually found in paste or powder form and it is very rare to find food material filaments. Chocolate is the best example of this type of 3DFP, and there are even commercial machines that offer the possibility of producing figures with complex geometries from this material[330,331,333,334]. In gel-forming extrusion, gelling can occur by different mechanisms. Unlike non-phase-change extrusion, in both melting extrusion and temperature-driven gel-forming processes, time-related factors (flow, printing speed...) and, more specifically, the relationship between these and thermal parameters (printing temperature, cooling of the deposited material...) take on special importance, as a too slow hardening would cause the material to flow long after it has been deposited, to the detriment of shape fidelity. In contrast, in processes based on gel formation by mixing components (see chemical cross-linking, ionotropic cross-linking, complex coacervate formation and enzymatic cross-linking in **FIGURE 32**), the opposite scenario is particularly problematic, since a premature hardening of the material inside the printer will result in clogging and potential printing failure[331,334,335].

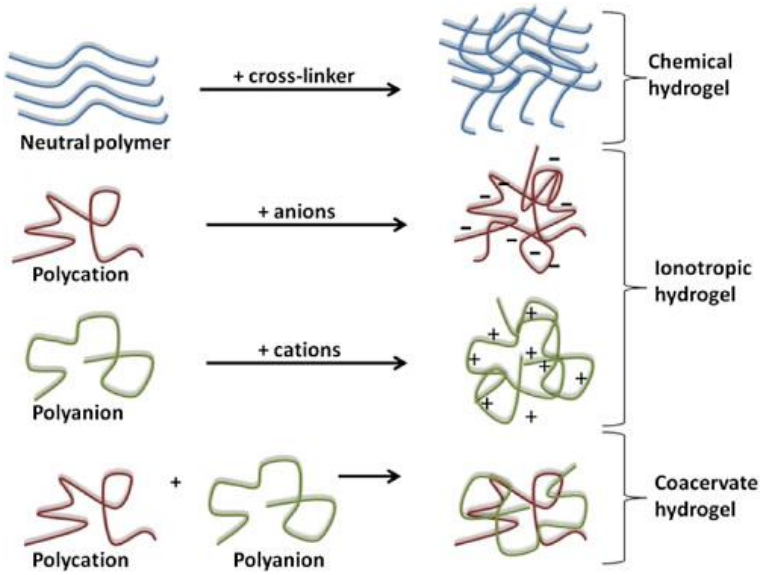

FIGURE 32. Schematic representation of hydrogel-forming mechanisms[334]

All these techniques, and the innovative alternatives that continue to emerge, make the variety of printable foods grow every day and, with it, the applications of 3D food printing. And it is precisely in this context that several authors raise the question of whether the use of 3D printing is really justified in all these applications. Lipton[336] finds two main reasons for customising food using 3D printing: health and preference. As well as its many advantages, this technology also has its drawbacks in replacing conventional food processing equipment. Production times, feeding systems with limited capacities and inefficient pre- and post-processing treatments are examples of the obstacles that are still to be overcome and the establishment of 3D printers as part of users' kitchens or industries based solely on the aesthetic improvement of preparations is —although possible or even probable— still uncertain[322,336–339]. However, there are cases where the use of 3D food printing can make a difference to conventional methods, and that is in the production of healthy products focused on the needs of specific population groups. Many diseases require specific nutrition as part of their treatment or management. Allergies and intolerances, swallowing or digestive problems, Celiac Disease, Crohn's Disease, Diverticulitis or Irritable Bowel Syndrome are examples of conditions where nutrition plays a

crucial role and the possibility of customising foods could result in a significant improvement in the quality of life of patients[336]. And it is not only people with illnesses who could benefit from the advantages of the 3DFP for the production of healthy products. It could also be the way to promote children's intake of fruit and vegetables, by making foods with shapes and colours that may be more attractive to them[340,341], and both the US Navy and NASA have launched their projects for the development of 3D printing systems for the preparation of meals on demand, customised to meet the energy and nutritional needs of each individual, which can also be prepared from their components separately and thus prolong shelf life of foods in long-duration missions[330]. And even outside of specific populations, it could mean a big change in the lives of the whole community. Already today, a great deal of information is available from anyone. Purchases, location, training items and even digitalised medical records can be used to estimate an individual's nutritional needs and automatically adjust the composition of meals based on this data[336,342]. In addition, 3DFP gives the possibility to create foods with structures that reduce their fat, sugar and salt content, as well as to control their textural properties[340].

The ability to make food more palatable could also be of great help in adopting new eating habits, such as making meals from what are now food by-products, to try to meet the needs of a growing world population and to do so in a sustainable way[340].

2.3.3. How can 3DFP improve dysphagia management?

So far, it has been seen that 3DFP may have advantages over conventional forms of food processing and preparation, which could be summarised in three fundamental aspects: appearance, texture and nutritional content. But, above all, the real strength of 3D printing is the possibility of personalisation. Not only can the appearance, texture and nutritional content be varied and controlled, but it can also be done in a totally personalised way, forgetting the limitations of the products available on the market. If the reader goes back to the first section of this chapter (section 2.1: Dysphagia and its nutritional management), it is not difficult to quickly realize how related these factors are to the nutritional management of dysphagia and, consequently, the important role that the 3DFP could play in this field.

2.3.3.1. Appealing appearance

There are different approaches to improving the appearance of meals. One of them is the preparation of meals with attractive shapes and colours and artistic motifs. This is precisely what Kouzani et al. did in their work. In the first of these[343], they printed a pavlova (a meringue-based dessert) in the shape of a map of Australia which, after being baked, they also decorated with a 3D printed chocolate garnish (**FIGURE 33A**). In a later work[344], Kouzani himself and his collaborators designed and printed a meal in the shape of a tuna fish by multi-material 3D printing (**FIGURE 33B**). They used purées of different colours (pumpkin, beet and tuna), cooked before being printed thanks to a piston-type system, without the need for additives to improve their printability. While this is a common strategy at 3DFP to create more eye-catching products that attract the attention of the general public, there is another one that could perhaps be more interesting for the production of meals suitable for dysphagia patients, and that is to try to make products that resemble conventional food as much as possible, such as the steak in **FIGURE 33C**, with textural properties that ensure its safe consumption by people with chewing and/or swallowing disorders[345].

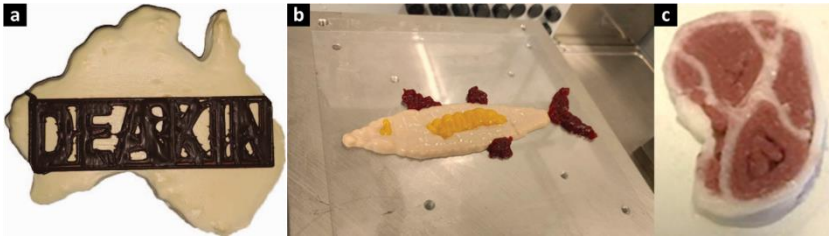

FIGURE 33. 3D printed meals with improved appearance for dysphagia patients (Images from (a) Kouzani, 2016[343]; (b) Kouzani, 2017[344]; (c) Dick, 2019[345])

As seen above, amorphous indistinguishable texture-modified meals not only make patients weary, but in many cases also cause them embarrassment when sharing a table with others, which can eventually lead to isolation[229]. 3D-printed dysphagia-oriented products could not only be more appealing to patients but also help them keep mealtimes as a social event. If the impact of modified diets on quality of life is minimised, it can be expected that the tendency for patients to reduce their food intake and discontinue treatments will also be reduced. Although studies on the influence of the appearance of food on the intake of patients with dysphagia are scarce, and even more so in the case of 3D printed

meals[231,346], the few available results are positive and it seems logical to think that they will be even more so when the technology advances enough to create truly 'realistic' 3D printed meals. 3D printed cultured meat represents a promising option in this regard, although it is a technology that is still in development and has yet to overcome several challenges, such as increased production capacity and cost reduction or the perception of unnaturalness by consumers[347].

2.3.3.2. Tailored textural properties

This is, of course, the main requirement that the 3DFP must meet in order to be a useful tool in the nutritional management of dysphagia. 3D printing of texture-controlled food products is one of the most frequently cited applications of 3DFP in the literature. However, not many studies address this aspect. Papers focused on rheological characterisation are, in many cases, more concerned about improving the printability of the material than about controlling its final properties[335,348–350]. Some 3D printed food products have been obtained with textural properties suitable for dysphagia-oriented nutrition[351–355]. Most of them contain hydrocolloids, either as a main component or as an additive to meat or vegetable pastes, to improve printability and/or their final texture, and the components are mixed —and cooked, if necessary— before being loaded into the 3D printer. This has the disadvantage of greatly limiting the automation possibilities offered by the 3DFP. Ideally, both formulation and the processing (the printing parameters in this case), should serve as a way for tuning the final properties of the printed products, so that different and customised consistencies can be obtained from the same starting ingredients. This would facilitate the preparation of these products by non-specialists, such as the patients themselves and their families, for whom this may sometimes not be an easy task [356], and would also reduce the chances of human error leading to the dispensing of food with inappropriate textures and bring closer the scenario where the patient, or their relatives, only have to 'push a button' to get food with the right texture.

2.3.3.3. Nutrient fortification

Despite being one of the main objectives of the 3DFP for dysphagia-oriented products, no work has been carried out, to our knowledge, in which these foods have been obtained specifically on the basis of their nutritional content or have

been nutritionally fortified. However, references can be found where 3D printing is used in the manufacture of drug dosage forms suitable for dysphagic patients, enabling the elaboration of customised formulations by frontline medical care members [357]. As a previous step to the automatic control of the nutritional content of foods for dysphagia, Farha et al.[342] have developed a software whose function is to estimate the nutritional needs of patients from data such as age, gender, physical constitution and hospital records.

2.3.3.4. Challenges in 3D printing of dysphagia-oriented products

Many hopes are placed on 3DFP as a way of obtaining food that is appealing to the eye and taste, with controlled textures and the ability to encapsulate additional nutrients or drugs, all in an automatic and totally personalised way[331,358]. However, this is a technology that, despite having attracted a lot of interest and experienced a rapid growth, still has much to improve in order to make the most of its potential. On the one hand, although it has already been possible to print meals that may be considered more attractive than conventional modified diets, there is still a need for much improvement in obtaining realistic-looking foods that truly resemble the originals and can offer a greater sense of 'normality' to patients. The variety of printable foods must also be widened and each of them deeply studied, in order to establish the relationships between printing parameters and the resulting rheological properties, so that different textures can be obtained from each formulation. These formulations should also be able to be prepared from their components separately, automatically mixing them in their correct proportions, allowing the preparation of more complex recipes or the incorporation of additional nutrients or drugs when necessary.

All this involves a great deal of multidisciplinary research and development work, in which specialists from very different fields will have to participate, but which could lead to a real change in the way dysphagia is managed nutritionally and also in our eating habits in general.

MATERIALS AND METHODS

CHAPTER 3
Materials and methods

3.1. MATERIALS

3.1.1. Raw materials

3.1.1.1. Carrageenan

κ-carrageenan (M_W 193 - 324 kDa, K ≤ 110 mg/g, Ca ≤ 35 mg/g, Na ≤ 20 mg/g, moisture ≤ 120 mg/g) was used as received from Sigma-Aldrich (Germany). Water used to prepare κ-carrageenan dispersions was directly taken from the Huelva water supply network, with an average content of cations Ca 15.7±2 mg/L, Mg 10.5±1.4 mg/L, Na 29.9±3.6 mg/L, K < 2 mg/L [359,360]. The content and proportions of cations have not been modified during the study to avoid interferences with the effects caused by the variation of the printing parameters.

3.1.1.2. Fresubin® Clear Thickener

The commercial powder thickener used in this work is Fresubin Clear Thickener® (FCT, see **FIGURE 34**), which was kindly provided by Fresenius Kabi Deutschland GmbH and used as received to be fed into the hopper of the MIX3D accessory for subsequent mixing with distilled water or alternative solvents.

FIGURE 34. Fresubin® Clear Thickener[361]

Orange juice with no added sugar (Juver SA, Spain) and skimmed milk (Covap, Spain), purchased in a local store, were used as alternative solvents.

3.1.2. Building materials

Commercial PLA filaments (BQ, Spain) have been used to 3D print the hopper and the casing of the mixing chamber. The conveyor screw has been printed in ABS (LEON3D, Spain), with a better thermal resistance than PLA, aiming to avoid deformations caused by the heat from the motor.

Non-printable parts, such as motors or screw, are standard components that can be purchased from commercial vendors.

3.1.3. 3D printers

3.1.3.1. Modified 3D printer

A BQ Hephestos 3D printer (FIGURE 35), with Marlin firmware, designed by BQ, was used for this study once previously adapted and submitted to modifications to print non-conventional materials.

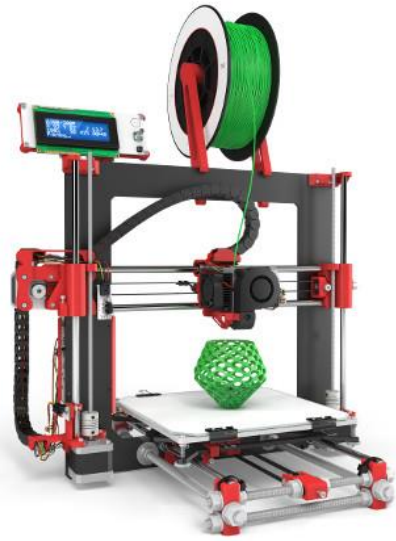

FIGURE 35. BQ Hephestos 3D printer[362]

A more comprehensive description of the modifications carried out for each part of the study can be found in the corresponding sections of Chapter 4: Results and discussion.

The BQ Hephestos 3D printer DIY kit designed by BQ (Spain) and the electronics (Arduino Mega 2560 and RAMPS 1.4 shield) were purchased from Ícarus Informática (Spain). All the additional components needed for its adaptation were supplied by 3DEspaña (Spain).

3.1.3.2. 3D printers used for fabrication of printable parts

3.1.3.2.1. BQ Hephestos

Another BQ Hephestos —unmodified, but equipped with a heated bed— was used to print most of the printable parts.

3.1.3.2.2. P3Steel

A P3Steel with dual extruder (HTA3D, Spain), as the one shown in FIGURE 36, was used to print the conveyor screw of the mixing device for thickened fluids.

FIGURE 36. P3Steel 3D printer[363]

Parts with overhanging areas require the use of supports for printing. These supports are structures that are printed at the same time as the part and serve to build up over them the overhanging areas of the model. The supports have to be removed from the part after the printing has been completed, but this can be a complicated task depending on the geometry, as is the case with the conveyor screw. The dual extruder allows to print the supports on a different material than that of the part and to remove them by dipping the print in a selective solvent.

In this case, the conveyor screw was printed on ABS and the supports on HIPS, which can be dissolved using limonene as a solvent without affecting the integrity of the ABS.

3.1.3.3. Software

The different shapes and models printed during this study, as well as all accessories required to modify the printer, were designed using AutoCAD 2018 software and Tinkercad online app. The slicing of the 3D models, necessary to obtain the .gcode extension files with all the information the printer needs to run, was carried out with Ultimaker Cura software and control of the 3D printer during operation was made possible by Repetier Host software.

3.2. Preparation methods

3.2.1. κ-carrageenan hydrogels

κ-carrageenan hydrogels studied were prepared by 3D printing. 3D printer feeding solutions were prepared by dispersing 3 wt.% κ-carrageenan in water at room temperature under vigorous mixing (1500 rpm), for 30 min, with a magnetic stirrer. These dispersions were fed on demand to the printer through a syringe pump system and gellified in situ during the 3D printing process. Main printing variables (printing speed, hotend temperature and layer height) were modified according to the experimental design described in section 4.1.2 (Experimental design and statistical analysis). Carrageenan gel discs of 50 mm diameter and 1 mm height were printed for rheological characterization.

In addition, a reference hydrogel sample was prepared from the same 3 wt.% carrageenan dispersion employed to feed the printer, using a conventional

protocol [364,365]. The carrageenan dispersion was heated by means of a heating plate at 80 °C for 2 h in a closed vessel, under vigorous stirring (1500 rpm) and then cooled down to room temperature by natural convection.

3.2.2. Thickened fluids

Thickener in powder form and solvent are directly fed into the mixing device. The desired texture or viscosity of thickened fluids is predefined by the respective amounts of solid thickener and aqueous liquid used in the mixture, i.e. the ratio between solid thickener and liquid. By mixing a liquid with a suitable solid thickener, thin liquids with a viscosity value of 1-50 mPa·s, nectar-like mixtures with a viscosity value between 51-350 mPa·s, honey-like mixtures with a viscosity value of 351-1750 mPa·s and spoon-thick mixtures with a viscosity value >1751 mPa·s can be provided. In compliance with the classification established by the National Dysphagia Diet Task Force, these values relate to a shear rate of 50 s^{-1} and a temperature of 25°C.

The hand-prepared systems were obtained by quickly adding the solvent over the appropriate amount of thickener, carefully stirring for 20 seconds and allowing to rest for 1 minute before characterisation, following the instructions provided on the package by the manufacturer.

3.3. Characterisation methods

3.3.1. Rheological characterisation

Rheological characterisation of gel samples was carried out with a controlled stress rheometer (Physica MCR-301, Anton Paar, Austria). Small-amplitude oscillatory shear (SAOS) tests were performed inside the linear viscoelastic region, using a plate-plate geometry (25 mm diameter, 1 mm gap) in a frequency range of 0.03-100 rad/s, at 25 °C.

Rheological characterisation of thickened fluids was also carried out with Physica MCR-301 rheometer. Viscous flow measurements were performed within a range of shear rates of 0.01–100 s^{-1} at 25 °C using a 50 mm serrated plate geometry and a gap of 1 mm.

3.3.2. Evaluation of thickener concentration

The actual solid content of each sample was gravimetrically quantified. To this end, each sample was weighed before being placed in a Selecta Digitronic convection oven (Selecta SA, Spain), dried overnight at 90 °C, and weighed again the day after.

Results and discussion

CHAPTER 4
Results and discussion

4.1. 3D PRINTING OF K-CARRAGEENAN HYDROGELS

The following subsection has been published in a form of research article to Food Hydrocolloids (see Annexes).

4.1.1. Introduction

3D printing is becoming a more important part of our lives every day, apart from already being used industrially, due to the wide variety of possibilities that it can deliver, especially in the development of customised and innovative products. There are several technologies that can be included in the category of 3D printing or additive manufacturing. However, those based on fused filament fabrication are probably the most extended, being suitable for a huge range of applications and materials [366–368]. Additive manufacturing refers to the process of building a 3D object by adding layer-upon-layer materials, such as plastic, metal, concrete…, or any material capable of forming stable self-supporting structures. The simplicity of this process is what makes it so versatile, since it does not need the use of materials with special reactive properties and/or initiators. In this context, many industries are focusing their interest on adapting 3D printing technology to the specific needs of each sector. Among many other fields, food processing, gastronomy and cooking are showing growing interest in 3D printing technologies (Lipton, Cutler, Nigl, Cohen, & Lipson, 2015; Pallottino et al., 2016; Sun et al., 2015; Sun, Zhou, Huang, Fuh, & Hong, 2015; Sun, Zhou, Yan, Huang, & Lin, 2018). In one hand, it can be used in food industry for the development of new products [334,337]. Moreover, it could also be the next cooking utensil present in our kitchens, as blenders or toasters are nowadays [371]. Beyond this, 3D printing can become an useful tool for pharmaceutical and clinical nutrition industries, since it could be a way to process fully customisable products, according to the needs of each specific patient [358,372], e.g. in the design of personalised foods for dysphagia management. In addition, the in situ product manufacture, just before administration or use, may solve some problems related to storage of unstable or incompatible components.

In all these fields, materials with specific gel characteristics are of great importance. Particularly interesting to form hydrogels is κ-carrageenan, which is considered a representative gel forming polysaccharide, with thermoreversible gelling capacity and widely extended use in many applications, especially in the food, pharmaceutical and cosmetic industries [313,365]. As well-known, κ-carrageenan is a sulphated polysaccharide extracted from different species of red seaweed [373], which needs to be heated and then cooled to gelify, what is known as "cold-setting" [374]. It is well accepted the two-step gelation mechanism involving the formation of helical dimers first, as proposed by Rochas and Rinaudo [375], followed by the aggregation of double helices [312,376]. In this aggregation process, the molecular chains extend and associate to other molecules favouring the formation of a three-dimensional network composed of double-helical aggregates as the junctions and flexible chains connecting the junctions [364,376]. To induce the gelation of κ-carrageenan in water, the temperature must be increased, yielding the hydration and swelling of particles in a range of between 40 and 60 °C, which causes an increase in its viscosity. Afterwards, between 70 and 80 °C, a further drop in viscosity occurs, due to the carrageenan molecules being organised in randomly arranged coils [311]. Typical procedures to prepare κ-carrageenan gels deal with heating at 70-90 °C under stirring for 30 min to 2h [313,364,373]. When the solution is cooled down, these coils are structured giving rise to the formation of the gel network [311,313]. Then, a thermal hysteresis is apparent in subsequent heating and cooling cycles above a critical concentration [373], being the melting temperature higher than the gelling temperature. However, as well known, this κ-carragenan gelification process is highly dependent on the salt concentration and the nature of the cations [377–379]. The need for all these thermal steps to take place in order to produce gelification complicates the use of continuous processes, as is the case of 3D printing. In addition, the specific conditions under which gelling takes place can lead to structures with different properties [380,381]. In this sense, rheology is presented as a powerful tool to assess the gel characteristics and final performance as a gel matrix in more complex formulations [364]. The possibility of preparing gel matrices with tailored rheological properties using efficient, quick and facile protocols is a big challenge that can be achieved by properly adapting the 3D printing technology. For instance, in the case of κ-carrageenan gels, it is worth mentioning that the transition from random coil to double helices is extremely fast [382]. However, subsequent aggregation of double helices to

complete the formation of a gel three dimensional network may take up to 15 h [383].

Up to now, the application of 3D printing in gel food processing has been mainly limited to extrude with sophisticated shapes previously gellified systems [384–387] or, in the best cases, a viscoelastic dispersion or solution [388]. Only a few works on 3D printing-induced gelation, i.e. the so-called 3D gel printing, have been reported for non-food systems [389] and most of them required a catalyst or initiator [368]. It is apparent that 3D printing-induced gelation could also have a relevant application for designing alternative, alpha-amylase-resistant, customised "fresh" pudding-like products for nutritional support of dysphagia patients (Gallegos, Brito-de la Fuente, Clavé, Costa, & Assegehegn, 2017; Turcanu et al., 2018).

Taking into account these considerations, the aim of this study was to take advantage of the potential and versatility of the 3D printing technology to induce the in situ gelification of κ-carrageenan aqueous solutions, subsequently studying, by means of a RSM experimental design, the influence of the main 3D printing variables on the rheological properties of the gel matrices obtained.

4.1.2. Experimental design and statistical analysis

The main printing parameters that have been considered throughout this study are the hotend temperature (T), printing speed (S) and layer height (H). The temperature of the hotend is the temperature of the heating block, which can be set to the desired value and measured continuously; the printing speed is the speed corresponding to the displacement movement of the hotend during the deposition of the material; and the layer height is the thickness of each of these deposited layers. In order to determine the effect of these printing parameters (printing speed, hotend temperature and layer height) and the interactions between them on the rheological response of the carrageenan gels, with the minimum possible number of experiments, a response surface methodology (RSM) experimental design was applied. In particular, a Box-Wilson three factors circumscribed central composite design (CCC) at 5 levels of each factor, with an α-value of ±1.682. Several replicates of the central point of the cube were carried out, with additional experiments lying at the cube vertices and side centres, originating 20 different case studies, which were rheologically characterized.

This experimental design enables the construction of second-order polynomials in the independent variables, as shown below:

$$Y = a + a_1x_1 + a_2x_2 + a_3x_3 + a_{12}x_1x_2 + a_{13}x_1x_3 + a_{23}x_2x_3 + a_{11}{x_1}^2 + a_{22}{x_2}^2 + a_{33}{x_3}^2 \quad (2)$$

Being Y the dependent variable, x_i the normalised values of the independent variables and a_{ij} the constants obtained from regression analysis.

In this way, a regression analysis was carried out on selected rheological parameters (see eq. 5 parameters defined below) as dependent variables and the printing parameters (printing speed, hotend temperature and layer height) as independent variables. Those variables whose significance level exceeds 0.05 in Student's *t* test were excluded from the analysis and the resulting polynomials.

The normalisation of the values of each variable, necessary to be able to compare its influence, was carried out by means of the following equation:

$$X_N = \frac{2\cdot(X - X_{med})}{(X_{max} - X_{min})} \quad (3)$$

Where X_N is the normalised value of the variable, X is its real value, X_{med} is the average value of the variable and X_{max} and X_{min} are the upper and lower limits, respectively, of the range considered for each variable. The range of each variable studied and their normalised values are detailed in TABLE 5.

TABLE 5. Independent variables studied and their normalised values used in the experimental design

Printing speed [mm/s]	Hotend temperature [°C]	Layer height [mm]	Normalised value
10.0	50	0.06	-1.682
20.1	62	0.11	-1
35.0	80	0.18	0
49.9	98	0.25	1
60.0	110	0.30	1.682

4.1.3. 3D printer setup

Nowadays, there are many different models of 3D printers available, fully assembled and ready to use, which are marketed by different companies. However, most of them do not allow to either handle fluid feed or to introduce

modifications to do it. Moreover, for the moment, their prices can be excessive for private consumers and small businesses or institutions. An alternative that is leading to what may be considered a new industrial revolution is the RepRap 3D printing technology. The RepRap (replicating rapid prototype) project is an initiative dedicated to designing and developing low-cost 3D printers. RepRap 3D printers are based on open-source hardware and software, which are able to print most of their own components, so they can self-replicate and repair themselves, making them freely available for everyone [321]. Their design, assembly and operating instructions can be found accessible and fully detailed on the web, as well as their firmware code. Thus, their tuning possibilities are almost unlimited. In fact, RepRap community is now made up of hundreds of collaborators, leading to a continuous open-source research and development activity. Therefore, RepRap appears as a technically and economically viable form of additive layer manufacturing of polymer-based products [390]. Moreover, it has the potential to have a lower environmental impact than conventional manufacturing for a variety of products [390,391].

The aim of this work was to go a step forward using a RepRap 3D printer instead of fully assembled commercial printers, in order to achieve gel structures through direct sol–gel transition, i.e. the in situ gelification. This requires the addition and/or replacement of some components of the original printer setup. The proposed self-adapted setup consists of a syringe pump that, through a polytetrafluoroethylene (PTFE) tube, feeds a watertight hotend that provokes the gelification of the carrageenan solution by temperature. Since feeding syringe is not attached to the printing head, it is possible to avoid problems associated with excessive inertia during movement, resulting in higher printing accuracy. A picture and a schematic depiction of this setup can be seen in FIGURE 37.

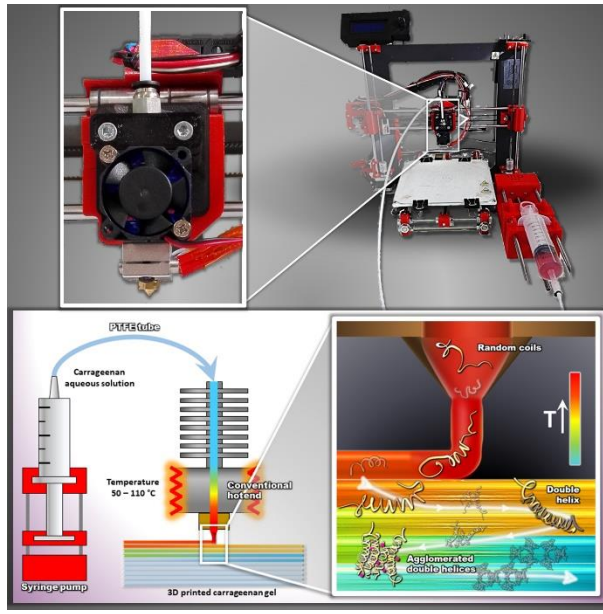

FIGURE 37. Schematic view of 3D printing setup to promote the in situ temperature-induced gelification

The syringe pump consists of a plastic structure, designed and printed with the printer itself prior to modification, metal rods as guides for its movement and a motor connected directly to the printer electronics, instead of the motor corresponding to the original extruder. This extruder, prepared to work with plastic filaments, had to be replaced by a Bowden type watertight hotend in order to handle low viscosity fluids. With these modifications, the printer operated as intended and there is no material leakage. Unfortunately, printing definition was very poor and the material flowed when deposited, so that the model was not able to gain height (FIGURE 38A). After several attempts under different printing conditions, it was concluded that there was not enough time between deposition of the different layers for cooling and structuring of the material, even when the printing speed was greatly reduced. The Bowden-type hotend does not allow to couple a standard layer fan, so there was no cooling system for the printed material apart from exposure to ambient air. Aiming to solve this drawback, a new piece was designed and printed on polylactic acid (PLA). This piece allows the layer fan of the old extruder to be adapted to the

new hotend, as well as distributing the air flow evenly thanks to a diffuser ring (see scheme in FIGURE 38B). This simple cooling system is based on ambient air at room temperature; but the mere fact of causing forced convection is sufficient to accelerate the cooling of the material, allowing the gel to structure in a way that the model can gain height. These modifications resulted in the printing of carrageenan gel models with an acceptable resolution and self-sustaining capability, as shown in FIGURE 38C.

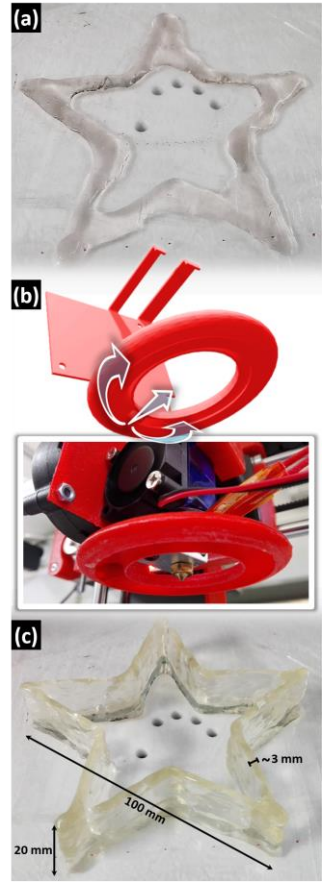

FIGURE 38. Star-shaped 3D printed κ-carrageenan gel model, (a) before and (c) after introducing the air distributor cooling ring (b)

However, the resolution in this case is limited by the nature of the material. When deposited, the material flows until it cools down sufficiently to structure itself. These is the reason why it was not possible to increase the height of the printed gels before the modification of the system with the cooling ring. In the same way, this brief flow of material means that the shapes are not preserved as faithfully as when working with other more conventional materials.

Due to these changes on the printer setup, the device had to be recalibrated, making some changes to the printer firmware for proper operation. Since the default extruder stepper motor was replaced by the one that drives the syringe pump, it was necessary to modify the value of axis steps per unit so that the feed flow was adequate for the geometry of the new feed system. From the values of printing speed, layer height and nozzle diameter (the same 0.4 mm diameter nozzle has been used for the entire study), the printer automatically adjusts the required material flow. The firmware was configured to give the correct reading of the new hotend thermocouple and the PID control constants for the new heater block were also determined.

4.1.4. Rheological behaviour

κ-carrageenan gels processed by 3D printing exhibited a qualitatively similar rheological response, characterized by a slight frequency dependence of the storage modulus (G') and a soft minimum in the evolution of the loss modulus (G''), being G' values almost one decade higher than G'' values. FIGURE 39 shows the evolution of both SAOS functions with frequency for selected 3D printed carrageenan gels.

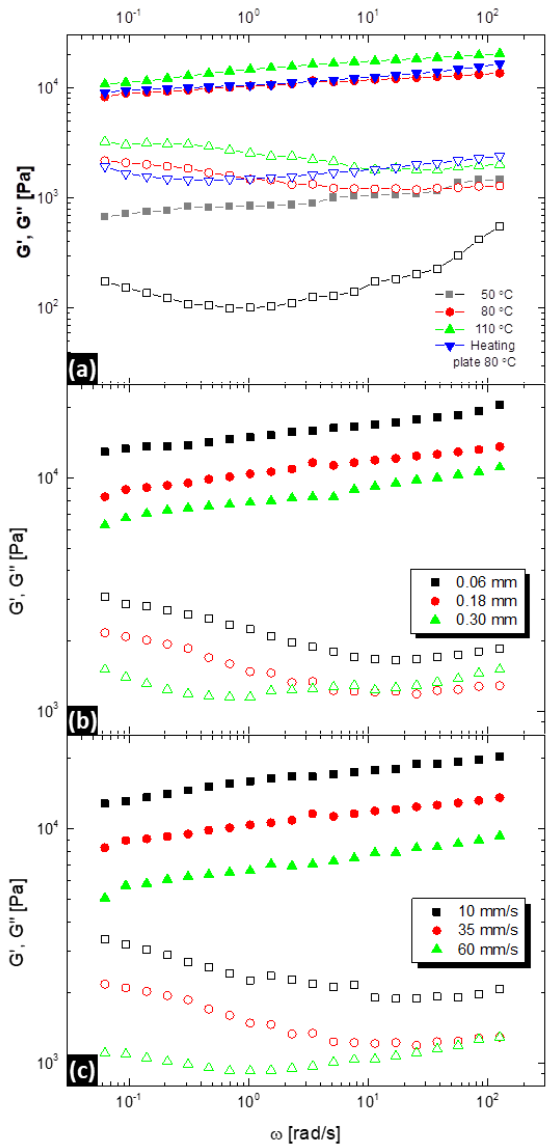

FIGURE 39. Evolution of storage (G') and loss (G") moduli with angular frequency of 3D printed and conventionally prepared κ-carrageenan gel samples, as a function of (a) temperature, (b) layer height and (c) printing speed

In particular, FIGURE 39A presents frequency sweeps of several samples, processed at the same speed (35 mm/s) and layer height (0.18 mm) but applying different temperatures at the hotend, compared with a carrageenan gel conventionally prepared at 80 °C. As can be seen, only the sample printed at 50 °C significantly differs from the others. As well known, at such a low temperature, the necessary mobility of the carrageenan coils is not reached in the solution phase and the gel network structure cannot fully develop when it was subsequently cooled. Once the temperature threshold required for the release of the coils has been exceeded, the structures obtained after gelling are quite similar to each other, even if the hotend temperature is significantly increased, i.e. 110 °C. Above this temperature threshold, both 3D printed and conventionally prepared gel samples have a similar rheological response. In fact, the linear viscoelastic functions of the carrageenan prepared in a conventional heating device, for 2 h under mixing, and those corresponding to the sample obtained by 3D printing at 80 °C are practically identical. FIGURE 39B, on the other hand, illustrates the effect of layer height at the same temperature (80 °C) and printing speed (35 mm/s), while, finally, FIGURE 39C compares the SAOS functions of printed gels at different speeds, keeping constant both hotend temperature (80 °C) and layer height (0.18 mm). As can be clearly seen, both higher layer height (H) and higher speed (S) lower the viscoelastic moduli over the entire frequency range considered.

The evolution of SAOS functions with frequency obtained in all cases show a slight decrease in G' when the frequency is reduced, due to the structural rearrangement and relaxation processes undergone by the gel network when it is subjected to a high enough stress. Moderate differences between G' and G'' values (less than one decade; in most cases, tanδ values higher than 0.1) is typically reported to be characteristic of relatively "weak gels" [392]. For all the printed gels, the loss tangent exhibited very similar values (tan δ=0.20±0.12) within the whole frequency range studied. For this reason, the complex modulus (G*), defined as:

$$|G^*|^2 = |G'|^2 + |G''|^2 \quad (4)$$

can be selected as an appropriate viscoelastic function to be modelled as a function of the 3D printing variables. G* has been fitted to a power-law model:

$$G^* = A\omega^n \quad (5)$$

where ω is the angular frequency (rad/s) and, according to the basic theory of gels, A represents the gel strength and n is a power-law relaxation exponent (Campo-Deaño & Tovar, 2009; Moresi, Bruno, & Parente, 2004; Munarin et al., 2014). In physical gelation, it has been widely reported that physical cross-links, i.e. entanglements, may change with time under the application of stress, causing an actual fluctuation in the state of gelation. For these so-called weak gels, Mita and Bholin [396] proposed that the real structure of such materials may be represented as a cooperative arrangement of flow units. In this context, the reciprocal of the above referred power law index, z=1/n, has been defined by different authors as a coordination number (Gabriele, De Cindio, & D'Antona, 2001) that assumes the meaning of the number of rheological units correlated with one other in the three dimensional structure, and applied to different gel systems (Antunes et al., 2008; Basu et al., 2011; Lupi et al., 2015). Therefore, in the present study, the coordination number could be related to the number of interacting rheological units within the 3D gel network, whilst A is a parameter associated to the strength of the interactions between them and therefore may be correlated to the bulk gel strength.

4.1.5. Response Surface modelling

TABLE 6 lists the values of fitting parameters A and z obtained for each case, as well as the normalised values of independent variables.

TABLE 6. Fitting parameters A and z obtained for each case study as a function of printing variables

Case	Normalised values of independent variables			A [Pa·s$^{1/z}$]	z	R^2
	S	T	H			
A	-1	-1	-1	13859.7	17.22	0.99
B	1	-1	-1	9719.1	17.89	0.99
C	-1	1	-1	18665.8	16.02	0.99
D	1	1	-1	12893.5	16.52	0.99
E	-1	-1	1	7444.0	13.91	0.97
F	1	-1	1	1662.3	12.11	0.95
G	-1	1	1	11754.5	15.36	0.98
H	1	1	1	7643.3	13.38	0.98
I	-1.682	0	0	15772.4	18.39	0.99
J	1.682	0	0	9593.0	15.44	0.99
K	0	-1.682	0	878.6	12.52	0.97
L	0	1.682	0	14506.7	13.28	0.99

M	0	0	-1.682	15125.7	18.19	0.99
N	0	0	1.682	7919.0	14.82	0.99
O1	0	0	0	10409.2	17.74	0.99
O2	0	0	0	9359.1	17.21	0.97
O3	0	0	0	10130.2	21.64	0.98
O4	0	0	0	11920.5	17.18	0.99
O5	0	0	0	11651.2	15.97	0.98
O6	0	0	0	11147.4	15.92	0.98

By applying the multivariate regression analysis, parameter A can be described as a function of the independent variables by means of the following equation:

$$A = 11224.0 - 1931.0 \cdot S + 3617.2 \cdot T - 2881.0 \cdot H - 1355.1 \cdot T^2 \quad (6)$$

$$(R^2 = 0.91; F = 37.33; df = 4.15)$$

This means that A linearly decreases with the printing speed (S) and layer height (H), as Fig. 3b and 3c suggest, whereas it depends quadratically on the temperature (T), in the range of printing variables studied. Moreover, good fitting results were obtained without the need to include terms of interaction among variables.

A similar dependence of the printing variables was found on parameter z, which can be modelled as follows:

$$z = 16.48 - 0.84 \cdot S + 1.11 \cdot T - 1.02 \cdot H - 1.82 \cdot T^2 \quad (7)$$

$$(R^2 = 0.93; F = 47.01; df = 4.15)$$

Since independent variables can only be associated with two of the axes of the 3D graphic (the third axis corresponds to the observed dependent variable), the response surfaces are drawn by giving values between -1.682 and +1.682 to two of the independent variables, while the third remains constant (see FIGURE 40).

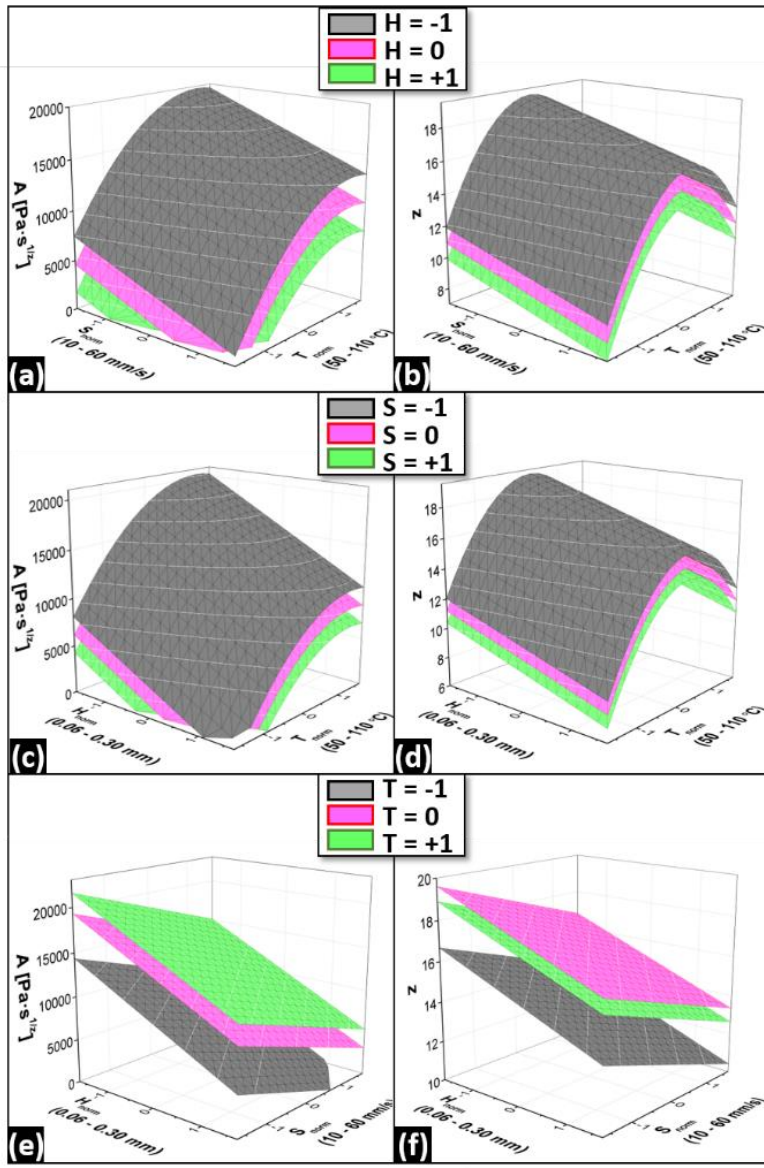

FIGURE 40. Values of A and z parameters as a function of printing variables at different levels of (a,b) layer height, (c,d) printing speed and (e,f) hotend temperature

4.1.5.1. Constant layer height (H) plots

As can be deduced from eqs. 6 and 7, A and z are linearly related to H, so that the surfaces corresponding to the different levels of H are parallel and equidistant from each other, as it is shown in FIGURE 40A and FIGURE 40B. As can be seen, parameter A decreases by increasing the layer height. An increase in layer height implies a larger amount of deposited material, so more time is required to cool down a given volume of sample before the next layer is deposited. Therefore, especially at high printing speed, the material does not have enough time to be properly cooled down and the network that is formed exhibits weaker interactions. As a result, the higher the layer height, the lower values of A and z were obtained, which in practice means lower gel strength.

For the same H-value, response surface model predicts a tendency to reach maximum A-values for low speeds and high temperatures, which corresponds to the expected behaviour, since it is the combination under which the material is most exposed to temperature increment, due to the longer residence time and the greater temperature gradient between the fed material and the hotend. As the coil-helix transition temperature is more widely exceeded, the carrageenan chains are more mobile and the creation of the gel structure is favoured upon cooling. However, the values of parameter A are levelled off at around 100 °C, whereas z reaches a maximum at around 80-85 °C. This means that no benefit can be taken by excessively heating the sample; on the contrary, a not so compact gel structure seems to be formed due to a partial non-reversible coil-helix transition and/or not so efficient aggregation of double helices. As Tanaka [400] pointed out, different associations of double helices, differing in the number of helices and average helix length, may be achieved at different temperatures. In particular, this theoretical study predicts that the number of helices per chain, which may be related with parameter z in eq. 5, passes through a maximum at a given temperature. In addition, low velocities also allow each layer of deposited material more time to cool down before it is covered by the next layer of hot material. So, the optimum point will be determined by the maximum time (minimum speed) that can be used in printing, ensuring that the limit value that allows the printer to work without clogging problems is reached. In this case, as a water-based material, conditions combining an excessively low flow rate with high temperature (e.g. printing speed below 2 mm/s and temperature above 85 °C) may result in drying of the material and consequent system clogging problems. However, in most applications, the aim is

to reduce total printing time and energy consumption, so that operating conditions would be closer to the upper limit: high layer height and printing speed at the lowest possible temperatures.

When hotend temperature is increased enough to allow the dispersion to exceed the hydration and dissolution threshold of carrageenan molecules, it is not necessary for the material to remain exposed to that temperature for so long, so that printing can be accelerated without major changes in the resulting rheological properties.

4.1.5.2. Constant printing speed (S) plots

As can be seen in FIGURE 40C and FIGURE 40D, the A and z response surfaces for constant S-values are very similar to those of constant H-values, since the relationship of both independent variables with the dependent variables are linear and comparable (eqs. 6 and 7). Both the layer height and printing speed are related to the material flow, which is being heated inside the hotend, since H determines the amount of material that goes through the 3D printing system and S is related to the hotend residence time. Moreover, once the material has been deposited on printing surface or on the previous layer, there is also an equivalent effect during cooling. The printing speed determines the time the material is cooled and therefore the time during which the material can be properly self-structured, whereas the layer height is related to the amount of material that needs to be self-structured.

4.1.5.3. Constant temperature (T) plots

Unlike those corresponding to constant H and S values, all graphs constructed for constant T-values are flat surfaces (FIGURE 40E and FIGURE 40F). Moreover, there are no interactions between the variables, so that all surfaces are parallel to each other. As just mentioned, the effects of layer height and print speed are somewhat equivalent. Therefore, the maximum values of A (stronger gel network) and z (higher number on interacting units) are predicted for the lowest values of H and S, while the minimum is exactly at the opposite corner, which tends to zero in the case of A, i.e. extremely low gel consistency. On the other hand, as previously discussed, A values are closer for hotend temperatures around 80-100 °C, and z reaches maximum values at around 80 °C (the higher plane in Fig. 4f).

4.1.6. Time as a variable

One of the goals of this study was to elaborate a practical model that allows predicting the rheological response of κ-carrageenan gels as a function of the main 3D printing variables directly involved in its manufacture: layer height, printing speed and temperature of the 3D printer hotend. In a typical product design process, the properties to be achieved would be set and the processing conditions should be established to achieve them at the lowest possible cost. In this context, the temperature would be an easily optimisable variable according to energy consumption: the most appropriate value would be the lowest value able to guarantee the desired final properties. For instance, as previously discussed, not noticeable improvement in gel strength was achieved by applying hotend temperatures above 80-85 °C. However, both layer height and printing speed are more complex to analyse. These variables are necessary to be able to define the conditions of the printing process, but do not have as much effect on the cost of the process as in the case of temperature. Nevertheless, the combination of both of them determines the value of a decisive variable in terms of cost optimization: the printing time.

Both the printer firmware and the software used in this study are the same as when printing with a conventional solid filament. In this way, the system can be treated analogously to a traditional solid filament printing system.

The printing speed, S, is the linear speed of the nozzle when printing. Thus:

$$t = \frac{L}{S} \tag{8}$$

where t is the total printing time and L is the length of the complete path the nozzle has to take to print a certain model. For a constant section 3D printed object, like the discs printed in this work for further rheological assessment of gel models:

$$L = L_c \cdot N_c \tag{9}$$

L_C being the length of the path necessary to print each layer and N_C being the number of layers of the model. By combining both equations (eqs. 8 and 9):

$$t = \frac{L_C \cdot N_C}{S} \tag{10}$$

The number of layers for a certain object would be the total height (h_m) divided by the height of each layer (H). So, the total printing time will be:

$$t = \frac{L_c \cdot h_m}{S \cdot H} \quad (11)$$

In this equation, h_m is a known value (1 mm in the gel discs) and L_C can be calculated from the "filament" length, $L_{filament}$. When the printer is operated conventionally by using a solid plastic filament that melts before being deposited, slicing software provides the length of filament to be used for printing a certain model. This value, included in the .gcode file, is the $L_{filament}$.

This filament is of a known diameter ($d_{filament}$) and, when it melts and passes through the nozzle, its section changes, taking the width of the outlet hole, d_{nozzle}, and the thickness corresponding to the layer height, H. If the volume of the material is considered to be constant before and after the nozzle (regardless of thermal expansion), the length of the filament consumed and the length of the deposited thread will be different. In this case, as it is not a solid filament, the internal diameter of the feed tube (2 mm) is taken as $d_{filament}$.

Thus, known $d_{filament}$ and d_{nozzle}, the $L_{filament}$ value can be used to calculate the length of the deposited thread. Moreover, if the value of $L_{filament}$ is taken as the data corresponding to laminate a single layer of the discs, the value of L_C can be obtained as follows:

$$L_c \cdot d_{nozzle} \cdot H = L_{filament} \cdot \frac{\pi}{4} \cdot \left(d_{filament}\right)^2 \quad (12)$$

$$L_c = \frac{L_{filament} \cdot \frac{\pi}{4} d_{filament}}{d_{nozzle} \cdot H} = \frac{L_{filament} \cdot \frac{\pi}{4} (2\ mm)^2}{0.4\ mm \cdot H} = 986.4\ mm \quad (13)$$

When considering discs printed with different H values, $L_{filament}$ also changes (the thicker the deposited thread, the more filament is consumed). Therefore, the path to be followed by the hotend to create a layer (L_C) is always the same, since the surface to be covered and the diameter of the nozzle are also the same. This value is provided by $L_{filament}$ and H-values, corresponding for each disc, and for all of them the same L_C value is obtained ($d_{filament}$ and d_{nozzle} are fixed values). So, for the case of this study:

$$t = \frac{L_c \cdot h_m}{S \cdot H} = \frac{986.4\ mm \cdot 1\ mm}{S \cdot H} = \frac{986.4\ mm^2}{S \cdot H} \quad (14)$$

The following procedure is an example of the utility of this relationship when, for instance, an A-value is imposed. Starting from the equation obtained to predict the behaviour of parameter A (eq. 5) and rearranging:

$$S = \frac{-A+11224.0+3617.2\cdot T-2881.0\cdot H-1355.1\cdot T^2}{2710.2} \quad (15)$$

Thus, for each pair of given H-T values and for a certain fixed value of A, S can be calculated. Subsequently, by substituting each calculated S-value and their corresponding H-values in the eq. 14, the printing time, t, is obtained.

It is important at this point to notice that, in eq. 14, the real values of variables S and H are entered, while, in eq. 15, it is necessary to use the normalized values of H and T between -1.682 and +1.682. Likewise, the printing speed values calculated from this equation also correspond to the normalised scale. Also, it is worth mentioning that fixed constant levels of H have been considered in this study, instead of S-values, because the layer height determines the resolution of the final 3D printed product and could, in some cases, be of interest for the optimisation of the printing process. However, when working with this kind of viscoelastic materials and in applications where the resolution of the final 3D object is not decisive, S instead of H may be chosen, following then the same procedure. Thus, for a given value of A (defined by product specifications), a new table can be elaborated from eqs. 14 and 15, which in this case has been calculated for A = 12000 Pa·s$^{1/z}$. Using these values, different curves can be plotted (**FIGURE 41**), from which the time and temperature required to obtain a gel with an imposed A-value can be determined.

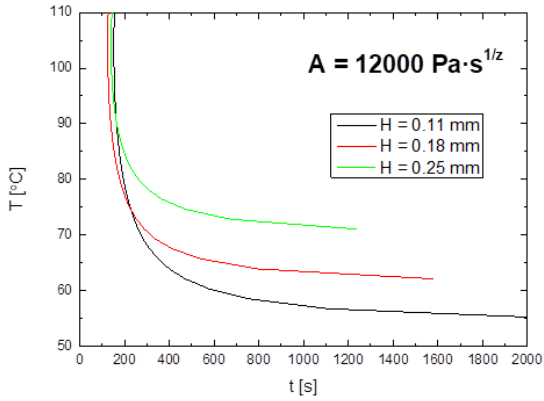

FIGURE 41. Time-temperature relationship for obtaining, by means of 3D printing, κ-carrageenan gels with an imposed A value of 12000 Pa·s$^{1/z}$

If there would be any restriction to raise the temperature (degradation of some component, for example), by drawing a horizontal line from that value, the first crossing with any of the plotted curves will indicate the minimum printing time that will be used in the process to achieve a target rheological parameter, a value of A=12000 $Pa \cdot s^{1/z}$ in this example. On the contrary, if it is time that determines, for example, whether it is profitable to print a certain product in 3D, the procedure would be the inverse: it could be determined what would be the minimum temperature value that could be used and, therefore, the associated energy consumption.

4.2. Design of a mixing device for fluid thickening

This design of the device described below has been submitted in a form of patent application by Fresenius Kabi Deutschland GmbH (Mixing chamber and device for preparing and optionally 3D-printing edible thickened aqueous compositions. Auths: I. Diañez, C. Gallegos, E. Brito-de la Fuente, I. Martínez, C. Valencia, M.C. Sánchez, M.J. Diaz, J.M. Franco).

4.2.1. Introduction

Dysphagia patients suffer from a swallowing problem which impairs their ability to swallow food in a controlled manner. Dysphagia can be a symptom of a multitude of neurological, muscular and structural pathologies. It can lead to serious complications, including malnutrition and dehydration, as well as severe respiratory problems —for instance, aspiration pneumonia— resulting from the aspiration of food or fluids into the airways.

One of the most widely used interventions in the management of dysphagia is the thickening of low-viscosity liquids, as these normally present the greatest risk of aspiration for the patient, especially due to delayed pharyngeal swallow or oral motor impairment. The thickener increases the viscosity of the liquids and thereby significantly reduces the flow rate of the bolus during swallowing. This increases the chances of the airways being secured in time during the swallowing process to prevent aspiration of the liquid into the airways.

Depending on the severity of the swallowing impairment, the viscosity required for safe swallowing varies from patient to patient. Consequently, several levels

of thickening have been established, the most common and accepted classification being that given by the National Dysphagia Diet Task Force (NDD) and published by the American Dietetic Association in 2002[150]. According to this classification, which is based on viscosity values determined at a shear rate of 50 s^{-1} and a temperature of 25°C, a liquid or liquid food with a viscosity in the range of 1 to 50 mPa·s is classified as a 'thin liquid', with a viscosity in the range of 51-350 mPa·s as 'nectar-like', with a viscosity in the range of 351-1750 mPa·s as 'honey-like', and finally, with a viscosity exceeding 1750 mPa·s it is classified as 'spoon-thick'.

Commercial products for thickening low viscosity beverages or liquid foods are provided either as dry powders or aqueous gels of starch- or gum-based thickeners. The provision of thickeners as aqueous gels instead of dry powders requires extra measures for insuring a sufficient shelf-life of the gels. These pre-gelled products are usually provided in small pre-packaged doses, which makes them relatively costly and produces significant amounts of waste packaging material after use. Additionally, as a dose of premixed gel comprises a relatively low amount of thickener dissolved in a large amount of a liquid base, shipping costs, relative to the amount of thickener provided, are significantly increased in comparison with the dry powder products, which are usually mixed manually into a beverage or liquid food by the patient, a caregiver or nursing staff immediately before consumption.

Commercial dry powder products are provided with instructions to the users on how to prepare thickened beverages or liquid foods with a viscosity within the above defined categories. Manual mixing of the thickener into the beverage or liquid food is relatively time-consuming and requires careful adherence to the mixing instructions, e.g. the amount of thickener required to obtain the desired viscosity and the time required by the thickener to increase the viscosity of the mixture. If these instructions are not adhered to by the person mixing the powder into the beverage or liquid food, the viscosity of the thickened product may not fall into the required category. Additionally, at higher viscosities, it becomes increasingly difficult to avoid the entrapment of air and the formation of bubbles in the thickened liquid. Air bubbles in the thickened liquid can lead to a significant reduction of the viscosity of the mixture, which therefore — although using the recommended amount of thickener— may not have the desired target viscosity.

Another problem that is encountered in dysphagia patients who consume a major part of their daily food in the form of thickened liquid nutrition is the development of 'diet fatigue'. Due to the limited sensorial attributes of thickened liquid nutrition, patients may tire of this food rather quickly and compliance to the dietary regime based on thickened beverages and thickened liquid food may be reduced.

Consequently, there exists a need to provide means for the preparation of viscosity-controlled thickened beverages or liquid food that overcomes or lessens the above described problems. Especially there is a need for a means to prepare more reliably thickened beverages or thickened liquid food having a predetermined viscosity, especially thickened compositions of nectar- or honey-like viscosity or spoon-thick compositions. Additionally, there is a need for a process by means of which such compositions can be prepared easily and in a less-time consuming way by users, especially caregivers or nursing-staff. There is also a need to provide thickened food with increased sensory attributes compared to thickened liquid food.

This chapter reports the design, fabrication and calibration of a mixing device which allows the reliable automated preparation of viscosity-controlled mixtures of a solid thickener and a liquid. This device is controlled by a RepRap 3D printer and is specially designed to be used as an extruder for 3D printing of thickened fluids, thus giving the possibility of preparing meals suitable for dysphagic patients that can be more appetising for them than conventional dysphagia-oriented products.

4.2.2. Device design

In this section, the device for preparing edible, viscosity-controlled mixtures starting from a liquid and a solid thickener is described. This device can also act as a print head in a 3D printer, as will be described in the following.

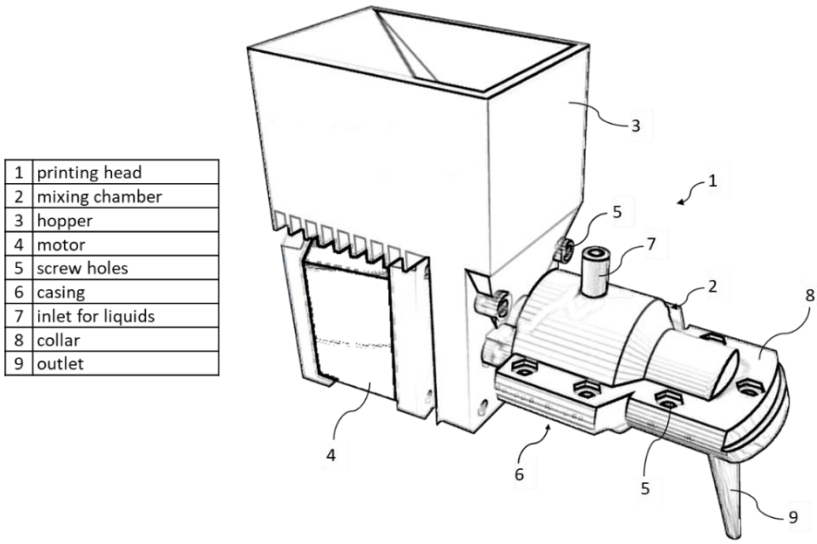

FIGURE 42. Three-dimensional view of the mixing chamber, hopper and motor

FIGURE 42 shows a three-dimensional view of the printing head (1), comprising the mixing chamber (2), coupled to the hopper (3) and the motor (4). The entire mixing chamber can be easily disengaged form the hopper and the motor, as they are only fastened by a press fit. The hopper is fastened to the motor by two screws (5). The casing (6) is divided into two halves, which are held together by seven additional screws inserted into screw holes (7) in the collar (8). It has an inlet for liquids (7) in its upper part and the outlet (9) for mixtures in its lower part.

The hopper is attached to the inlet for solids, through which the solid thickener is transported into the mixing chamber. A liquid feed is attached to the inlet for liquids, through which the fluid can enter the mixing chamber. A motor is connected to the screw conveyor. Furthermore, the device comprises a control unit for regulating the dosage of the liquid and/or the dosage of the solid thickener. In this case, the electronics of a RepRap 3D printer acts as the control unit, which can be connected to a PC or another user interface, via which it can be programmed by the user and different elements of the device can be controlled.

This device allows the preparation of single doses as well as in situ and continuous mixing of a solid thickener and a liquid to prepare batches comprising multiple doses of viscosity-controlled mixtures.

4.2.2.1. Mixing chamber

The mixing chamber is the main part of the device.

2	mixing chamber
3	hopper
4	motor
6	casing
7	inlet for liquids
9	outlet
10	central axis
11	solid dosage area
12	first end
13	liquid dosage area
14	transport area
15	second end
16	inlet for solids
17	screw conveyor

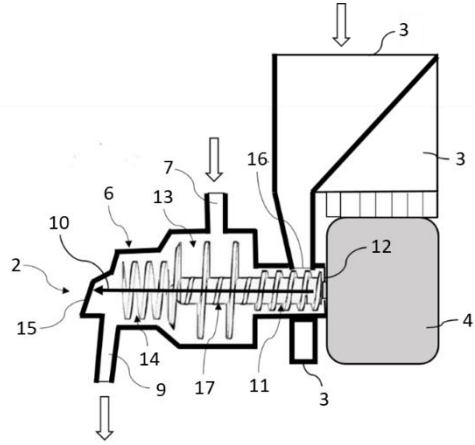

FIGURE 43. Vertical cross section along the long axis of the mixing chamber

FIGURE 43 shows a vertical cross section along the central axis (10) of the mixing chamber. The three arrows indicate solid thickener and liquid input into the mixing chamber and output of the prepared mixture out of the mixing chamber. The mixing chamber comprises the casing, which defines, with its inner walls, an inner volume with three cylindrical areas. The three areas follow one another along the central axis, starting with the solid dosage area (11) at the first end (12), followed by the liquid dosage area (13) and the transport area (14) at the second end (15) of the inner volume. In other words, the liquid dosage area is arranged between the solid dosage area and the transport area. The inlet for solids (16) is located in the upper part of the solid dosage area and the conveyor screw (17) extends along the three areas of the mixing chamber.

5	screw holes
7	inlet for liquids
8	collar
10	central axis
11	solid dosage area
12	first end
13	liquid dosage area
14	transport area
15	second end
16	inlet for solids
18	upper half of the casing
19	transition area
20	counter flanks
21	inner wall of upper half

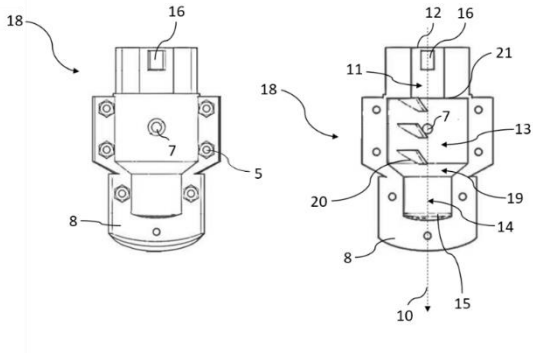

FIGURE 44. Outside (left) and inside (right) view of the upper half of the casing

FIGURE 44 shows a top and inside view of the upper half (18) of the casing. The transition area (19) connects the liquid dosage and the transport areas. The counter flanks (20) are arranged on the inner wall (21) of the upper half of the casing. The counter flanks or baffles are designed and arranged in a way that they engage with the truncated helical flanks of the screw conveyor (see section 4.2.2.2: Screw conveyor). This means that, in an assembled state, during rotation of the screw conveyor, the counter flanks brush against the truncated helical flanks of the screw conveyor. Thus, undissolved solids or only partially dissolved thickener are removed from the surface of the helical flanks, promoting solid flow and mixing.

The mixing chamber consists of a casing defining with its walls an inner volume, designed to minimise dead zones and to avoid the adhesion of solid or only partially dissolved thickener to the surfaces of the screw conveyor and the inner walls of the casing. It comprises three cylindrical areas, whose diameters may be the same or differ from each other. These different cylindrical areas follow one another along a central axis and act as solid dosage, a liquid dosage and a transport area. The outermost inner wall of the solid dosage area defines the first end of the inner volume. The solid dosage area is followed by the liquid dosage area, which is followed by the transport area. The outermost inner wall of the transport area defines the second end of the inner volume. The solid dosage area comprises an inlet for solids and the liquid dosage area comprises at least one inlet for an aqueous liquid, while the transport area comprises an outlet by means of which the prepared mixture of solid thickener and aqueous

liquid leaves the mixing chamber. Preferably the inlets are arranged at an upper part of the casing to reduce the probability of clogging of only partially wetted and/or dissolved solid thickener. The outlet, on the other hand, is arranged at a lower part of the casing close to the second end of the inner volume.

The diameters of the solid dosage area (D_s), the liquid dosage area (D_l) and the transport area (D_t) may all be identical or different from each other. However, preferably, the mixing chamber has cylindrical areas of different diameters, to enhance each of the mixing stages. The solid dosage area has the smallest diameter of all three cylindrical areas. The central zone, i.e. the liquid dosage zone, is the largest in diameter, thereby creating a large reservoir in which solid thickener and liquid are brought into contact to effectively dissolve the thickener in the liquid. Thus, the diameter of the solid dosage area is smaller than the diameter of the liquid dosage area and smaller than the diameter of the transport area. The diameter of the transport area is smaller than the diameter of the liquid dosage area too. This arrangement is favourable because it helps to avoid backward flow to the solid dosage area and, in the area of the outlet, the weight of the prepared mixture supports its transport out of the mixing chamber. If the viscosity of the prepared mixture is sufficiently low, the mixture could simply flow out of the outlet and not require the transportation via screw conveyor.

There is a transition area between the liquid dosage area and the transport area, so the transition between the liquid dosage area and the transport area is continuous. This transition area is shaped as a truncated cone in which the inner wall is tapered with decreasing diameter from the liquid dosage area towards the transport area. This allows the mixture to flow continuously from the liquid dosage area into the transport area. No dead zones are created where the mixture can accumulate without movement.

If the mass to be transported into the liquid dosage area needs to be increased (to include bigger amounts of macro- or micronutrients, for instance), it may be beneficial to increase D_s in relation to D_l to allow a higher mass flow from the solid dosage area into the liquid dosage area.

Additionally, new inlets for liquid and/or solids can be arranged in the liquid and solid dosage areas, respectively. Additional liquid and solid feeds can therefore be connected to these inlets for independently controlling the concentration of selected ingredients in more complex mixtures, such as macro- and

micronutrients, pharmaceutical effective agents or additional ingredients, such as colorants, flavours, stabilisers, or the like.

An array of counter flanks is arranged on the inner wall of the casing in the liquid dosage area, engaging with the flanks of the screw conveyor. In the liquid dosage area, the liquid and the solid thickener come into contact with each other. Thus, the surface of the solid thickener is initially wetted by the liquid and may form a highly viscous film on the surface of the thickener particle. Such wetted particles may adhere to the inner walls of the casing or the flanks. Similarly, as the liquid further penetrates the thickener particle during the dissolving process, the particle may swell and form a highly viscous body of only partially dissolved thickener, which again may adhere to the inner wall of the casing or the flanks. Thus, there is an increased need for preventing the solid thickener to adhere to the inner walls of the liquid dosage area or the flanks of the screw conveyor situated in the liquid dosage area. Additionally, the at least one counter flank or, preferably, the array of counter flanks hinder liquid to pass through the inlet for solids into an attached solid feed, which could result in a clogging up of the inlet for solids by highly viscous, only partially dissolved thickener. Additionally, as already discussed above, the counter flank or flanks, especially when formed as baffles arranged only in the upper half of the casing, help to reduce or avoid the accumulation of solid or only partially dissolved thickener at the bottom of the casing.

The provision of the one or more counter flanks only in this area of the mixing chamber has proven to be sufficiently effective in reducing or minimizing the adherence of solid or only partially dissolved thickener to the inner walls of the mixing chamber, the surface of the flanks of the screw conveyor, and for hindering liquid passing through the solid inlet into an attached solid feed.

The casing of the mixing chamber is divided into two detachable halves, preferably an upper and a lower half. This allows an easy assembly or disassembly of the mixing chamber, the insertion and removal of the screw conveyor, as well as the easy cleaning of all components. Such ease of cleaning is of great importance, as the mixtures produced using the mixing chamber are intended for human consumption, especially for patients with an already impaired health. Additionally, it reduces the time required for the maintenance of the mixing chamber. The upper and the lower half of the casing each comprises a circumferential collar to build a sealed, detachable connection to

one another. For this purpose, connection elements, such as screws or clamps, can be used.

4.2.2.2. Screw conveyor

A screw conveyor extends through all three areas of the inner volume of the mixing chamber. This screw will drive and mix the material during its flow through the mixing chamber.

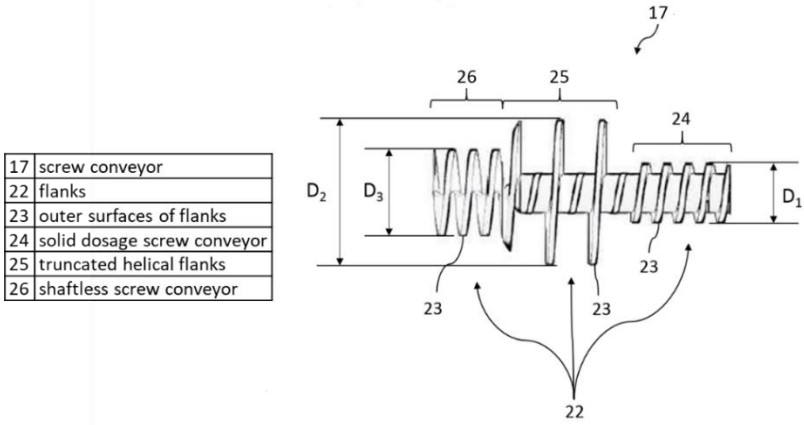

17	screw conveyor
22	flanks
23	outer surfaces of flanks
24	solid dosage screw conveyor
25	truncated helical flanks
26	shaftless screw conveyor

FIGURE 45. Side view of the screw conveyor

FIGURE 45 shows a more detailed drawing of the screw conveyor. The screw conveyor comprises flanks (22) arranged helically along the long axis of the screw conveyor. Helically arranged flanks mean that the outer surfaces (23) of the flanks describe a curve that winds around the jacket of a cylinder with a constant slope. There are three different kind of flanks shown. Namely, flanks that continuously wind around the long axis of the screw conveyor, forming the solid dosage screw conveyor (24); flanks that are designed as truncated open flanks (25), winding along the long axis; and flanks forming a shaftless screw conveyor (26).

The screw conveyor comprises flanks, arranged helically along its long axis. Within this chapter, the diameter of the (imaginary) cylinder the outer surfaces of the flanks wind around is referred to as the outer diameter of the helical flanks. It is not mandatory that the outer surface of the flanks describe a continuous helix or cylindrical spiral along the entire screw conveyor. Instead, the flanks may only be present in specific sections along the long axis of the screw conveyor.

The outer diameter of the helical flanks is equal to or only slightly smaller than the diameter of the cylindrical area they are arranged in. In other words, an outer diameter D_1 of the flanks in the solid dosage area corresponds to the diameter D_s. An outer diameter D_2 of the flanks in the liquid dosage area corresponds to the diameter D_l and an outer diameter D_3 of the flanks arranged in the transport area corresponds to the diameter D_t. In the transition area, the outer surface of the flank is tapered, corresponding to the decreasing diameter of this part of the casing. The adhesion of solid or partially dissolved solid to the inner wall is thereby effectively reduced or prevented. The outer area of the flanks may also be designed as flexible wing elements, which brush over the inner wall of the mixing chamber as the screw conveyor rotates. Thus, solid thickener or only partially dissolved thickener that adheres to the inner wall is scraped off the inner wall of the casing, whilst dead zones are minimised.

Hence, dead zones in which solids or highly viscous, partially dissolved, solids can accumulate are minimised, as well as those zones in which the mixture is not properly transported in the direction of the outlet. Minimising the dead zones in the mixing chamber ensures an effective contact between all the solid thickener and the liquid fed into the liquid dosage area and, thereby, enables the solid thickener to be effectively mixed and dissolved into the aqueous liquid. This allows the preparation of mixtures having an increased homogeneity and ensures that the whole solid thickener fed into the liquid dosage area is used to thicken the liquid, thus minimising variability in the concentration of thickener in the mixture and, therefore, its viscosity. This is of great importance for reliably producing mixtures of solid thickener and a liquid having a predetermined, aimed-for viscosity.

Also, with this aim, as commented before, an array of counter flanks is arranged on the inner wall of the casing. While the conveyor screw rotates, counter flanks are brought into contact, or into very close proximity, to the flanks of the screw

conveyor to wipe over their surface at a distance that is small enough to scrape off any solid, or only partially dissolved solid, that adheres to said flanks. In other words, the counter flanks and the flanks engage with each other, such that the counter flanks scrape off solid, or only partially dissolved solid, that adheres to the flanks and vice versa. If both the flanks and counter flanks are made of a rigid material, e.g. of metal or plastic material, the flanks and counter flanks may only be brought into close proximity to each other (e.g. 1 mm or less), so not to touch each other. On the contrary, if either the flanks or counter flanks, or both, are made of a sufficiently flexible material, e.g. of a silicone-type material, flanks and counter flanks may come into contact with each other whilst solid or semi-solid material is scraped off their surfaces.

Preferably, counter flanks or baffles are arranged only in the upper half of the casing, especially in the liquid dosage area. In this way, the accumulation of any solid or only partially dissolved thickener in the bottom half of the casing is reduced or avoided.

The part of the screw conveyor extending through the solid dosage area is designed as a screw conveyor for transportation of the solid thickener. While the flanks in this part of the screw conveyor continuously wind around its long axis, the flanks of the screw conveyor in the liquid dosage area are designed as truncated helical flanks. These truncated flanks can be described as radially cut discs, each of which is stretched or distorted by pushing apart the two cutting edges resulting from the cut, said stretched or distorted discs then being arranged along the long axis of the screw conveyor in this area. Thus, the counter flanks can engage with the truncated flanks and scrape or wipe over their front surfaces during movement of the screw conveyor, as described above.

Finally, the part of the screw conveyor extending through the transport area is designed as a shaftless spiral conveyor. Thus, the helical flanks wind continuously around an open axis. This form is similar to the form of a dough hook and is, therefore, especially suitable for exerting force onto thickened mixtures, resulting in an effective transport thereof in the direction of the outlet.

All the different kind of flanks wind around the long axis of the screw conveyor. Hence, when the device is assembled and running, the screw conveyor generates

a mass flow through the cylindrical areas from the first end to the second end of the inner volume.

4.2.2.3. Liquid and solid feeds

The liquid feed is a pump with an associated motor and reservoir for liquids. The control unit (the 3D printer, see section 4.2.2.4) controls the motor of the pump to provide a mass flow of the liquid to the inlet.

The solid feed may be any device providing a constant supply of solid thickener, as the hopper does in this case. It is attached to the inlet for solids. The hopper comprises a receptacle area extending therethrough, said receptacle area being designed in such a way that the mixing chamber and the screw conveyor can be connected to the motor positioned at the lower end of the hopper. Once the mixing chamber has been inserted into the receptacle area of the hopper, the opening at the bottom of the hopper is situated above the solid inlet of the mixing chamber. Solid thickener may then enter the solid dosage area of the mixing chamber via the solid inlet. Together with the screw conveyor in the solid dosage area, a certain mass flow can be provided. Therefore, the control unit regulates the motor driving the screw conveyor connected thereto. Mass flow of the solid depends on the size of the inlet and the solid dosage area, the rotation speed of the screw conveyor and its design in said area. Lower rotation speed results in a lower flow rate of the solid thickener. The screw conveyor will also mix and transport the material of the mixture during its flow through the inner volume of the mixing chamber.

It is advantageous to choose a diameter D_s for the solid dosage area that is smaller than the diameter D_l of the liquid dosage area. Therefore, a low flow rate for the solid can be provided at a sufficiently high rotation speed to ensure homogeneous mixing of the material during its flow through the inner volume of the mixing chamber.

4.2.2.4. The control unit (3D printer)

The mixing extruder is designed and manufactured to be adapted to a 3D printer and controlled by its firmware, allowing the continuous and automatic in-situ mixing of at least one solid thickener and at least one aqueous liquid, fed into the mixing chamber via the respective feeds. Furthermore, the device can

simply be used as an automatic mixer controlled via software, to obtain mixtures having a viscosity in a predetermined range.

A conventional fused filament 3D printer can be modified by replacing the original filament extruder with the mixing extruder. In this work, a BQ Hephestos RepRap 3D printer has been used as the control unit for the mixing extruder.

1	printing head
2	mixing chamber
3	hopper
4	motor
7	inlet for liquids
9	outlet
27	modified 3d printer
28	build area
29	x-carriage
30	electronics and pc/user interface connection
31	pump

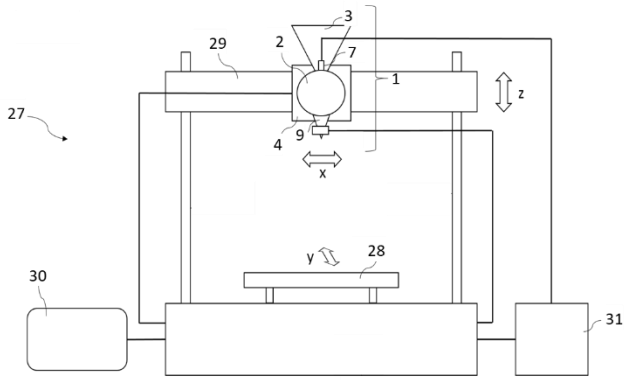

FIGURE 46. Schematic diagram of a 3D printer modified according to the proposed setup

FIGURE 46 shows a schematic representation of a 3D printer according to the described setup. The Figure shows only selected elements of the device. Additional constructions elements are required to run the device, the build area and print head, such as transmission belts for moving the print head, power supply, etc.

The modified 3D printing device (27) comprises drive mechanisms for moving selected parts of the 3D printer, such as the print head, build area (28), and the x-carriage (29). A PC or another type of user interface can be connected to the electronics (30) to operate the 3D printer. The pump (31) for liquids is also connected to and controlled by 3D printer electronics.

Build area is movable only in one direction (y-direction), as indicated by the arrow above it. it is located between two vertical frame elements, onto which a movable horizontal frame element (x-carriage) is mounted in such a way that it can be moved in vertical direction (z-direction) relative to the surface of build

area, as indicated by the arrow shown beside it. Build area is a flat rectangular heatable or non-heatable work plate made of any material suitable for depositing the printed material thereon, e.g. ceramic, plastic, metal, etc. Print head is mounted movably using a custom-made holder in such a way that it can be moved along the x-carriage, in a direction (x-direction) parallel to the surface of movable build area, by means of a driving mechanism. During use, the control unit can simultaneously regulate the movement of build area, x-carriage and print head. Furthermore, it controls the mass transport rate of aqueous liquid from the liquid feed into mixing chamber by controlling the rotation speed of the pump motor, and the mass transport rate of solid thickener from the solid feed by regulating the rotation speed of motor to which the screw conveyor of the mixing chamber is attached.

The 3D printer can be built using conventional and commercially available mechanical and electronic components (such as controller boards), frame construction parts, motion controllers (such as belts and stepper motors), threaded rods and end stops, power supply units, print beds used as the building area, including heated and non-heated print beds, heating units including thermocouples, cooling fans, and user interfaces.

When used to obtain highly viscous mixtures with viscosities that allow them to self-sustain a defined three-dimensional form, the mixing chamber coupled to a 3D printer can be used to design meals with appealing shapes or simulating conventional food, which can help to make clinical nutrition more attractive to patients, thereby increasing compliance of patients to a prescribed texture-modified diet.

4.2.3. Use and calibration

All parts of the mixing device must be clean and dry before assembly. The two casing halves are secured with screws, having previously placed the screw conveyor inside. The mixing device is then coupled to the solid feed, so that the motor shaft fits with the cavity made for this purpose in the screw conveyor. Once this is done, the solid feed is loaded with the solid thickener and the liquid feed, previously loaded with the liquid to be thickened, is connected to the liquid inlet in the upper half of the casing. When the device is loaded and ready for use, the desired flow ratio is set via software running on the control unit.

Preferably, the process further comprises a calibration sequence for the control unit to configure the dosage of the solid thickener and the dosage of the liquid.

The liquid and solid feeds, working as conventional extruders, can operate simultaneously and independently due to the creation in Repetier-Host of a virtual extruder for which the flow ratio of both feeds can be controlled by means of a simple software script.

When a conventional 3D printer has two extruders, they are usually of the same type and geometry, so the flow ratio can be assigned directly. That is, by setting a weight of 50 (over 100) for each extruder, the material flow for each extruder would be the same. This is not the case here, where the liquid feed and the solid feed are feeding systems with completely different geometries that, for equal motor movement, provide different material flows. Thus, individually calibration of each of the feeds is necessary.

The firmware of the 3D printer used as the control unit measures the advance of the motors (their rotation) in units of length. Thus, by sending orders to the printer to print different distances and weighing the amount of material printed in each case, a flow rate value in g/mm can be obtained. This flow rate value, in turn, can be converted into mass flow rate directly by means of the printing speed used:

$$\dot{m} = fr \cdot v \tag{16}$$

$\dot{m}$: mass flow rate [g/min]

fr: flow rate [g/mm]

v: printing speed [mm/min]

Since the geometries of the two feed systems are different, as are the flow rate values for the liquid solvent (fr_l) and the solid (fr_{solid}), therefore each of the flows has to be calibrated independently by weighing the amount of material supplied by the liquid pump, for example a syringe pump, and the mixing screw, i.e. screw conveyor for given motor advance lengths, for example resulting in:

$$fr_{solid} = 1.13 \cdot 10^{-3} g/mm \qquad fr_l = 0.33\ g/mm$$

Once the characteristic flow rate of each feed system is known, a weight from 0 to 100 is applied to each motor to control mixing ratio. A weight of 1 is assigned to the liquid pump motor (w_l), as it is the one with higher feeding

capacity. Then, the weight for the motor driving the mixing screw, i.e. screw conveyor (w_{solid}), is calculated to get the correct ratio in each case. However, the sum of the weights of the different motors is required to be equal to 100, so that a third 'ghost' motor is defined in order to absorb the excess weights. Different mass flows can be achieved by multiplying the weights for the solid and liquid solvent. For instance, considering the nectar-like concentration (1.6 wt.%):

$$\dot{m} = 2\ g/min \begin{cases} w_l = 1 \\ w_{solid} = 4 \\ w_g = 95 \end{cases} \qquad \dot{m} = 4\ g/min \begin{cases} w_l = 2 \\ w_{solid} = 8 \\ w_g = 90 \end{cases}$$

w_l: weight for liquid solvent feeding motor

w_{solid}: weight for solid feeding motor

w_g: weight for "ghost" motor

Thus, mixing mass flow rate also named as total mass flow rate is then calculated by means of this expression:

$$\dot{m} = (w_{solid} \cdot fr_{solid} + w_l \cdot fr_l) \cdot v \qquad (17)$$

Printing speed is set, for example, at 600 mm/min for nectar-like blends and slightly varied to compensate the increased solid flow for the two higher concentrations.

4.3. Obtention of thickened fluids by means of the designed mixing device

The following subsection has been submitted in a form of research article to Food Hydrocolloids.

4.3.1. Introduction

Swallowing difficulty (dysphagia) is a problem that, according to the most conservative estimates, affects approximately 8% of the world's population [125]. Dysphagia can be a consequence of a multitude of neurological, muscular, and structural pathologies or can even be drug-induced [23]. It can lead to very serious complications, including malnutrition and dehydration as well as severe respiratory problems, such as aspiration pneumonia, resulting from the

aspiration of food or fluids into the airways [91]. As a result, dysphagia is associated with increased morbidity, worse prognoses, longer hospital stays, more frequent readmissions, and, in turn, higher mortality rates [86,109].

One of the most widely used interventions in the management of dysphagia is the thickening of low-viscosity liquids, as these normally present the greatest risk of aspiration [122,145]. Fresubin® Clear Thickener (FCT) is a gum-based α-amylase-resistant powder thickener that is widely used for modifying the rheological behaviour of fluids in dysphagia management [175]. As the thickener increases the viscosity of the fluids, the flow rate of the bolus during swallowing is significantly reduced, increasing the chances of the airways being secured in time to prevent aspiration [139,142]. However, because the viscosity required for safe swallowing varies from patient to patient [144], several levels of thickening are established. The most common and accepted classification is that given by the National Dysphagia Diet Task Force (NDD); according to this classification, at a shear rate of 50 s^{-1} and a temperature of 25 °C the viscosity values are as follows [150]:

- Thin liquid: 1–50 mPa·s
- Nectar-like: 51–350 mPa·s
- Honey-like: 351–1750 mPa·s
- Spoon-thick: <1750 mPa·s

However, although this classification is universally accepted at the level of the medical community, it is excessively simplistic, as it does not consider the non-Newtonian character of these thickened fluids or the different effective shear rates along the upper digestive tract [22,156,401].

The dose of FCT required to obtain these consistencies (nectar-like and higher) starting from Newtonian fluids as well as the way to prepare thickened liquids by manual mixing are indicated on the FCT packaging. However, although these instructions indicate how to reduce the inlet of air and consequent formation of bubbles in the mixture as much as possible, this is almost impossible in manual mixing and even more difficult with other mechanical means (such as blenders) [287]. Furthermore, it can be difficult for this process to be repeated from one preparation to another, especially if mixing is performed by different people. These complications, in the worst case, can lead to a significant decrease in the

viscosity of the mixture, thus the failure to meet the specific requirements for each texture.

To minimise these drawbacks while providing new and interesting features, in this study, a new mixing device was designed and manufactured to be adapted to a 3D printer and controlled by its firmware, allowing the continuous and automatic in situ mixing of (at least) one solid and one liquid feed. This device can simply be used as an automatic mixer to obtain mixtures with proportions controlled via software. In this way, it exhibits advantages over manual preparation, because the introduction of air into the system during manual mixing is unavoidable (especially in mixtures with high viscosity). This new preparation method allows mixing without letting air enter the system; the few small air bubbles that can be observed in mixtures are due solely to the air trapped between the solid particles, which can be minimised by controlling the granulometry.

In addition, through the use of additional feeds, more complex mixtures containing nutrients, drugs, or even colouring and/or flavouring agents can be prepared. When used to obtain concentrated systems (>10 wt.%) with viscosities that allow self-sustainment to form three-dimensional configurations, shape can be another key element in making thickened fluids more palatable and appealing for dysphagia patients. With the device coupled to a 3D printer, which allows it to be moved in three dimensions, gel models can be designed and printed with appealing shapes similar to conventional foods, which could make clinical nutrition more attractive to patients and less repetitive in long-term treatments [402]. Making thickened fluids more attractive is of utmost importance, as the lack of acceptance of these products by patients is a well-known issue. Patients' dislike of thickened fluids has, on the one hand, a very significant negative effect on their quality of life and, on the other hand, negative effects due to the potential non-compliance with treatment or reduced fluid and food intake [105,202,203].

The objective of this study was to develop and validate a novel device designed for the continuous mixing of solids and liquids, hereinafter referred to as the MIX3D accessory, controlled by the firmware of a RepRap 3D printer to which it is attached in order to be applied for dysphagia management. This device can mix a liquid (water, juice, and milk) with FCT to obtain mixtures at different concentrations covering the range from nectar-like to spoon-thick consistencies.

The actual content of solids and the final rheological behaviour of the mixtures obtained with the proposed device were evaluated.

4.3.2. 3D printer setup

To mix solids and liquids during printing, the equipment must handle both types

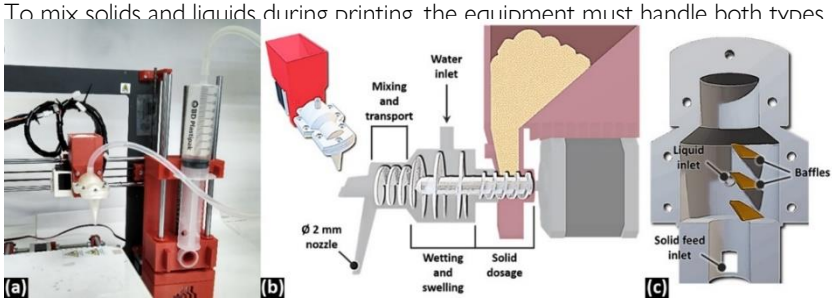

FIGURE 47B).

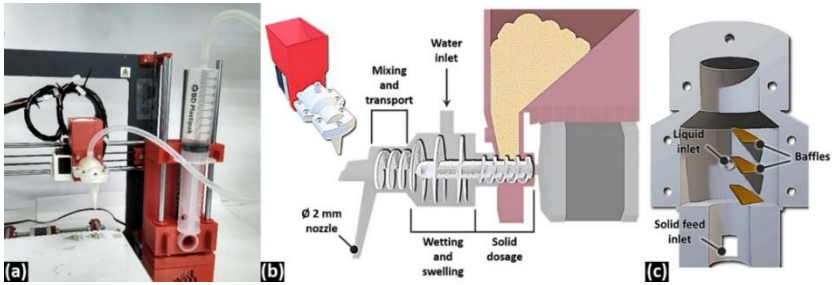

FIGURE 47. MIX3D accessory layout. (a) photograph of device and syringe pump setup, (b) schematic representation of the mixing device, (c) inside view of the upper half of the mixing device casing

The mixing screw is directly attached and driven by a NEMA 17 motor, which, like the one in the syringe pump, is configured as a conventional extruder to be controlled via software. The extruders can be operated simultaneously through a virtual extruder in Repetier-Host for which the flow ratio of both feeds can be controlled by means of a simple script. However, when a conventional 3D printer has multiple extruders, they are usually of the same type and geometry, so the flow ratio can be assigned directly. That is, by setting a weight of 50 (over 100) for each extruder, the material flow would be the same. This is not the

case in the proposed system, where the syringe pump and hopper are feeding systems with completely different geometries; for equal motor movement, they provide different material flows. Therefore, the first step to set a specific concentration is to calibrate each of the feeds passing through the system individually. Once each feed has been calibrated separately, it is possible to correct the weights and obtain the desired solid content.

The casing of the device is divided into two halves (upper and lower) to allow the insertion and removal of the screw as well as the cleaning of all components. The feeding inlets are located in the upper half to reduce the probability of clogging, while the mixing outlet is located at the end of the lower half. In addition, the upper part contains an array of baffles (FIGURE 47C) matching the truncated segments of the screw for the removal of the wet solid from the surface of the screw. The device has no heating or cooling system, so prints were performed at room temperature.

All parts of the mixing device must be perfectly clean and dry before assembly. The two casing halves were secured with screws after inserting the feeder screw. This whole set is coupled to the hopper so that the motor shaft fits with the cavity in the feeder screw. Then, the hopper is loaded with the FCT powder, and the syringe pump, previously loaded with the liquid to be thickened, is connected to the upper inlet of the casing. When the device is loaded and ready for use, the desired flow ratio is configured via software. The resulting configurations for each concentration and mass flow are summarised in Table 7.

TABLE 7. Summary of the thickened fluids studied in this work

Texture	FCT concentration setpoint [wt.%][a]	Printing speed [mm/min]	w_s/w_{FCT}	Mass flow rate [g/min]
Nectar-like	1.6	600	1/4	2
			2/8	4
			3/12	6
			5/20	10
Honey-like	5.0	583	1/13	2
			2/26	4
			3/39	6
			4/52	8

Spoon-thick[b]	9.5	555	1/26	2
			2/52	4

[a] Manufacturer's recommended concentrations, indicated on product packaging
[b] The same mass flow rates have not been studied for all textures because, with shorter residence times, the mixing was not adequate, and very heterogeneous systems were obtained

However, owing to the high viscosity and stickiness of the system, the complexity in the mixing and flow of the material causes fluctuations in the final concentration. One of the goals of this work was to optimise the operating parameters and routines of the device to improve the accuracy of the concentrations obtained and thus ensure that the resulting thickened fluids had the right viscosity for each texture. Thus, the actual solid content of each sample was gravimetrically quantified.

4.3.3. Solid content accuracy

The first step in the evaluation of the applicability of the MIX3D accessory is to check that the concentrations obtained are correct according to the setpoint established via software in each case. Although this may seem trivial because the feeds have been correctly calibrated separately and without fluctuations in their flow, it is not. When FCT and water come into contact, a very sticky, highly viscous wet dough is created, whose flow properties change as it moves through the accessory and the degree of mixing increases. In addition, this process significantly depends on the concentration set. The handling of this wet dough is very complex and has led to numerous changes in the design of the device to avoid blockages, accumulations of solids, and total or partial clogging of the feed inlets, which were the main reasons why the concentrations obtained were very different from those expected. While the current design solves all these complications, there are still some fluctuations and variations in concentration among printed replicates. **FIGURE 48** shows the actual concentrations of all the blends processed with the MIX3D accessory throughout this study, and their deviation from the target concentrations.

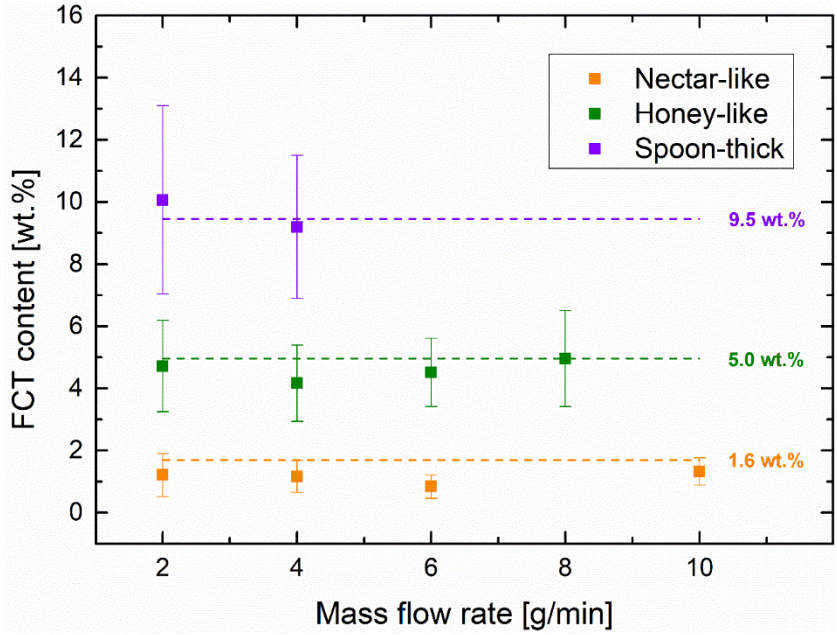

FIGURE 48. Actual FCT content of thickened fluids obtained with the MIX3D accessory at different mass flow rates

FIGURE 48 illustrate the complexity of the flow of the solid/liquid blend and its dependence on concentration, as discussed previously. At all flow rates, the average solid content of the nectar-like blends was 1.1 ± 0.5 wt.%. The variability among the concentrations obtained was minimal in this case. However, this value

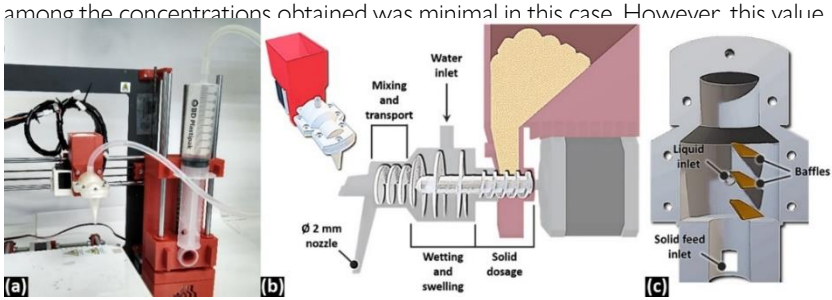

FIGURE 47) and the slight accumulation of solid stuck to the different elements of the accessory. In the first case, the moistened solid in the feed zone causes a

reduction in the flow of the solid, which results in a concentration drop. In fact, this is most likely the cause of the average solids content below the setpoint for nectar- and honey-like textures, as the lower linear velocity induced by the screw and the presence of a greater amount of water within the device induces the liquid to flow back more easily. In the second case, the solid accumulated in the small dead zones of the device causes the concentration to be slightly lower at the beginning of the operation and higher afterwards. However, the variation caused by this effect is minor (the device is designed to minimise dead zones and baffles avoid the adhesion of solid to the surface of the screw) and is only noticeable for the more concentrated blends (spoon-thick samples) since, in those with a higher water content, the solid dissolves better and does not accumulate.

FIGURE 48 also shows that, for nectar- and honey-like textures, the concentrations are more accurate at both low (2 g/min) and high (8 or 10 g/min, depending on the case) flow rates, with intermediate flows being more distant from the setpoint. At low rates, the residence time is higher and the solid is better dissolved in most of its path. When the solid is properly dissolved, the gel formed is not sticky, as in the case of the initial mixture; instead, it is slippery and flows easily. On the other hand, at high flow rates, the rapid linear advance of the screw rotating at high speed prevents the liquid from flowing back into the dry solid feeding zone, which has already been described as one of the most common complications. Thus, the intermediate flow values, in which none of these favourable situations occur, are those that present the greatest difficulty; thus, they are the values that are generally farthest from the setpoint.

4.3.4. Flow measurements

One of the main goals of the design of products for patients with dysphagia is to meet the prescribed requirements in terms of viscosity/consistency for a safe swallowing process. The addition of beverages and foods with inadequate viscosity increases the risk of aspiration and poses a real threat to their health, especially when the viscosity is lower than specified, as most patients with dysphagia have more problems swallowing thin liquids [22,122,128,136,152,403].

FIGURE 49A shows the viscosity values of FCT/water blends processed with the MIX3D accessory measured at 50 s^{-1} and 25 °C (η_{50}) according to NDD

criteria. The largest points correspond to the average values and their standard deviations from the values obtained for each target concentration setpoint (1.6, 5.0, and 9.5 wt.%). On the other hand, black unfilled points refer to η_{50} values measured for hand-prepared blends, i.e. the conventional preparation method.

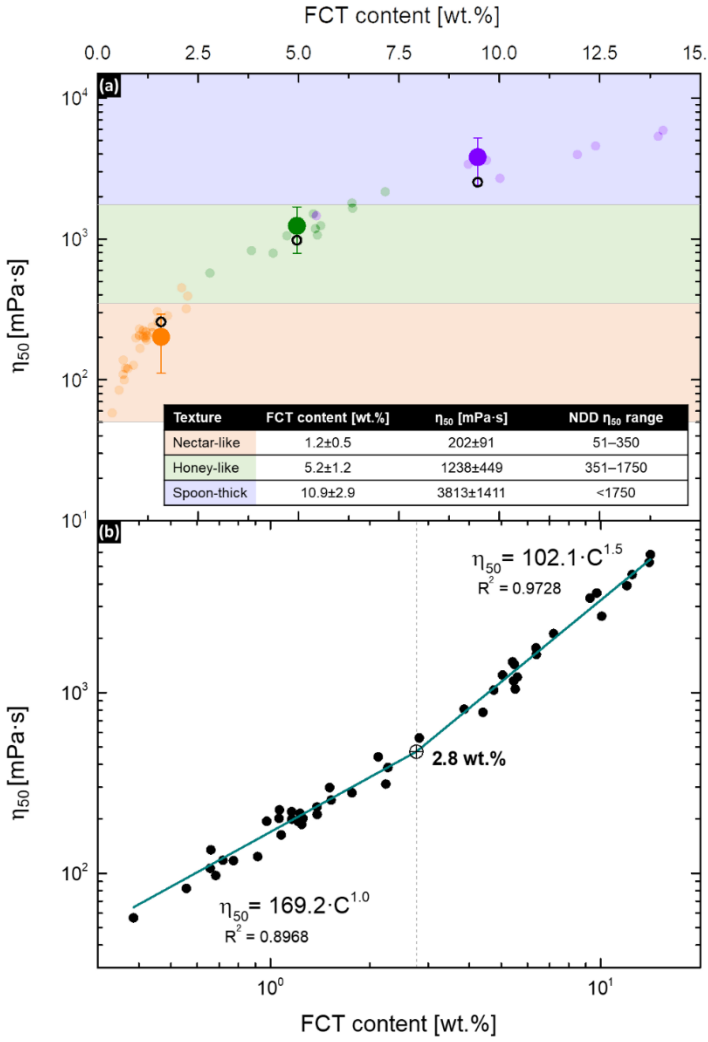

FIGURE 49. Viscosity at a shear rate of 50 s^{-1} and a temperature of 25 °C versus FCT content in (a) semi-log scale (bigger points represent mean values for each texture, and black unfilled points represent the values of hand-prepared samples) and (b) log-log scale, fitted to intersecting power-law models

As can be seen from the figure, most of the values are within the recommended viscosity range, and only a few printed replicates, such as the intended honey-like sample showing the lowest viscosity of the spoon-thick texture (highest green point), or the intended spoon-thick sample showing the highest viscosity of the honey-like texture (lowest violet point), have textures different from the target ones. Above all, it must be emphasised that the averages of the viscosity values and their standard deviations are within the limits established for the three textures.

The η_{50} as a function of the concentration in a log-log scale (**FIGURE 49B**) follow a linear trend, corresponding to a power-law expression, with a change in slope at a concentration of approximately 2.8 wt.%. This type of viscosity dependence on concentration is very common in hydrocolloid solutions, with changes in slope (or intersection between different potential models) being taken as critical concentrations and boundaries between different concentration regimes. The overlap concentration (C*), which separates the diluted and semi-diluted unentangled regimes, and the entanglement concentration (C_e), which is the boundary between the semi-diluted unentangled/entangled regimes, are the critical concentrations most commonly found in polymer solutions, although more or less regions may be observed depending on the type of polymer [246,404,405]. Critical concentrations are usually obtained from the evaluation of zero-shear or specific viscosities and, because the increase in viscosity with concentration in shear-thinning fluids becomes less significant with increasing shear rate [240], the slopes obtained are smaller than those obtained in zero-shear conditions. Hence, the results obtained in this study are difficult to compare with those of previous studies, regarding the determination of the critical concentration. However, the critical concentration value found in this study (2.8 wt.%) is in good agreement with the entanglement concentrations of different starches [406], which is, along with xanthan gum, one of the major components of FCT. On the contrary, the overlap concentration is usually found at much lower concentrations for starch and xanthan gum solutions [246,407].

As mentioned in the Introduction section, although the NDD criterion for classifying textures is only the viscosity at 50 s^{-1}, there are different shear rates to which foods and beverages are subjected to during swallowing [22,142,156,163,401]. Therefore, it is interesting to evaluate the viscous flow properties of these

products over a wide range of shear rates. **FIGURE 50** shows the shear rate dependence of the viscosity for some selected blends.

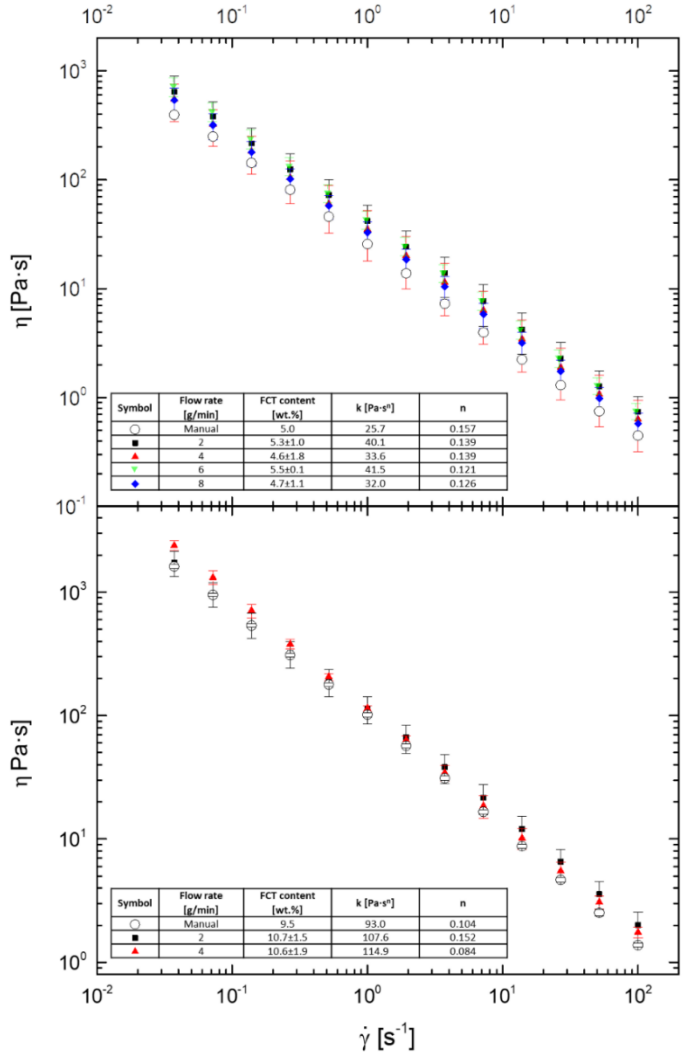

FIGURE 50. Flow curves and values of power-law fitting parameters for nectar-like and spoon-thick blends processed with the MIX3D accessory and for hand-prepared blends

Independently from the printing flow rate, the MIX3D accessory generally provides thickened samples with viscosity values and shear rate dependence comparable to those prepared by hand. The flow curves included in Figure 4 correspond to the average data for each flow rate. The standard deviation of the viscosities is represented as error bars, whereas the variability of the thickener concentration is indicated in the legends. The legends of Figure 4 also shows the parameters resulting from the fitting of the different average flow curves to the power-law model performed as follows (the inclusion of the fittings has been avoided for the sake of clarity):

$$\eta = k\dot{\gamma}^{n-1} \tag{18}$$

where η is the apparent viscosity, $\dot{\gamma}$ is the shear rate, k is the consistency index, and n is the flow index. The power-law fitting parameters also reflect the previously discussed differences in η_{50}. The consistency index (k) is very sensitive to changes in concentration and, considering the fact that it represents the viscosity value at 1 s^{-1}, it also reflects the variations at low or moderate shear rates. Although the flow response of printed systems is very similar to that of hand-prepared ones, it is apparent that the former generally show slightly higher viscosity values than manually mixed blends, which could be due to the significantly lower bulk viscosity induced by the lower amount of air trapped in the printed samples, as illustrated in **FIGURE 51**.

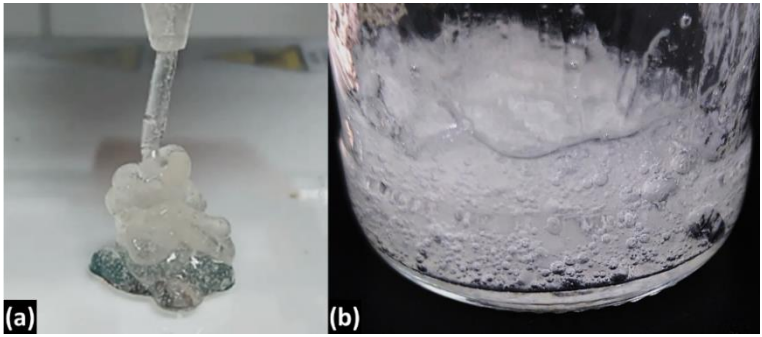

FIGURE 51. Images of spoon-thick blends (a) processed with MIX3D accessory and (b) prepared by hand

As a result, hand-mixed samples had lower viscosity than the MIX3D accessory processed samples with the same (or even lower) effective concentrations.

4.3.5. Linear viscoelasticity

The viscoelastic responses of the obtained blends in SAOS experiments were also analysed, and the results for selected blends printed at a 2 g/min flow rate are shown in Figure 52. The samples were subjected to frequency sweeps within the linear viscoelasticity regime. From **FIGURE 52**, it can be observed that the dependence of the moduli on frequency is weaker as the thickener concentration increases, yielding gel-like responses, which evolve from soft gel, for the nectar-like texture, to a strong gel, for the spoon-thick consistency.

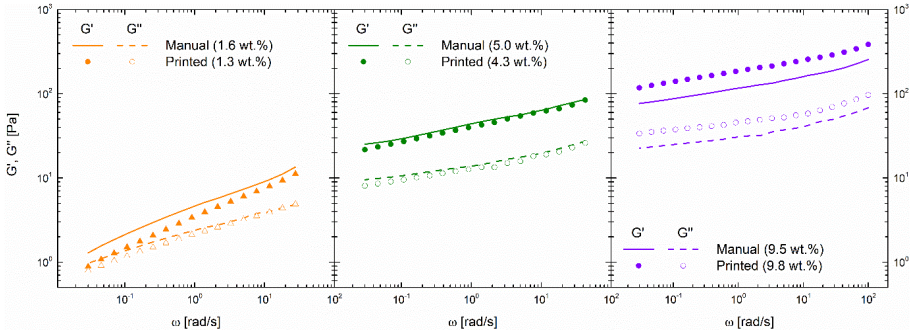

FIGURE 52. Viscoelastic response of FCT/water (a) nectar-like, (b) honey-like, and (c) spoon-thick blends processed with the MIX3D accessory

A well-developed plateau region, with low values of the slope of the plots of G' and G" as a function of the angular frequency, characteristic of strong gels, is apparent in the spoon-thick system, whereas a tendency to reach a crossover between the G' and G' curves can be observed at low frequencies for the nectar-like system. However, in all cases, a predominant solid-like behaviour is observed; in particular, the storage modulus (G') is higher than the loss modulus (G") over the entire frequency range considered. This confirms that the concentration of all the mixtures studied are above the overlap concentration because, below this concentration, the diluted solutions must show a viscoelastic response characterised by G" values higher than G' in a wide frequency range as well as a high dependence of both SAOS functions on the frequency [242].

Again, samples obtained with the MIX3D accessory show values of both moduli very close to those of the samples obtained by manual mixing, despite having a FCT content sometimes lower than that of hand-mixed samples. However,

blends with spoon-thick textures processing with the MIX3D accessory generally have higher SAOS moduli than those obtained by manual mixing, probably owing to the lower amount of air bubbles incorporated, as discussed in the previous section.

4.3.6. Thickening of common beverages

The MIX3D accessory was also used to thicken both commercial orange juice and skimmed milk. Samples were mixed at 2 g/min to obtain the spoon-thick target texture, as this is the most interesting consistency to take advantage of all features of 3D printing. **FIGURE 53** shows plots of the viscosity and linear viscoelasticity as functions of the shear rate/frequency of the FCT-thickened orange juice, skimmed milk, and water obtained with the MIX3D accessory and by manual mixing.

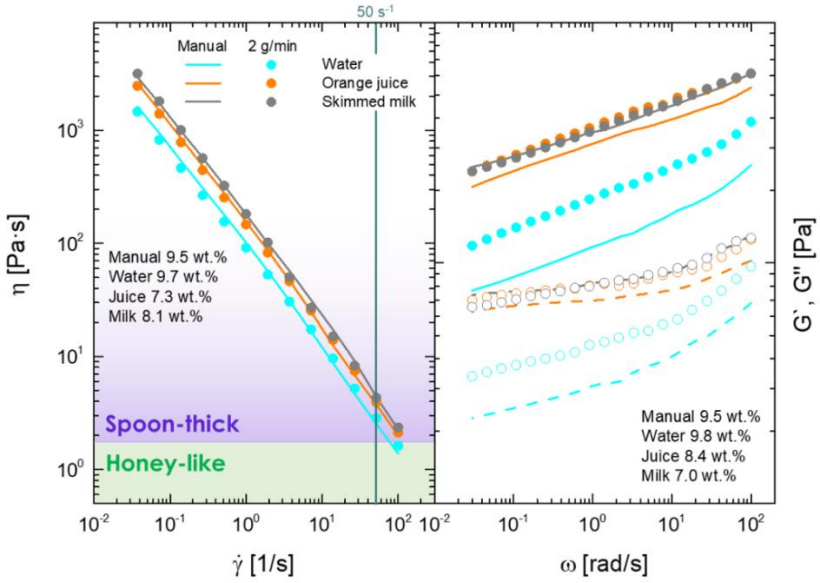

FIGURE 53. (a) Viscosity vs. shear rate and (b) linear viscoelastic functions vs. frequency of FCT-thickened orange juice, skimmed milk, and water

From **FIGURE 53**, it can be seen that higher values of viscosity and linear viscoelastic functions are obtained for thickened juice and milk than for thickened water. This is not surprising because the influence of the dispersing fluid on the

rheological properties of thickened fluids is a well-known issue; the thickening effect of a given hydrocolloid is different for different dispersing media [280,286–288].

The most remarkable aspect of these results is that, by using the MIX3D accessory, similar viscous and linear viscoelastic responses to those obtained by manual mixing may be obtained, although a lower amount of thickener is needed (see inlets in Figure 7). More specifically, similar viscosity and linear viscoelastic values as those shown by a 9.5 wt.% hand-prepared thickened milk have been achieved by using 8.1 wt.% (for viscosity) and a 7.0 wt.% (for linear viscoelasticity functions) skimmed milk, respectively, with the mixing accessory. In the case of orange juice, the viscosity of the manually thickened fluid was matched by using a 7.3 wt.% thickener concentration. On the other hand, the 8.4 wt.% thickener mixed with the accessory has storage and loss moduli values slightly higher than those of the manually mixed 9.5 wt.% thickener.

Conclusions

CHAPTER 5
Conclusions

Based on the results obtained throughout this research work, the following conclusions can be highlighted:

- 3D printed κ-carrageenan gels were successfully obtained by means of a RepRap 3D printer, which was modified to be able to in situ gellify carrageenan-in-water dispersions.
- Thus printed gels can be obtained in a few minutes, exhibiting a rheological response comparable to that prepared conventionally by a process of 2 h duration. This seems to mean that, in spite of how briefly the material is inside the 3D printer, it is sufficient for the different transitions necessary for the development of the gel network.
- The multivariate analysis carried out on SAOS parameters obtained for 3D printed κ-carrageenan allowed to determine the effect of the main printing parameters (layer height, printing speed and hotend temperature) on the rheological response of gel structures created during printing process. In general, it can be concluded that an elevated temperature, together with a reduced velocity and layer height, favours the structuring of carrageenan, giving rise to gel networks with more intense interactions.
- Taking into account the influence of speed and layer height on printing time, printing variables can be optimised to obtain a final product with a given specification.
- The results of this study validate the proposed MIX3D accessory for the development of dysphagia-oriented products for in-situ application.
- The proposed accessory overcomes the limitations of the in situ mixing of solids and liquids.
- The proposed accessory is compatible with and operated by the firmware and hardware of a 3D printer and allows the implementation of additional feeds without complications, as well as the automatic and simple processing of foods with controlled rheological characteristics. This allows the design of foods with appetising colours, odours, and tastes and attractive shape to favour patient acceptance.

- The in situ mixing of solid and liquid feed during a continuous 3D printing process was successfully achieved in this study. The accessory was shown to successfully thicken water, orange juice, and skimmed milk.
- Although there are some fluctuations in the final thickener concentration as well as in the flow of the mixture along the device, they are low enough to achieve viscosity values within the range required for each texture (nectar-like, honey-like, and spoon-thick). These fluctuations are mainly due to the stickiness and high viscosity of the product during mixing and therefore become more evident as the solid content increases.
- The introduction of air into the blends prepared with the accessory is minimal compared to that observed in the manual preparation, resulting in slightly higher viscosities and more homogeneous and transparent blends.
- The MIX3D device could be improved by designing it with more resistant materials (e.g. machined metal), which allow the reduction in the size of the accessory (note that small plastic pieces are too fragile). In this way, contact between phases could be improved, the residence time required for mixing could be reduced, and the response speed of the system to changes in setpoint could be increased. Increasing the contact between phases also allows the increase in the mass flow rates while ensuring adequate mixing.

Annexes

ANNEXES

El artículo "3D printing in situ gelification of κ- carrageenan solutions: effect of printing variables on the rheological response" que forma parte del apartado Annexes, ha sido retirados de la tesis debido a restricciones relativas a derechos de autor. En sustitución del artículo ofrecemos la siguiente información: referencia bibliográfica, enlace a la revista y resumen.

-Diañez, I., Gallegos, C., Brito-de la Fuente, E., Martínez, I., Valencia, C., Sánchez, M. C., Diaz, M. J., & Franco, J. M. (2019). 3D printing in situ gelification of κ-carrageenan solutions: Effect of printing variables on the rheological response. Food Hydrocolloids, 87, 321–330. https://doi.org/10.1016/j.foodhyd.2018.08.010

Enlace al texto completo del artículo: https://doi.org/10.1016/j.foodhyd.2018.08.010

RESUMEN:
This work reports a successful 3D printing-based in situ temperature-induced gelification procedure of κ-carrageenan aqueous dispersions. 3D printer was modified to handle low viscosity fluid feeding and more efficiently distribute ambient air at room temperature causing forced convection to accelerate the cooling of the printed layer. Thus, obtained gel samples, containing 30 mg/g κ-carrageenan in water, showed self-sustaining capability and a rheological response comparable with a reference conventionally prepared gel. Moreover, the effect of main printing variables, such as temperature of the hotend, printing speed and layer height, on the linear viscoelastic response of the gels was analysed by application of the response surface methodology (RSM). In general, gel strength linearly increases by decreasing printing speed and layer height whereas not noticeable improvement in gel strength was achieved by applying hotend temperatures above 80–85 °C. Based on the results obtained from this analysis, an optimisation method is proposed to minimise the temperature and time needed to 3D print a gel with pre-set rheological properties. Overall, this study demonstrates that it is possible to generate in situ 3D printed gel materials with potential uses in food and pharmaco-nutrition, without the aid of reactive additives or initiators, and using a facile protocol.

Annexes

PUBLISHED ARTICLE

3D PRINTING IN SITU GELIFICATION OF K-CARRAGEENAN SOLUTIONS: EFFECT OF PRINTING VARIABLES ON THE RHEOLOGICAL RESPONSE

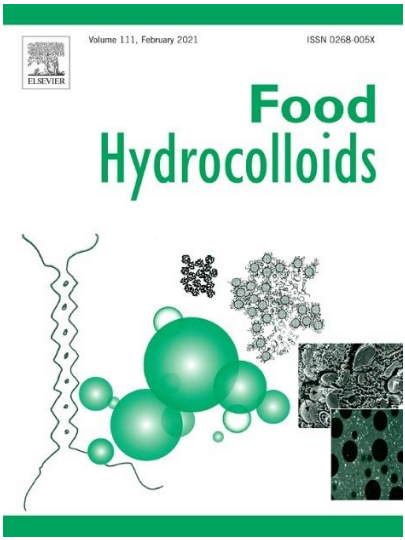

Author:
I. Diañez, C. Gallegos, E. Brito-de la Fuente, I. Martínez, C. Valencia, M.C. Sánchez, M.J. Diaz, J.M. Franco

Publication:
Food Hydrocolloids (Volume 87, Pages 321-330)

Publisher:
Elsevier

Date:
February 2019

ARTICLE UNDER REVIEW

IMPLEMENTATION OF A NOVEL CONTINUOUS SOLID/LIQUID MIXING ACCESSORY FOR 3D PRINTING OF DYSPHAGIA-ORIENTED THICKENED FLUIDS

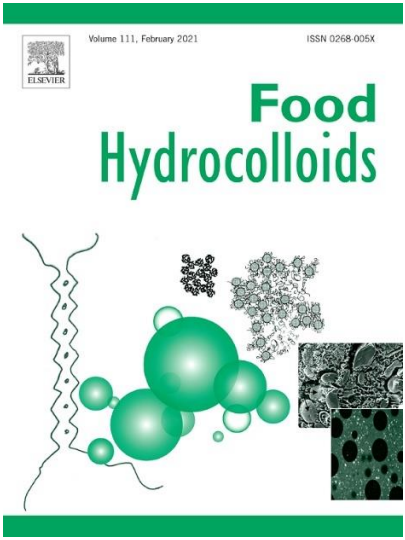

Author:
I. Diañez, C. Gallegos, E. Brito-de la Fuente, I. Martínez, C. Valencia, M.C. Sánchez, J.M. Franco

Publication:
Food Hydrocolloids

Publisher:
Elsevier

Submission date:
December 2020

Manuscript File

Implementation of a novel continuous solid/liquid mixing accessory for 3D printing of dysphagia-oriented thickened fluids

I. Diañez[a], C. Gallegos[b], E. Brito-de la Fuente[b], I. Martínez[a], C. Valencia[a], M.C. Sánchez[a], J.M. Franco[a,*]

[a] Pro²TecS – Chemical Process and Product Technology Center. Dpto. Ingeniería Química. ETSI. Campus de "El Carmen". Universidad de Huelva. 21071, Huelva. Spain.

[b] Product & Process Engineering Centre, Fresenius Kabi Deutschland GmbH, 61352 Bad Homburg, Germany

ABSTRACT

This paper describes the implementation and evaluation of an accessory designed and manufactured to be adapted to a 3D printer to allow the in situ and continuous mixing of solid and liquid feeds. In particular, the capacity of this accessory to correctly mix a dysphagia-oriented commercial powder thickener with several conventional fluids (i.e. water, juice, and milk) was studied. Target thickener concentrations were defined in order to achieve mixtures with viscosities corresponding to the textures established by the National Dysphagia Diet Task Force (NDD)—nectar-like, honey-like, and spoon-thick—for thickened fluids. Both the accuracy of the solid content and the rheological response of the obtained mixtures were evaluated. Although fluctuations were observed in the concentrations of the mixtures obtained by continuous mixing with respect to the target values, the viscosities obtained were within the limits established for each of the desired textures. The thickened fluids processed using the 3D printing mixing accessory showed viscosities very similar to their hand-mixed counterparts and a higher degree of structuration, especially when printed at low mass flow rates, as well as a lower amount of entrapped air. This method of preparation allows the production of thickened fluids with more appealing shapes and colours for the long-term dysphagia management, improving the quality of life of patients with dysphagia, and promoting treatment compliance.

Keywords: 3D printing; dysphagia; gels; mixing; thickened fluids; rheology.

1. Introduction

Swallowing difficulty (dysphagia) is a problem that, according to the most conservative estimates, affects approximately 8% of the world's population (Cichero et al., 2013). Dysphagia can be a consequence of a multitude of neurological, muscular, and structural pathologies or can even be drug-induced (Shaker, 2006). It can lead to very serious complications, including malnutrition and

dehydration as well as severe respiratory problems, such as aspiration pneumonia, resulting from the aspiration of food or fluids into the airways (Carrión et al., 2019; Pere Clavé & Shaker, 2015). As a result, dysphagia is associated with increased morbidity, worse prognoses, longer hospital stays, more frequent readmissions, and, in turn, higher mortality rates (Attrill et al., 2018; Cabré et al., 2013).

One of the most widely used interventions in the management of dysphagia is the thickening of low-viscosity liquids, as these normally present the greatest risk of aspiration (Andersen et al., 2013; Newman et al., 2016). Fresubin® Clear Thickener (FCT) is a gum-based α-amylase-resistant powder thickener that is widely used for modifying the rheological behaviour of fluids in dysphagia management (Turcanu et al., 2018). As the thickener increases the viscosity of the fluids, the flow rate of the bolus during swallowing is significantly reduced, increasing the chances of the airways being secured in time to prevent aspiration (Inamoto et al., 2013; Qazi et al., 2019). However, because the viscosity required for safe swallowing varies from patient to patient (Choi et al., 2011; P. Clavé et al., 2006), several levels of thickening are established. The most common and accepted classification is that given by the National Dysphagia Diet Task Force (NDD); according to this classification, at a shear rate of 50 s^{-1} and a temperature of 25 °C the viscosity values are as follows (American Dietetic Association, 2002):

- Thin liquid: 1–50 mPa·s
- Nectar-like: 51–350 mPa·s
- Honey-like: 351–1750 mPa·s
- Spoon-thick: <1750 mPa·s

However, although this classification is universally accepted at the level of the medical community, it is excessively simplistic, as it does not consider the non-Newtonian character of these thickened fluids or the different effective shear rates along the upper digestive tract (Brito-de la Fuente et al., 2019; Nutritional Aspects of Dysphagia Management, 2017; Salinas-Vázquez et al., 2014). In addition, the influence of saliva in the rheological properties of these thickened products should also be taken into account to improve the management of dysphagia (Herranz et al., 2021).

The dose of FCT required to obtain these consistencies (nectar-like and higher) starting from Newtonian fluids as well as the way to prepare thickened liquids by manual mixing are indicated on the FCT packaging. However, although these instructions indicate how to reduce the inlet of air and consequent formation of bubbles in the mixture as much as possible, this is almost impossible in manual mixing and even more difficult with other mechanical means (such as blenders) (Sopade, Halley, Cichero, Ward, Hui, et al., 2008). Furthermore, it can be difficult for this process to be repeated from one preparation to another, especially if mixing is performed by different people.

These complications, in the worst case, can lead to a significant decrease in the viscosity of the mixture, thus the failure to meet the specific requirements for each texture.

To minimise these drawbacks while providing new and interesting features, in this study, a new mixing device was designed and manufactured to be adapted to a 3D printer and controlled by its firmware, allowing the continuous and automatic in situ mixing of (at least) one solid and one liquid feed. This device can simply be used as an automatic mixer to obtain mixtures with proportions controlled via software. In this way, it exhibits advantages over manual preparation, because the introduction of air into the system during manual mixing is unavoidable (especially in mixtures with high viscosity). This new preparation method allows mixing without letting air enter the system; the few small air bubbles that can be observed in mixtures are due solely to the air trapped between the solid particles, which can be minimised by controlling the granulometry.

In addition, through the use of additional feeds, more complex mixtures containing nutrients, drugs, or even colouring and/or flavouring agents can be prepared. When used to obtain concentrated systems (>10 wt.%) with viscosities that allow self-sustainment to form three-dimensional configurations, shape can be another key element in making thickened fluids more palatable and appealing for dysphagia patients. With the device coupled to a 3D printer, which allows it to be moved in three dimensions, gel models can be designed and printed with appealing shapes similar to conventional foods, which could make clinical nutrition more attractive to patients and less repetitive in long-term treatments (Diañez et al., 2019). Making thickened fluids more attractive is of utmost importance, as the lack of acceptance of these products by patients is a well-known issue. Patients' dislike of thickened fluids has, on the one hand, a very significant negative effect on their quality of life and, on the other hand, negative effects due to the potential non-compliance with treatment or reduced fluid and food intake (Colodny, 2005; Lim et al., 2016; Low et al., 2001).

The objective of this study was to develop and validate a novel device designed for the continuous mixing of solids and liquids, hereinafter referred to as the MIX3D accessory, controlled by the firmware of a RepRap 3D printer to which it is attached in order to be applied for dysphagia management. This device can mix a liquid (water, juice, and milk) with FCT to obtain mixtures at different concentrations covering the range from nectar-like to spoon-thick consistencies. The actual content of solids and the final rheological behaviour of the mixtures obtained with the proposed device were evaluated.

2. Experimental

2.1. Materials

FCT was provided by Fresenius Kabi Deutschland GmbH and used as received to be fed into the hopper of the MIX3D accessory for subsequent mixing with distilled water. Orange juice with no added sugar (Juver SA, Spain) and skimmed milk (Covap, Spain), purchased in a local store, were also used as alternative solvents.

2.2. 3D printer

The BQ Hephestos 3D printer DIY kit designed by BQ (Spain) and the electronics (Arduino Mega 2560 and RAMPS 1.4 shield) were purchased from Ícarus Informática (Spain). All parts of the MIX3D accessory (excluding stepper motor and screws) were designed in our laboratory and printed with an unmodified BQ Hephestos.

The different models printed during this study were designed using the AutoCAD 2018 software and Tinkercad online app. The 3D models were sliced using the Ultimaker Cura software, and the 3D printer was controlled during operation using the Repetier-Host software.

To mix solids and liquids during printing, the equipment must handle both types of feeds separately. The liquid feed is dosed using a syringe pump driven by a motor directly connected to the printer electronics to be controlled as a conventional extruder (Figure 1a). This syringe pump was also designed and assembled from 3D printed parts and non-printable components supplied by 3DEspana (Spain). The solid, in powder form, is fed through a hopper and dosed by a feeder screw, which will also drive and mix the material during its flow through the MIX3D accessory (Figure 1b).

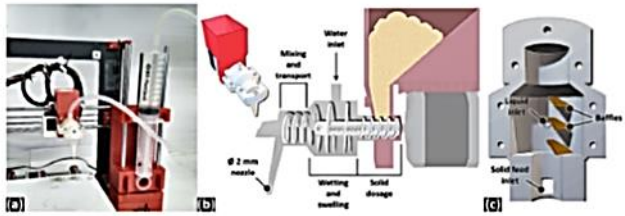

Figure 1. MIX3D accessory layout. (a) photograph of device and syringe pump setup, (b) schematic representation of the mixing device, (c) inside view of the upper half of the mixing device casing

The mixing screw is directly attached and driven by a NEMA 17 motor, which, like the one in the syringe pump, is configured as a conventional extruder to be controlled via software. The extruders can be operated simultaneously through a virtual extruder in Repetier-Host for which the flow ratio of both feeds can be controlled by means of a simple script. However, when a conventional 3D printer has multiple extruders, they are usually of the same type and geometry, so the flow ratio can be assigned directly. That is, by setting a weight of 50 (over 100) for each extruder, the material flow

would be the same. This is not the case in the proposed system, where the syringe pump and hopper are feeding systems with completely different geometries; for equal motor movement, they provide different material flows. Therefore, the first step to set a specific concentration is to calibrate each of the feeds passing through the system individually. Once each feed has been calibrated separately, it is possible to correct the weights and obtain the desired solid content.

The casing of the device is divided into two halves (upper and lower) to allow the insertion and removal of the screw as well as the cleaning of all components. The feeding inlets are located in the upper half to reduce the probability of clogging, while the mixing outlet is located at the end of the lower half. In addition, the upper part contains an array of baffles (Figure 1c) matching the truncated segments of the screw for the removal of the wet solid from the surface of the screw. The device has no heating or cooling system, so prints were performed at room temperature.

All parts of the mixing device must be perfectly clean and dry before assembly. The two casing halves were secured with screws after inserting the feeder screw. This whole set is coupled to the hopper so that the motor shaft fits with the cavity in the feeder screw. Then, the hopper is loaded with the FCT powder, and the syringe pump, previously loaded with the liquid to be thickened, is connected to the upper inlet of the casing. When the device is loaded and ready for use, the desired flow ratio is configured via software.

2.3. Calibration of the device and printing parameters

The firmware of the printer measures the advance of the motors (their rotation) in units of length. Thus, by setting the printer to print different distances and weighing the amount of material printed in each case, a flow rate value in g/mm can be obtained. This flow rate value, in turn, can be converted into the mass flow rate directly by means of the printing speed used (Eq. 1):

$$\dot{m} = fr \cdot v, \tag{1}$$

where $\dot{m}$ is the mass flow rate [g/min], fr is the flow rate [g/mm], and v is the printing speed [mm/min].

Since the geometries of the two feed systems are different, as are the flow rate values for the solvent (fr_s) and the solid (fr_{FCT}), therefore each of the flows has to be calibrated independently by weighing the amount of material supplied by the syringe pump and the screw for given motor advance lengths, resulting in:

$$fr_{FCT} = 1.13 \cdot \frac{10^{-3} g}{mm}, \qquad fr_s = 0.33 \frac{g}{mm}.$$

Once the characteristic flow rate of each feed system is known, a weight from 0 to 100 is applied to each motor to control the mixing ratio. A weight of 1 was assigned to the syringe pump motor (w_s), as it was the one with the highest feeding capacity. Then, the weight for the motor driving the screw

(w_{FCT}) was calculated to obtain the correct ratio in each case. However, the sum of the weights of the different motors must be equal to 100, so that a third 'ghost' motor is defined in order to absorb the excess weights. Different mass flows can be achieved by multiplying the weights of the FCT and solvent. For instance, considering the nectar-like concentration (1.6 wt.%),

$$\dot{m} = 2\ g/min \begin{cases} w_s = 1 \\ w_{FCT} = 4, \\ w_g = 95 \end{cases} \qquad \dot{m} = 4\ g/min \begin{cases} w_s = 2 \\ w_{FCT} = 8, \\ w_g = 90 \end{cases}$$

where w_s, w_{FCT}, and w_g are the weights of the solvent feeding motor, the FCT feeding motor, and "ghost" motor, respectively. Thus, the mixing mass flow rate can be calculated as follows:

$$\dot{m} = (w_{FCT} \cdot fr_{FCT} + w_s \cdot fr_s) \cdot v. \tag{2}$$

The printing speed was set to 600 mm/min for nectar-like blends and was slightly changed to compensate for the increased solid flow for the two higher concentrations. The resulting configurations for each concentration and mass flow are summarised in Table 1.

Table 1. Summary of the samples studied in this work

Texture	FCT concentration setpoint [wt.%][a]	Printing speed [mm/min]	w_s/w_{FCT}	Mass flow rate [g/min]
Nectar-like	1.6	600	1/4	2
			2/8	4
			3/12	6
			5/20	10
Honey-like	5.0	583	1/13	2
			2/26	4
			3/39	6
			4/52	8
Spoon-thick[b]	9.5	555	1/26	2
			2/52	4

[a] Manufacturer's recommended concentrations, indicated on product packaging
[b] The same mass flow rates have not been studied for all textures because, with shorter residence times, the mixing was not adequate, and very heterogeneous systems were obtained

However, owing to the high viscosity and stickiness of the system, the complexity in the mixing and flow of the material causes fluctuations in the final concentration. One of the goals of this work was to optimise the operating parameters and routines of the device to improve the accuracy of the concentrations obtained and thus ensure that the resulting thickened fluids had the right viscosity for each texture. Thus, the actual solid content of each sample was gravimetrically quantified. To this end, each sample was weighed before being placed in a Selecta Digitronic convection oven (Selecta SA, Spain), dried overnight at 90 °C, and weighed again the day after.

2.4. Rheological characterisation

Rheological characterisation of the MIX3D accessory-processed prints was carried out with a controlled stress rheometer (Physica MCR-301, Anton Paar, Austria). Viscous flow measurements

were performed within a range of shear rates of 0.01–100 s^{-1} at 25 °C using a 50 mm serrated plate geometry and a gap of 1 mm.
The same plate-plate geometry was used to perform small-amplitude oscillatory shear (SAOS) tests inside the linear viscoelastic region in a frequency range of 100–0.03 rad/s.

2.5. Statistical Analysis

For the evaluation of concentration accuracy, the solids content of at least seven samples was checked for each texture and flow rate. Among them, a minimum of eight samples (at least two at each flow rate) per level of consistency were subjected to viscous flow measurements, and four samples (two per flow rate) were subjected to SAOS tests. The standard deviation was calculated for each mean value as a measure of variability.

3. Results and discussion

3.1. Solid content accuracy

The first step in the evaluation of the applicability of the MIX3D accessory is to check that the concentrations obtained are correct according to the setpoint established via software in each case. Although this may seem trivial because the feeds have been correctly calibrated separately and without fluctuations in their flow, it is not. When FCT and water come into contact, a very sticky, highly viscous wet dough is created, whose flow properties change as it moves through the accessory and the degree of mixing increases. In addition, this process significantly depends on the concentration set. The handling of this wet dough is very complex and has led to numerous changes in the design of the device to avoid blockages, accumulations of solids, and total or partial clogging of the feed inlets, which were the main reasons why the concentrations obtained were very different from those expected. While the current design solves all these complications, there are still some fluctuations and variations in concentration among printed replicates. Figure 2 shows the actual concentrations of all the blends processed with the MIX3D accessory throughout this study, and their deviation from the target concentrations.

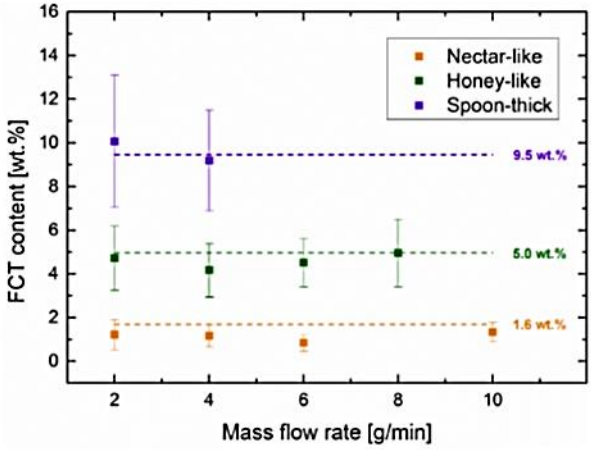

Figure 2. Actual FCT content of thickened fluids obtained with the MIX3D accessory at different mass flow rates

The figures illustrate the complexity of the flow of the solid/liquid blend and its dependence on concentration, as discussed previously. At all flow rates, the average solid content of the nectar-like blends was 1.1 ± 0.5 wt.%. The variability among the concentrations obtained was minimal in this case. However, this value is slightly lower than the target value. At all mass flows, the mean concentration values for honey-like and spoon-thick textures were 4.5 ± 1.3 and 9.6 ± 2.6 wt.%, respectively. For these consistencies, the variability was greater. Nevertheless, the averages are proportionally much closer to the set value, especially in the case of the spoon-thick blends. The sources of error in the concentration, as observed during the experimentation with the device, are the backward movement of liquid into the dry solid feed zone (Figure 1) and the slight accumulation of solid stuck to the different elements of the accessory. In the first case, the moistened solid in the feed zone causes a reduction in the flow of the solid, which results in a concentration drop. In fact, this is most likely the cause of the average solids content below the setpoint for nectar- and honey-like textures, as the lower linear velocity induced by the screw and the presence of a greater amount of water within the device induces the liquid to flow back more easily. In the second case, the solid accumulated in the small dead zones of the device causes the concentration to be slightly lower at the beginning of the operation and higher afterwards. However, the variation caused by this effect is minor (the device is designed to minimise dead zones and baffles avoid the adhesion of solid to the

surface of the screw) and is only noticeable for the more concentrated blends (spoon-thick samples) since, in those with a higher water content, the solid dissolves better and does not accumulate. Figure 2 also shows that, for nectar- and honey-like textures, the concentrations are more accurate at both low (2 g/min) and high (8 or 10 g/min, depending on the case) flow rates, with intermediate flows being more distant from the setpoint. At low rates, the residence time is higher and the solid is better dissolved in most of its path. When the solid is properly dissolved, the gel formed is not sticky, as in the case of the initial mixture; instead, it is slippery and flows easily. On the other hand, at high flow rates, the rapid linear advance of the screw rotating at high speed prevents the liquid from flowing back into the dry solid feeding zone, which has already been described as one of the most common complications. Thus, the intermediate flow values, in which none of these favourable situations occur, are those that present the greatest difficulty; thus, they are the values that are generally farthest from the setpoint.

3.2. Flow measurements

One of the main goals of the design of products for patients with dysphagia is to meet the prescribed requirements in terms of viscosity/consistency for a safe swallowing process. The addition of beverages and foods with inadequate viscosity increases the risk of aspiration and poses a real threat to their health, especially when the viscosity is lower than specified, as most patients with dysphagia have more problems swallowing thin liquids (Bolivar-Prados et al., 2019; Nutritional Aspects of Dysphagia Management, 2017; Leonard et al., 2014; Newman et al., 2016; Ortega et al., 2020; Quinchia et al., 2011).

Figure 3a shows the viscosity values of FCT/water blends processed with the MIX3D accessory measured at 50 s^{-1} and 25 °C (η_{50}) according to NDD criteria. The largest points correspond to the average values and their standard deviations from the values obtained for each target concentration setpoint (1.6, 5.0, and 9.5 wt.%). On the other hand, black unfilled points refer to η_{50} values measured for hand-prepared blends, i.e. the conventional preparation method.

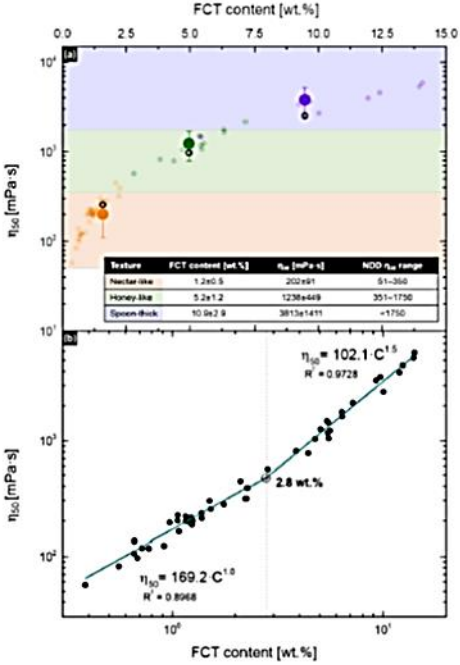

Figure 3. Viscosity at a shear rate of 50 s^{-1} and a temperature of 25 °C versus FCT content in (a) semi-log scale (bigger points represent mean values for each texture, and black unfilled points represent the values of hand-prepared samples) and (b) log-log scale, fitted to intersecting power-law models

As can be seen from the figure, most of the values are within the recommended viscosity range, and only a few printed replicates, such as the intended honey-like sample showing the lowest viscosity of the spoon-thick texture (highest green point), or the intended spoon-thick sample showing the highest viscosity of the honey-like texture (lowest violet point), have textures different from the target ones. Above all, it must be emphasised that the averages of the viscosity values and their standard deviations are within the limits established for the three textures.

266 The η_{50} as a function of the concentration in a log-log scale (Figure 3b) follow a linear trend,
267 corresponding to a power-law expression, with a change in slope at a concentration of
268 approximately 2.8 wt.%. This type of viscosity dependence on concentration is very common in
269 hydrocolloid solutions, with changes in slope (or intersection between different potential models)
270 being taken as critical concentrations and boundaries between different concentration regimes. The
271 overlap concentration (C*), which separates the diluted and semi-diluted unentangled regimes, and
272 the entanglement concentration (C_e), which is the boundary between the semi-diluted
273 unentangled/entangled regimes, are the critical concentrations most commonly found in polymer
274 solutions, although more or less regions may be observed depending on the type of polymer (Pollard
275 & Fischer, 2014; Wyatt & Liberatore, 2009; Zhang et al., 2016). Critical concentrations are usually
276 obtained from the evaluation of zero-shear or specific viscosities and, because the increase in
277 viscosity with concentration in shear-thinning fluids becomes less significant with increasing shear
278 rate (Lapasin et al., 1995), the slopes obtained are smaller than those obtained in zero-shear
279 conditions. Hence, the results obtained in this study are difficult to compare with those of previous
280 studies, regarding the determination of the critical concentration. However, the critical
281 concentration value found in this study (2.8 wt.%) is in good agreement with the entanglement
282 concentrations of different starches (Li et al., 2016), which is, along with xanthan gum, one of the
283 major components of FCT. On the contrary, the overlap concentration is usually found at much
284 lower concentrations for starch and xanthan gum solutions (Wang et al., 2001; Wyatt & Liberatore,
285 2009).
286 As mentioned in the Introduction section, although the NDD criterion for classifying textures is only
287 the viscosity at 50 s^{-1}, there are different shear rates to which foods and beverages are subjected to
288 during swallowing (Brito-de la Fuente et al., 2012, 2019; Nutritional Aspects of Dysphagia
289 Management, 2017; Qazi et al., 2019; Salinas-Vázquez et al., 2014). Therefore, it is interesting to
290 evaluate the viscous flow properties of these products over a wide range of shear rates. Figure 4
291 shows the shear rate dependence of the viscosity for some selected blends.

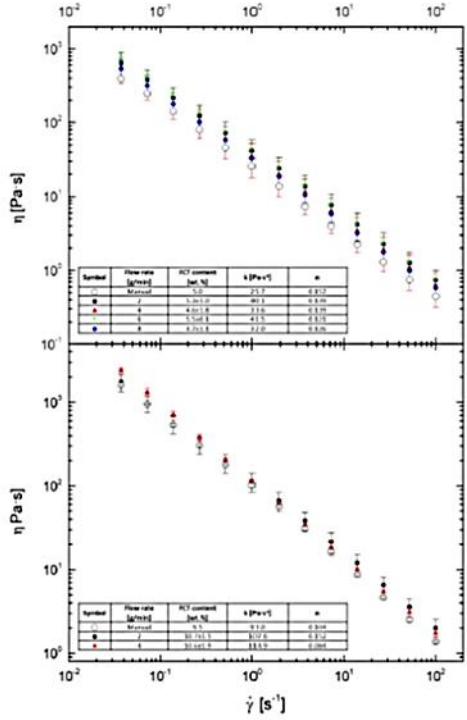

292

293 *Figure 4. Flow curves and values of power-law fitting parameters for nectar-like and spoon-thick blends*
294 *processed with the MIX3D accessory and for hand-prepared blends*

295 Independently from the printing flow rate, the MIX3D accessory generally provides thickened
296 samples with viscosity values and shear rate dependence comparable to those prepared by hand.
297 The flow curves included in Figure 4 correspond to the average data for each flow rate. The standard
298 deviation of the viscosities is represented as error bars, whereas the variability of the thickener
299 concentration is indicated in the legends. The legends of Figure 4 also shows the parameters

resulting from the fitting of the different average flow curves to the power-law model performed as follows (the inclusion of the fittings has been avoided for the sake of clarity):

$$\eta = k\dot{\gamma}^{n-1}, \quad [3]$$

where η is the apparent viscosity, $\dot{\gamma}$ is the shear rate, k is the consistency index, and n is the flow index. The power-law fitting parameters also reflect the previously discussed differences in η_{∞}. The consistency index (k) is very sensitive to changes in concentration and, considering the fact that it represents the viscosity value at 1 s^{-1}, it also reflects the variations at low or moderate shear rates. Although the flow response of printed systems is very similar to that of hand-prepared ones, it is apparent that the former generally show slightly higher viscosity values than manually mixed blends, which could be due to the significantly lower bulk viscosity induced by the lower amount of air trapped in the printed samples, as illustrated in Figure 5.

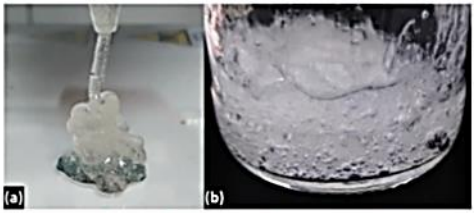

Figure 5. Images of spoon-thick blends (a) processed with MIX3D accessory and (b) prepared by hand

As a result, hand-mixed samples had lower viscosity than the MIX3D accessory processed samples with the same (or even lower) effective concentrations.

3.3. Linear viscoelasticity

The viscoelastic responses of the obtained blends in SAOS experiments were also analysed, and the results for selected blends printed at a 2 g/min flow rate are shown in Figure 6. The samples were subjected to frequency sweeps within the linear viscoelasticity regime. From Figure 6, it can be observed that the dependence of the moduli on frequency is weaker as the thickener concentration increases, yielding gel-like responses, which evolve from soft gel, for the nectar-like texture, to a strong gel, for the spoon-think consistency.

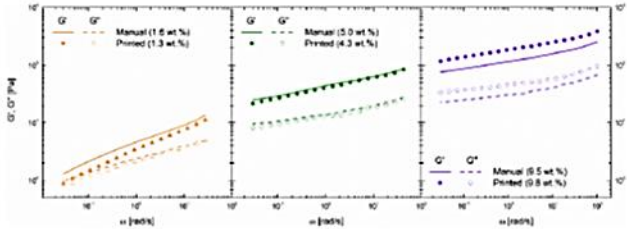

Figure 6. Viscoelastic response of FCT/water (a) nectar-like, (b) honey-like, and (c) spoon-thick blends processed with the MIX3D accessory

A well-developed plateau region, with low values of the slope of the plots of G' and G" as a function of the angular frequency, characteristic of strong gels, is apparent in the spoon-thick system, whereas a tendency to reach a crossover between the G' and G' curves can be observed at low frequencies for the nectar-like system. However, in all cases, a predominant solid-like behaviour is observed; in particular, the storage modulus (G') is higher than the loss modulus (G") over the entire frequency range considered. This confirms that the concentration of all the mixtures studied are above the overlap concentration because, below this concentration, the diluted solutions must show a viscoelastic response characterised by G" values higher than G' in a wide frequency range as well as a high dependence of both SAOS functions on the frequency (Sworn, 2007).

Again, samples obtained with the MIX3D accessory show values of both moduli very close to those of the samples obtained by manual mixing, despite having a FCT content sometimes lower than that of hand-mixed samples. However, blends with spoon-thick textures processing with the MIX3D accessory generally have higher SAOS moduli than those obtained by manual mixing, probably owing to the lower amount of air bubbles incorporated, as discussed in the previous section.

3.4. Thickening of common beverages

The MIX3D accessory was also used to thicken both commercial orange juice and skimmed milk. Samples were mixed at 2 g/min to obtain the spoon-thick target texture, as this is the most interesting consistency to take advantage of all features of 3D printing (see example of printing a thickened-orange juice in movie M1 of the supporting information). Figure 7 shows plots of the viscosity and linear viscoelasticity as functions of the shear rate/frequency of the FCT-thickened orange juice, skimmed milk, and water obtained with the MIX3D accessory and by manual mixing.

348

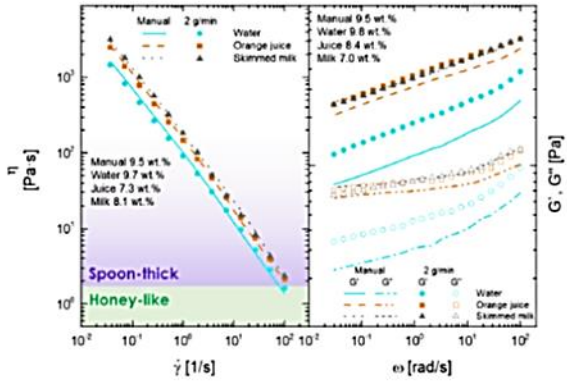

349

350 *Figure 7. (a) Viscosity vs. shear rate and (b) linear viscoelastic functions vs. frequency of FCT-thickened orange*
351 *juice, skimmed milk, and water*

352 From Figure 7, it can be seen that higher values of viscosity and linear viscoelastic functions are
353 obtained for thickened juice and milk than for thickened water. This is not surprising because the
354 influence of the dispersing fluid on the rheological properties of thickened fluids is a well-known
355 issue; the thickening effect of a given hydrocolloid is different for different dispersing media (Moret-
356 Tatay et al., 2015; Sopade et al., 2007; Sopade, Halley, Cichero, Ward, Hui, et al., 2008; Sopade,
357 Halley, Cichero, Ward, Liu, et al., 2008).
358 The most remarkable aspect of these results is that, by using the MIX3D accessory, similar viscous
359 and linear viscoelastic responses to those obtained by manual mixing may be obtained, although a
360 lower amount of thickener is needed (see inlets in Figure 7). More specifically, similar viscosity and
361 linear viscoelastic values as those shown by a 9.5 wt.% hand-prepared thickened milk have been
362 achieved by using 8.1 wt.% (for viscosity) and a 7.0 wt.% (for linear viscoelasticity functions)
363 skimmed milk, respectively, with the mixing accessory. In the case of orange juice, the viscosity of
364 the manually thickened fluid was matched by using a 7.3 wt.% thickener concentration. On the other
365 hand, the 8.4 wt.% thickener mixed with the accessory has storage and loss moduli values slightly
366 higher than those of the manually mixed 9.5 wt.% thickener.
367

4. Concluding remarks

The results of this study validate the proposed MIX3D accessory for the development of dysphagia-oriented products for in-situ application. The proposed accessory overcomes the limitations of the in situ mixing of solids and liquids. The proposed accessory is compatible with and operated by the firmware and hardware of a 3D printer and allows the implementation of additional feeds without complications, as well as the automatic and simple processing of foods with controlled rheological characteristics. This allows the design of foods with appetising colours, odours, and tastes and attractive shape to favour patient acceptance.

The in situ mixing of solid and liquid feed during a continuous 3D printing process was successfully achieved in this study. The accessory was shown to successfully thicken water, orange juice, and skimmed milk. Although there are some fluctuations in the final thickener concentration as well as in the flow of the mixture along the device, they are low enough to achieve viscosity values within the range required for each texture (nectar-like, honey-like, and spoon-thick). These fluctuations are mainly due to the stickiness and high viscosity of the product during mixing and therefore become more evident as the solid content increases.

Furthermore, the introduction of air into the blends prepared with the accessory is minimal compared to that observed in the manual preparation, resulting in slightly higher viscosities and more homogeneous and transparent blends.

The MIX3D device could be improved by designing it with more resistant materials (e.g. machined metal), which allow the reduction in the size of the accessory (note that small plastic pieces are too fragile). In this way, contact between phases could be improved, the residence time required for mixing could be reduced, and the response speed of the system to changes in setpoint could be increased. Increasing the contact between phases also allows the increase in the mass flow rates while ensuring adequate mixing.

5. References

American Dietetic Association. (2002). *National Dysphagia Diet: Standardization for Optimal Care*. American Dietetic Association. https://books.google.es/books?id=MZ5mSbGPOE4C

Andersen, U. T., Beck, A. M., Kjaersgaard, A., Hansen, T., & Poulsen, I. (2013). Systematic review and evidence based recommendations on texture modified foods and thickened fluids for adults (≥18 years) with oropharyngeal dysphagia. *E-SPEN Journal*, *8*(4), e127–e134. https://doi.org/10.1016/j.clnme.2013.05.003

Attrill, S., White, S., Murray, J., Hammond, S., & Doeltgen, S. (2018). Impact of oropharyngeal dysphagia on healthcare cost and length of stay in hospital: A systematic review. In *BMC Health*

Services Research (Vol. 18, Issue 1, p. 594). BioMed Central Ltd. https://doi.org/10.1186/s12913-018-3376-3

Bolivar-Prados, M., Rofes, L., Arreola, V., Guida, S., Nascimento, W. V., Martin, A., Vilardell, N., Ortega Fernández, O., Ripken, D., Lansink, M., & Clavé, P. (2019). Effect of a gum-based thickener on the safety of swallowing in patients with poststroke oropharyngeal dysphagia. *Neurogastroenterology & Motility*, *31*(11). https://doi.org/10.1111/nmo.13695

Brito-de la Fuente, E., Staudinger-Prevost, N., Quinchia, L. A., Valencia, C., Partal, P., Franco, J. M., & Gallegos, C. (2012). Design of a New Spoon-Thick Consistency Oral Nutrition Supplement Using Rheological Similarity with a Swallow Barium Test Feed. *Applied Rheology*, *22*(5), 53365. https://doi.org/https://doi.org/10.3933/applrheol-22-53365

Brito-de la Fuente, E., Turcanu, M., Ekberg, O., & Gallegos, C. (2019). *Rheological Aspects of Swallowing and Dysphagia: Shear and Elongational Flows BT - Dysphagia: Diagnosis and Treatment* (O. Ekberg (ed.); pp. 687–716). Springer International Publishing. https://doi.org/10.1007/174_2017_119

Cabré, M., Serra-Prat, M., Force, L., Almirall, J., Palomera, E., & Clavé, P. (2013). Oropharyngeal Dysphagia is a Risk Factor for Readmission for Pneumonia in the Very Elderly Persons: Observational Prospective Study. *The Journals of Gerontology: Series A*, *69A*(3), 330–337. https://doi.org/10.1093/gerona/glt099

Carrión, S., Costa, A., Ortega, O., Verin, E., Clavé, P., & Laviano, A. (2019). *Complications of Oropharyngeal Dysphagia: Malnutrition and Aspiration Pneumonia BT - Dysphagia: Diagnosis and Treatment* (O. Ekberg (ed.); pp. 823–857). Springer International Publishing. https://doi.org/10.1007/174_2017_168

Choi, K. H., Ryu, J. S., Kim, M. Y., Kang, J. Y., & Yoo, S. D. (2011). Kinematic analysis of dysphagia: Significant parameters of aspiration related to bolus viscosity. *Dysphagia*, *26*(4), 392–398. https://doi.org/10.1007/s00455-011-9325-5

Cichero, J. A. Y., Steele, C., Duivestein, J., Clavé, P., Chen, J., Kayashita, J., Dantas, R., Lecko, C., Speyer, R., Lam, P., & Murray, J. (2013). The Need for International Terminology and Definitions for Texture-Modified Foods and Thickened Liquids Used in Dysphagia Management: Foundations of a Global Initiative. *Current Physical Medicine and Rehabilitation Reports*, *1*(4), 280–291. https://doi.org/10.1007/s40141-013-0024-z

Clavé, P., De Kraa, M., Arreola, V., Girvent, M., Farré, R., Palomera, E., & Serra-Prat, M. (2006). The effect of bolus viscosity on swallowing function in neurogenic dysphagia. *Alimentary Pharmacology and Therapeutics*, *24*(9), 1385–1394. https://doi.org/10.1111/j.1365-2036.2006.03118.x

436 Clavé, Pere, & Shaker, R. (2015). Dysphagia: Current reality and scope of the problem. In *Nature*
437 *Reviews Gastroenterology and Hepatology* (Vol. 12, Issue 5, pp. 259–270). Nature Publishing
438 Group. https://doi.org/10.1038/nrgastro.2015.49
439 Colodny, N. (2005). Dysphagic Independent Feeders' Justifications for Noncompliance With
440 Recommendations by a Speech-Language Pathologist. *American Journal of Speech-Language*
441 *Pathology*. https://doi.org/10.1044/1058-0360(2005/008)
442 Diañez, I., Gallegos, C., Brito-de la Fuente, E., Martínez, I., Valencia, C., Sánchez, M. C., Diaz, M. J., &
443 Franco, J. M. (2019). 3D printing in situ gelification of κ-carrageenan solutions: Effect of printing
444 variables on the rheological response. *Food Hydrocolloids*, *87*, 321–330.
445 https://doi.org/10.1016/j.foodhyd.2018.08.010
446 Nutritional Aspects of Dysphagia Management, 81 Advances in Food and Nutrition Research 271
447 (2017). https://www.sciencedirect.com/science/article/pii/S1043452616300687
448 Herranz, B., Criado, C., Pozo-Bayón, M. Á., & Álvarez, M. D. (2021). Effect of addition of human saliva
449 on steady and viscoelastic rheological properties of some commercial dysphagia-oriented
450 products. *Food Hydrocolloids*, *111*, 106403. https://doi.org/10.1016/j.foodhyd.2020.106403
451 Inamoto, Y., Saitoh, E., Okada, S., Kagaya, H., Shibata, S., Ota, K., Baba, M., Fujii, N., Katada, K.,
452 Wattanapan, P., & Palmer, J. B. (2013). The effect of bolus viscosity on laryngeal closure in
453 swallowing: Kinematic analysis using 320-row area detector CT. *Dysphagia*, *28*(1), 33–42.
454 https://doi.org/10.1007/s00455-012-9410-4
455 Lapasin, R., Pricl, S., Lapasin, R., & Pricl, S. (1995). Industrial applications of polysaccharides. In
456 *Rheology of Industrial Polysaccharides: Theory and Applications* (pp. 134–161). Springer US.
457 https://doi.org/10.1007/978-1-4615-2185-3_2
458 Leonard, R. J., White, C., McKenzie, S., & Belafsky, P. C. (2014). Effects of bolus rheology on
459 aspiration in patients with dysphagia. *Journal of the Academy of Nutrition and Dietetics*, *114*(4),
460 590–594. https://doi.org/10.1016/j.jand.2013.07.037
461 Li, X., Chen, H., & Yang, B. (2016). Centrifugally spun starch-based fibers from amylopectin rich
462 starches. *Carbohydrate Polymers*, *137*, 459–465. https://doi.org/10.1016/j.carbpol.2015.10.079
463 Lim, D. J. H., Mulkerrin, S. M., Mulkerrin, E. C., & O'Keeffe, S. T. (2016). A randomised trial of the
464 effect of different fluid consistencies used in the management of dysphagia on quality of life: a
465 time trade-off study. *Age and Ageing*, *45*(2), 309–312. https://doi.org/10.1093/ageing/afv194
466 Low, J., Wyles, C., Wilkinson, T., & Sainsbury, R. (2001). The effect of compliance on clinical
467 outcomes for patients with dysphagia on videofluoroscopy. *Dysphagia*, *16*(2), 123–127.
468 https://doi.org/10.1007/s004550011002
469 Moret-Tatay, A., Rodríguez-García, J., Martí-Bonmatí, E., Hernando, I., & Hernández, M. J. (2015).

Commercial thickeners used by patients with dysphagia: Rheological and structural behaviour in different food matrices. *Food Hydrocolloids*, *51*, 318–326. https://doi.org/10.1016/j.foodhyd.2015.05.019

Newman, R., Vilardell, N., Clavé, P., & Speyer, R. (2016). Effect of Bolus Viscosity on the Safety and Efficacy of Swallowing and the Kinematics of the Swallow Response in Patients with Oropharyngeal Dysphagia: White Paper by the European Society for Swallowing Disorders (ESSD). In *Dysphagia* (Vol. 31, Issue 2, pp. 232–249). Springer New York LLC. https://doi.org/10.1007/s00455-016-9696-8

Ortega, O., Bolívar-Prados, M., Arreola, V., Nascimento, W. V., Tomsen, N., Gallegos, C., Brito-de La Fuente, E., & Clavé, P. (2020). Therapeutic Effect, Rheological Properties and α-Amylase Resistance of a New Mixed Starch and Xanthan Gum Thickener on Four Different Phenotypes of Patients with Oropharyngeal Dysphagia. *Nutrients*, *12*(6), 1873. https://doi.org/10.3390/nu12061873

Pollard, M. A., & Fischer, P. (2014). Semi-dilute galactomannan solutions: observations on viscosity scaling behavior of guar gum. *Journal of Physics: Condensed Matter*, *26*(46), 464107. https://doi.org/10.1088/0953-8984/26/46/464107

Qazi, W. M., Ekberg, O., Wiklund, J., Kotze, R., & Stading, M. (2019). Assessment of the Food-Swallowing Process Using Bolus Visualisation and Manometry Simultaneously in a Device that Models Human Swallowing. In *Dysphagia* (Vol. 34, Issue 6, pp. 821–833). Springer New York LLC. https://doi.org/10.1007/s00455-019-09995-8

Quinchia, L. A., Valencia, C., Partal, P., Franco, J. M., Brito-de la Fuente, E., & Gallegos, C. (2011). Linear and non-linear viscoelasticity of puddings for nutritional management of dysphagia. *Food Hydrocolloids*, *25*(4), 586–593. https://doi.org/10.1016/j.foodhyd.2010.07.006

Salinas-Vázquez, M., Vicente, W., Brito-de la Fuente, E., Gallegos, C., Márquez, J., & Ascanio, G. (2014). Early Numerical Studies on the Peristaltic Flow through the Pharynx. *Journal of Texture Studies*, *45*(2), 155–163. https://doi.org/10.1111/jtxs.12060

Shaker, R. (2006). Oropharyngeal Dysphagia. *Gastroenterology & Hepatology*, *2*(9), 633–634. https://pubmed.ncbi.nlm.nih.gov/28316533

Sopade, P. A., Halley, P. J., Cichero, J. A. Y., & Ward, L. C. (2007). Rheological characterisation of food thickeners marketed in Australia in various media for the management of dysphagia. I: Water and cordial. *Journal of Food Engineering*, *79*(1), 69–82. https://doi.org/10.1016/j.jfoodeng.2006.01.045

Sopade, P. A., Halley, P. J., Cichero, J. A. Y., Ward, L. C., Hui, L. S., & Teo, K. H. (2008). Rheological characterisation of food thickeners marketed in Australia in various media for the management

of dysphagia. II. Milk as a dispersing medium. *Journal of Food Engineering*, *84*(4), 553–562. https://doi.org/10.1016/j.jfoodeng.2007.06.024

Sopade, P. A., Halley, P. J., Cichero, J. A. Y., Ward, L. C., Liu, J., & Varliveli, S. (2008). Rheological characterization of food thickeners marketed in Australia in various media for the management of dysphagia. III. Fruit juice as a dispersing medium. *Journal of Food Engineering*, *86*(4), 604–615. https://doi.org/10.1016/j.jfoodeng.2007.11.013

Sworn, G. (2007). Natural Thickeners. In *Handbook of Industrial Water Soluble Polymers* (pp. 10–31). Blackwell Publishing Ltd. https://doi.org/10.1002/9780470988701.ch2

Turcanu, M., Siegert, N., Secouard, S., Brito-de la Fuente, E., Balan, C., & Gallegos, C. (2018). An alternative elongational method to study the effect of saliva on thickened fluids for dysphagia nutritional support. *Journal of Food Engineering*, *228*, 79–83. https://www.sciencedirect.com/science/article/pii/S0260877418300700

Wang, F., Sun, Z., & Wang, Y. J. (2001). Study of xanthan gum/waxy corn starch interaction in solution by viscometry. *Food Hydrocolloids*, *15*(4–6), 575–581. https://doi.org/10.1016/S0268-005X(01)00065-0

Wyatt, N. B., & Liberatore, M. W. (2009). Rheology and viscosity scaling of the polyelectrolyte xanthan gum. *Journal of Applied Polymer Science*, *114*(6), 4076–4084. https://doi.org/10.1002/app.31093

Zhang, E., Dai, X., Dong, Z., Qiu, X., & Ji, X. (2016). Critical concentration and scaling exponents of one soluble polyimide - From dilute to semidilute entangled solutions. *Polymer*, *84*, 275–285. https://doi.org/10.1016/j.polymer.2016.01.001

List of tables

List of figures

References

1. World Health Organization. WHO | International Classification of Functioning, Disability and Health (ICF). *International Classification of Functioning, Disability and Health (ICF)* https://apps.who.int/classifications/icfbrowser/.

2. World Health Organization. WHO | International Classification of Diseases, 11th Revision (ICD-11). *Internation Classification of Diseases 11th Revision (ICD-11)* https://icd.who.int/browse11/l-m/en#/http://id.who.int/icd/entity/968461848.

3. Malagelada, J. R. *et al.* World gastroenterology organisation global guidelines. *Journal of Clinical Gastroenterology* vol. 49 370–378 (2015).

4. Aslam, M. & Vaezi, M. F. Dysphagia in the Elderly. *Gastroenterol. Hepatol. (N. Y).* **9**, 784 (2013).

5. Philpott, H., Garg, M., Tomic, D., Balasubramanian, S. & Sweis, R. Dysphagia: Thinking outside the box. *World Journal of Gastroenterology* vol. 23 6942–6951 (2017).

6. Lynch, K. L. & Katzka, D. A. Dysphagia: How to Recognize and Narrow the Differential. in *Evaluation and Management of Dysphagia* 1–12 (Springer International Publishing, 2020). doi:10.1007/978-3-030-26554-0_1.

7. Owen, W. Dysphagia. *Bmj* **323**, 850 (2001).

8. Tack, J. & Zaninotto, G. Therapeutic options in oesophageal dysphagia. *Nature Reviews Gastroenterology and Hepatology* vol. 12 332–341 (2015).

9. Johnston, B. T. Oesophageal dysphagia: a stepwise approach to diagnosis and management. *The Lancet Gastroenterology and Hepatology* vol. 2 604–609 (2017).

10. Baijens, L. W. J. *et al.* European society for swallowing disorders - European union geriatric medicine society white paper: Oropharyngeal dysphagia as a geriatric syndrome. *Clinical Interventions in Aging* vol. 11 1403–1428 (2016).

11. Rommel, N. & Hamdy, S. Oropharyngeal dysphagia: Manifestations and

diagnosis. *Nature Reviews Gastroenterology and Hepatology* vol. 13 49–59 (2016).

12. Barczi, S. R., Sullivan, P. A. & Robbins, J. How Should Dysphagia Care of Older Adults Differ? Establishing Optimal Practice Patterns. *Semin. Speech Lang.* **Volume 21**, 0347–0364 (2000).

13. Ferrero López, M. I., García Gollarte, J. F., Botella Trelis, J. J. & Juan Vidal, O. Detección de disfagia en mayores institucionalizados. *Rev. Esp. Geriatr. Gerontol.* **47**, 143–147 (2012).

14. Clavé, P. & Shaker, R. Dysphagia: Current reality and scope of the problem. *Nature Reviews Gastroenterology and Hepatology* vol. 12 259–270 (2015).

15. Streicher, M. *et al.* Dysphagia in Nursing Homes—Results From the NutritionDay Project. *J. Am. Med. Dir. Assoc.* **19**, 141-147.e2 (2018).

16. Eslick, G. D. & Talley, N. J. Dysphagia: Epidemiology, risk factors and impact on quality of life - A population-based study. *Aliment. Pharmacol. Ther.* **27**, 971–979 (2008).

17. Roden, D. F. & Altman, K. W. Causes of dysphagia among different age groups: A systematic review of the literature. *Otolaryngologic Clinics of North America* vol. 46 965–987 (2013).

18. Bhattacharyya, N. The Prevalence of Dysphagia among Adults in the United States. *Otolaryngol. Neck Surg.* **151**, 765–769 (2014).

19. Adkins, C. *et al.* Prevalence and Characteristics of Dysphagia Based on a Population-Based Survey. *Clin. Gastroenterol. Hepatol.* (2019) doi:10.1016/j.cgh.2019.10.029.

20. Kertscher, B., Speyer, R., Fong, E., Georgiou, A. M. & Smith, M. Prevalence of Oropharyngeal Dysphagia in the Netherlands: A Telephone Survey. *Dysphagia* **30**, 114–120 (2015).

21. Cook, I. J. & Kahrilas, P. J. AGA technical review on management of oropharyngeal dysphagia. *Gastroenterology* **116**, 455–478 (1999).

22. Gallegos, C., Brito-de la Fuente, E., Clavé, P., Costa, A. & Assegehegn, G. *Nutritional Aspects of Dysphagia Management*. *Advances in Food and Nutrition Research* vol. 81 271–318 (2017).

23. Shaker, R. Oropharyngeal Dysphagia. *Gastroenterol. Hepatol. (N. Y).* **2**,

633–634 (2006).

24. Cook, I. J. Oropharyngeal Dysphagia. *Gastroenterology Clinics of North America* vol. 38 411–431 (2009).

25. Falsetti, P. *et al.* Oropharyngeal Dysphagia after Stroke: Incidence, Diagnosis, and Clinical Predictors in Patients Admitted to a Neurorehabilitation Unit. *J. Stroke Cerebrovasc. Dis.* **18**, 329–335 (2009).

26. Kopey, S. A., Chae, J. & Vargo, M. M. Does a 3-Sip Test Detect Dysphagia in Acute Stroke Rehabilitation Patients. *PM R* **2**, 822–828 (2010).

27. Flowers, H. L., Silver, F. L., Fang, J., Rochon, E. & Martino, R. The incidence, co-occurrence, and predictors of dysphagia, dysarthria, and aphasia after first-ever acute ischemic stroke. *J. Commun. Disord.* **46**, 238–248 (2013).

28. Rofes, L. *et al.* Prevalence, risk factors and complications of oropharyngeal dysphagia in stroke patients: A cohort study. *Neurogastroenterol. Motil.* **30**, e13338 (2018).

29. Howle, A. A., Baguley, I. J. & Brown, L. Management of Dysphagia Following Traumatic Brain Injury. *Curr. Phys. Med. Rehabil. Reports* **2**, 219–230 (2014).

30. Mandaville, A., Ray, A., Robertson, H., Foster, C. & Jesser, C. A retrospective review of swallow dysfunction in patients with severe traumatic brain injury. *Dysphagia* vol. 29 310–318 (2014).

31. Nilsson, H., Ekberg, O., Olsson, R. & Hindfelt, B. Quantitative assessment of oral and pharyngeal function in Parkinson's disease. *Dysphagia* **11**, 144–150 (1996).

32. Coates, C. & Bakheit, A. M. O. Dysphagia in Parkinson's Disease. *Eur. Neurol.* **38**, 49–52 (1997).

33. Pflug, C. *et al.* Critical Dysphagia is Common in Parkinson Disease and Occurs Even in Early Stages: A Prospective Cohort Study. *Dysphagia* **33**, 41–50 (2018).

34. Feinberg, M. J., Ekberg, O., Segall, L. & Tully, J. Deglutition in elderly patients with dementia: Findings of videofluorographic evaluation and impact on staging and management. *Radiology* **183**, 811–814 (1992).

35. Horner, J., Alberts, M. J., Dawson, D. V. & Cook, G. M. Swallowing in Alzheimer's disease. *Alzheimer Dis. Assoc. Disord.* **8**, 177–189 (1994).

36. Seçil, Y. *et al.* Dysphagie dans la maladie d'Alzheimer. *Neurophysiol. Clin.* **46**, 171–178 (2016).

37. Benfer, K. A. *et al.* Oropharyngeal dysphagia and gross motor skills in children with cerebral palsy. *Pediatrics* **131**, e1553–e1562 (2013).

38. Asgarshirazi, M., Farokhzadeh-Soltani, M., Keihanidost, Z. & Shariat, M. Evaluation of Feeding Disorders Including Gastro-Esophageal Reflux and Oropharyngeal Dysfunction in Children With Cerebral Palsy. *J. Fam. Reprod. Heal.* **11**, 197–201 (2017).

39. Calcagno, P., Ruoppolo, G., Grasso, M. G., De Vincentiis, M. & Paolucci, S. Dysphagia in multiple sclerosis - prevalence and prognostic factors. *Acta Neurol. Scand.* **105**, 40–43 (2002).

40. Terré-Boliart, R. *et al.* [Oropharyngeal dysphagia in patients with multiple sclerosis]. *Rev. Neurol.* **39**, 707–10.

41. Poorjavad, M. *et al.* Oropharyngeal dysphagia in multiple sclerosis. *Mult. Scler.* **16**, 362–5 (2010).

42. Solaro, C. *et al.* Prevalence of dysphagia in a consecutive cohort of subjects with MS using fibre-optic endoscopy. *Neurol. Sci.* 1–5 (2019) doi:10.1007/s10072-019-04198-3.

43. Leighton, S. E. J., Burton, M. J., Lund, W. S. & Cochrane, G. M. Swallowing in motor neurone disease. *J. R. Soc. Med.* **87**, 801–805 (1994).

44. Briani, C. *et al.* Radiological evidence of subclinical dysphagia in motor neuron disease. *J. Neurol.* **245**, 211–216 (1998).

45. Ruoppolo, G. *et al.* Dysphagia in amyotrophic lateral sclerosis: prevalence and clinical findings. *Acta Neurol. Scand.* **128**, 397–401 (2013).

46. Platteaux, N., Dirix, P., Dejaeger, E. & Nuyts, S. Dysphagia in head and neck cancer patients treated with chemoradiotherapy. *Dysphagia* vol. 25 139–152 (2010).

47. Denaro, N., Merlano, M. C. & Russi, E. G. Dysphagia in head and neck cancer patients: Pretreatment evaluation, predictive factors, and assessment during radio-chemotherapy, recommendations. *Clinical and Experimental Otorhinolaryngology* vol. 6 117–126 (2013).

48. García-Peris, P. *et al.* Long-term prevalence of oropharyngeal dysphagia in head and neck cancer patients: Impact on quality of life. *Clin. Nutr.* **26**,

710–717 (2007).

49. Hey, C. *et al.* Water swallow screening test for patients after surgery for head and neck cancer: Early identification of dysphagia, aspiration and limitations of oral intake. *Anticancer Res.* **33**, 4017–4022 (2013).

50. Rinkel, R. N. *et al.* Prevalence of swallowing and speech problems in daily life after chemoradiation for head and neck cancer based on cut-off scores of the patient-reported outcome measures SWAL-QOL and SHI. *Eur. Arch. Oto-Rhino-Laryngology* **273**, 1849–1855 (2016).

51. Hutcheson, K. A. *et al.* Two-year prevalence of dysphagia and related outcomes in head and neck cancer survivors: An updated SEER-Medicare analysis. *Head Neck* **41**, 479–487 (2019).

52. Buchholz, D. W. Oropharyngeal dysphagia due to iatrogenic neurological dysfunction. *Dysphagia* **10**, 248–254 (1995).

53. Ekberg, O. The Geriatric Pharynx and Esophagus BT - Dysphagia: Diagnosis and Treatment. in (ed. Ekberg, O.) 247–256 (Springer International Publishing, 2019). doi:10.1007/174_2017_62.

54. Serra-Prat, M. *et al.* Prevalence of oropharyngeal dysphagia and impaired safety and efficacy of swallow in independently living older persons. *Journal of the American Geriatrics Society* vol. 59 186–187 (2011).

55. Holland, G. *et al.* Prevalence and symptom profiling of oropharyngeal dysphagia in a community dwelling of an elderly population: a self-reporting questionnaire survey. *Dis. Esophagus* **24**, 476–480 (2011).

56. Yang, E. J., Kim, M. H., Lim, J. Y. & Paik, N. J. Oropharyngeal dysphagia in a community-based elderly cohort: The Korean longitudinal study on health and aging. *J. Korean Med. Sci.* **28**, 1534–1539 (2013).

57. Nogueira, D. & Reis, E. Swallowing disorders in nursing home residents: How can the problem be explained? *Clin. Interv. Aging* **8**, 221–227 (2013).

58. Sarabia-Cobo, C. M. *et al.* The incidence and prognostic implications of dysphagia in elderly patients institutionalized: A multicenter study in Spain. *Appl. Nurs. Res.* **30**, e6–e9 (2016).

59. Huppertz, V. A. L. *et al.* Association Between Oropharyngeal Dysphagia and Malnutrition in Dutch Nursing Home Residents: Results of the National Prevalence Measurement of Quality of Care. *J. Nutr. Heal. Aging*

22, 1246–1252 (2018).

60. Prasse, J. E. & Kikano, G. E. An overview of pediatric dysphagia. *Clin. Pediatr. (Phila).* **48**, 247–51 (2009).

61. Abadie, V. & Couly, G. Congenital feeding and swallowing disorders. in *Handbook of Clinical Neurology* vol. 113 1539–1549 (Elsevier B.V., 2013).

62. Duncan, D. R., Amirault, J., Mitchell, P. D., Larson, K. & Rosen, R. L. Oropharyngeal Dysphagia Is Strongly Correlated with Apparent Life-Threatening Events. *J. Pediatr. Gastroenterol. Nutr.* **65**, 168–172 (2017).

63. Dusick, A. Investigation and Management of Dysphagia. *Seminars in Pediatric Neurology* vol. 10 255–264 (2003).

64. Lefton-Greif, M. A., Carroll, J. L. & Loughlin, G. M. Long-term follow-up of oropharyngeal dysphagia in children without apparent risk factors. *Pediatr. Pulmonol.* **41**, 1040–1048 (2006).

65. Bourin, P. F., Puech, M. & Woisard, V. Pediatric Aspect of Dysphagia BT - Dysphagia: Diagnosis and Treatment. in (ed. Ekberg, O.) 213–236 (Springer International Publishing, 2019). doi:10.1007/174_2017_138.

66. Cichero, J. A. Y. & Altman, K. W. Definition, Prevalence and Burden of Oropharyngeal Dysphagia: A Serious Problem among Older Adults Worldwide and the Impact on Prognosis and Hospital Resources. in *Nestlé Nutrition Institute workshop series* vol. 72 1–11 (Karger Publishers, 2012).

67. Altman, K. W., Yu, G. P. & Schaefer, S. D. Consequence of dysphagia in the hospitalized patient: Impact on prognosis and hospital resources. *Arch. Otolaryngol. - Head Neck Surg.* **136**, 784–789 (2010).

68. Rosenbek, J. C., Robbins, J. A., Roecker, E. B., Coyle, J. L. & Wood, J. L. A penetration-aspiration scale. *Dysphagia* **11**, 93–98 (1996).

69. Matsuo, K. & Palmer, J. B. Coordination of mastication, swallowing and breathing. *Japanese Dental Science Review* vol. 45 31–40 (2009).

70. Ekberg, O. *et al.* Feeding and Respiration BT - Dysphagia: Diagnosis and Treatment. in (ed. Ekberg, O.) 49–54 (Springer Berlin Heidelberg, 2012). doi:10.1007/174_2012_587.

71. Ekberg, O. Oral and Pharyngeal Function and Dysfunction BT - Dysphagia: Diagnosis and Treatment. in (ed. Ekberg, O.) 65–80 (Springer

International Publishing, 2019). doi:10.1007/174_2017_60.

72. Denk-Linnert, D.-M. Evaluation of Symptoms BT - Dysphagia: Diagnosis and Treatment. in (ed. Ekberg, O.) 71–81 (Springer Berlin Heidelberg, 2012). doi:10.1007/174_2012_620.

73. Garon, B. R., Sierzant, T. & Ormiston, C. Silent Aspiration. *J. Neurosci. Nurs.* **41**, 178–185 (2009).

74. Arvedson, J., Rogers, B., Buck, G., Smart, P. & Msall, M. Silent aspiration prominent in children with dysphagia. *Int. J. Pediatr. Otorhinolaryngol.* **28**, 173–181 (1994).

75. Smith, C. H., Logemann, J. A., Colangelo, L. A., Rademaker, A. W. & Pauloski, B. R. Incidence and patient characteristics associated with silent aspiration in the acute care setting. *Dysphagia* **14**, 1–7 (1999).

76. Weir, K. A., McMahon, S., Taylor, S. & Chang, A. B. Oropharyngeal aspiration and silent aspiration in children. *Chest* **140**, 589–597 (2011).

77. Sekizawa, K., Ujiie, Y., Itabashi, S., Sasaki, H. & Takishima, T. Lack of cough reflex in aspiration pneumonia. *The Lancet* vol. 335 1228–1229 (1990).

78. Kikuchi, R. *et al.* High incidence of silent aspiration in elderly patients with community- acquired pneumonia. *Am. J. Respir. Crit. Care Med.* **150**, 251–253 (1994).

79. Almirall, J., Cabré, M. & Clavé, P. Complications of Oropharyngeal Dysphagia: Aspiration Pneumonia. in *Nestlé Nutrition Institute workshop series* vol. 72 67–76 (Karger Publishers, 2012).

80. Marik, P. E. Pulmonary aspiration syndromes. *Curr. Opin. Pulm. Med.* **17**, 148–154 (2011).

81. Valenti, W. M., Trudell, R. G. & Bentley, D. W. Factors Predisposing to Oropharyngeal Colonization with Gram-Negative Bacilli in the Aged. *N. Engl. J. Med.* **298**, 1108–1111 (1978).

82. El-Solh, A. A. *et al.* Colonization of Dental Plaques. *Chest* **126**, 1575–1582 (2004).

83. Langmore, S. E. *et al.* Predictors of aspiration pneumonia: How important is dysphagia? *Dysphagia* **13**, 69–81 (1998).

84. DeLegge, M. H. Aspiration Pneumonia: Incidence, Mortality, and At-Risk Populations. *J. Parenter. Enter. Nutr.* **26**, S19–S25 (2002).

85. Cabre, M. *et al.* Prevalence and prognostic implications of dysphagia in elderly patients with pneumonia. *Age Ageing* **39**, 39–45 (2009).

86. Cabré, M. *et al.* Oropharyngeal Dysphagia is a Risk Factor for Readmission for Pneumonia in the Very Elderly Persons: Observational Prospective Study. *Journals Gerontol. Ser. A* **69A**, 330–337 (2013).

87. Hayashi, M. *et al.* Clinical features and outcomes of aspiration pneumonia compared with non-aspiration pneumonia: A retrospective cohort study. *J. Infect. Chemother.* **20**, 436–442 (2014).

88. Lanspa, M. J. *et al.* Characteristics associated with clinician diagnosis of aspiration pneumonia: A descriptive study of afflicted patients and their outcomes. *J. Hosp. Med.* **10**, 90–96 (2015).

89. Carnaby, G., Hankey, G. J. & Pizzi, J. Behavioural intervention for dysphagia in acute stroke: A randomised controlled trial. *Lancet Neurol.* **5**, 31–37 (2006).

90. Li, M., Wang, Z., Han, W.-J., Lu, S.-Y. & Fang, Y.-Z. Effect of feeding management on aspiration pneumonia in elderly patients with dysphagia. *Chinese Nurs. Res.* **2**, 40–44 (2015).

91. Carrión, S. *et al.* Complications of Oropharyngeal Dysphagia: Malnutrition and Aspiration Pneumonia BT - Dysphagia: Diagnosis and Treatment. in (ed. Ekberg, O.) 823–857 (Springer International Publishing, 2019). doi:10.1007/174_2017_168.

92. Malnutrition. https://www.who.int/news-room/fact-sheets/detail/malnutrition.

93. Clavé, P. *et al.* The effect of bolus viscosity on swallowing function in neurogenic dysphagia. *Aliment. Pharmacol. Ther.* **24**, 1385–1394 (2006).

94. Carrión, S. *et al.* Nutritional status of older patients with oropharyngeal dysphagia in a chronic versus an acute clinical situation. *Clin. Nutr.* **36**, 1110–1116 (2017).

95. Keusch, G. T. The History of Nutrition: Malnutrition, Infection and Immunity. *J. Nutr.* **133**, 336S-340S (2003).

96. Vivanti, A., Ward, N. & Haines, T. Nutritional status and associations with falls, balance, mobility and functionality during hospital admission. *J. Nutr. Heal. Aging* **15**, 388–391 (2011).

97. Barker, L. A., Gout, B. S. & Crowe, T. C. Hospital malnutrition: Prevalence, identification and impact on patients and the healthcare system. *International Journal of Environmental Research and Public Health* vol. 8 514–527 (2011).

98. Hickson, M. & Julian, A. Consequences of undernutrition. in *Advanced Nutrition and Dietetics in Nutrition Support* 33–41 (John Wiley & Sons, Ltd, 2018). doi:10.1002/9781118993880.ch1.5.

99. Correia, M. I. T. D. & Waitzberg, D. L. The impact of malnutrition on morbidity, mortality, length of hospital stay and costs evaluated through a multivariate model analysis. *Clin. Nutr.* **22**, 235–239 (2003).

100. Leibovitz, A. *et al.* Dehydration among Long-Term Care Elderly Patients with Oropharyngeal Dysphagia. *Gerontology* **53**, 179–183 (2007).

101. Stanga, Z. & Aubry, E. Dehydration in Dysphagia BT - Dysphagia: Diagnosis and Treatment. in (ed. Ekberg, O.) 859–871 (Springer International Publishing, 2019). doi:10.1007/174_2017_56.

102. Karagiannis, M. J., Chivers, L. & Karagiannis, T. C. Effects of oral intake of water in patients with oropharyngeal dysphagia. *BMC Geriatr.* **11**, 1–10 (2011).

103. Verdonschot, R. J. C. G. *et al.* Affective symptoms in patients with oropharyngeal dysphagia: A systematic review. *Journal of Psychosomatic Research* vol. 97 102–110 (2017).

104. Ekberg, O., Hamdy, S., Woisard, V., Wuttge-Hannig, A. & Ortega, P. Social and psychological burden of dysphagia: Its impact on diagnosis and treatment. *Dysphagia* **17**, 139–146 (2002).

105. Colodny, N. Dysphagic Independent Feeders' Justifications for Noncompliance With Recommendations by a Speech-Language Pathologist. *Am. J. Speech-Language Pathol.* (2005) doi:10.1044/1058-0360(2005/008).

106. Farri, A., Accornero, A. & Burdese, C. Social importance of dysphagia: its impact on diagnosis and therapy. *Acta Otorhinolaryngol. Ital.* **27**, 83–86 (2007).

107. Martino, R., Beaton, D. & Diamant, N. E. Using different perspectives to generate items for a new scale measuring medical outcomes of dysphagia (MOD). *J. Clin. Epidemiol.* **62**, 518–526 (2009).

108. Martino, R., Beaton, D. & Diamant, N. E. Perceptions of psychological issues related to dysphagia differ in acute and chronic patients. *Dysphagia* **25**, 26–34 (2010).

109. Attrill, S., White, S., Murray, J., Hammond, S. & Doeltgen, S. Impact of oropharyngeal dysphagia on healthcare cost and length of stay in hospital: A systematic review. *BMC Health Services Research* vol. 18 594 (2018).

110. Westmark, S., Melgaard, D., Rethmeier, L. O. & Ehlers, L. H. The cost of dysphagia in geriatric patients. *Clin. Outcomes Res.* **10**, 321–326 (2018).

111. Martino, R. *et al.* Feasibility of assessing patient health benefits and incurred costs resulting from early dysphagia intervention during and immediately after chemoradiotherapy for head-and-neck cancer. *Curr. Oncol.* **24**, e466–e476 (2017).

112. Odderson, I. R., Keaton, J. C. & McKenna, B. S. Swallow management in patients on an acute stroke pathway: Quality is cost effective. *Arch. Phys. Med. Rehabil.* **76**, 1130–1133 (1995).

113. Walzer, S., Droeschel, D., Nuijten, M. & Chevrou-Séverac, H. Health economics evidence for medical nutrition: Are these interventions value for money in integrated care? *ClinicoEconomics and Outcomes Research* vol. 6 241–251 (2014).

114. Tay, W. Y., Low, L. L., Tan, S. Y. & Vasanwala, F. F. Evidence-Based Measures for Preventing Aspiration Pneumonia in Patients with Dysphagia. *Proc. Singapore Healthc.* **23**, 158–165 (2014).

115. Martín, A., Ortega, O., Roca, M., Arús, M. & Clavé Civit, P. Effect of a Minimal-Massive Intervention in Hospitalized Older Patients with Oropharyngeal Dysphagia: A Proof of Concept Study. *J. Nutr. Heal. Aging* **22**, 739–747 (2018).

116. Eltringham, S. A. *et al.* Impact of Dysphagia Assessment and Management on Risk of Stroke-Associated Pneumonia: A Systematic Review. *Cerebrovasc. Dis.* **46**, 99–107 (2018).

117. Bisch, E. M., Logemann, J. A., Rademaker, A. W., Kahrilas, P. J. & Lazarus, C. L. Pharyngeal Effects of Bolus Volume, Viscosity, and Temperature in Patients With Dysphagia Resulting From Neurologic Impairment and in Normal Subjects. *J. Speech, Lang. Hear. Res.* **37**, 1041–1049 (1994).

118. Engmann, J. & Burbidge, A. S. Fluid mechanics of eating, swallowing and digestion-overview and perspectives. *Food Funct.* **4**, 443–447 (2013).

119. American Gastroenterological Association medical position statement on management of oropharyngeal dysphagia. *Gastroenterology* (1999) doi:10.1016/S0016-5085(99)70143-5.

120. McCullough, G., Pelletier, C. & Steele, C. National Dysphagia Diet: What to Swallow? *ASHA Lead.* **8**, 16–27 (2003).

121. Wirth, R. *et al.* Oropharyngeal dysphagia in older persons – from pathophysiology to adequate intervention: A review and summary of an international expert meeting. *Clin. Interv. Aging* **11**, 189–208 (2016).

122. Newman, R., Vilardell, N., Clavé, P. & Speyer, R. Effect of Bolus Viscosity on the Safety and Efficacy of Swallowing and the Kinematics of the Swallow Response in Patients with Oropharyngeal Dysphagia: White Paper by the European Society for Swallowing Disorders (ESSD). *Dysphagia* vol. 31 232–249 (2016).

123. Volkert, D. *et al.* ESPEN guideline on clinical nutrition and hydration in geriatrics. *Clin. Nutr.* **38**, 10–47 (2019).

124. Atherton, M., Bellis-Smith, N., Cichero, J. A. Y. & Suter, M. Texture-modified foods and thickened fluids as used for individuals with dysphagia: Australian standardised labels and definitions. *Nutr. Diet.* **64**, S53–S76 (2007).

125. Cichero, J. A. Y. *et al.* The Need for International Terminology and Definitions for Texture-Modified Foods and Thickened Liquids Used in Dysphagia Management: Foundations of a Global Initiative. *Curr. Phys. Med. Rehabil. Reports* **1**, 280–291 (2013).

126. Steele, C. M. *et al.* The Influence of Food Texture and Liquid Consistency Modification on Swallowing Physiology and Function: A Systematic Review. *Dysphagia* **30**, 2–26 (2015).

127. Miles, A., McFarlane, M., Scott, S. & Hunting, A. Cough response to aspiration in thin and thick fluids during FEES in hospitalized inpatients. *Int. J. Lang. Commun. Disord.* **53**, 909–918 (2018).

128. Bolivar-Prados, M. *et al.* Effect of a gum-based thickener on the safety of swallowing in patients with poststroke oropharyngeal dysphagia. *Neurogastroenterol. Motil.* **31**, (2019).

129. Chen, M. Y. M., Ott, D. J., Peele, V. N. & Gelfand, D. W. Oropharynx in patients with cerebrovascular disease: Evaluation with videofluoroscopy. *Radiology* **176**, 641–643 (1990).

130. Kuhlemeier, K. V., Palmer, J. B. & Rosenberg, D. Effect of liquid bolus consistency and delivery method on aspiration and pharyngeal retention in dysphagia patients. *Dysphagia* **16**, 119–122 (2001).

131. Bhattacharyya, N., Kotz, T. & Shapiro, J. The effect of bolus consistency on dysphagia in unilateral vocal cord paralysis. *Otolaryngol. - Head Neck Surg.* **129**, 632–636 (2003).

132. Logemann, J. A. *et al.* A Randomized Study of Three Interventions for Aspiration of Thin Liquids in Patients With Dementia or Parkinson's Disease. *J. Speech, Lang. Hear. Res.* (2008) doi:10.1044/1092-4388(2008/013).

133. Diniz, P. B., Vanin, G., Xavier, R. & Parente, M. A. Reduced Incidence of Aspiration With Spoon-Thick Consistency in Stroke Patients. *Nutr. Clin. Pract.* **24**, 414–418 (2009).

134. Leder, S. B., Judson, B. L., Sliwinski, E. & Madson, L. Promoting safe Swallowing when puree is swallowed without aspiration but thin liquid is aspirated: Nectar is enough. *Dysphagia* **28**, 58–62 (2013).

135. Rofes, L., Arreola, V., Mukherjee, R., Swanson, J. & Clavé, P. The effects of a xanthan gum-based thickener on the swallowing function of patients with dysphagia. *Aliment. Pharmacol. Ther.* **39**, 1169–1179 (2014).

136. Leonard, R. J., White, C., McKenzie, S. & Belafsky, P. C. Effects of bolus rheology on aspiration in patients with dysphagia. *J. Acad. Nutr. Diet.* **114**, 590–594 (2014).

137. Clavé, P. *et al.* Accuracy of the volume-viscosity swallow test for clinical screening of oropharyngeal dysphagia and aspiration. *Clin. Nutr.* **27**, 806–815 (2008).

138. Rofes, L., Arreola, V., Mukherjee, R. & Clavé, P. Sensitivity and specificity of the Eating Assessment Tool and the Volume-Viscosity Swallow Test for clinical evaluation of oropharyngeal dysphagia. *Neurogastroenterol. Motil.* **26**, 1256–1265 (2014).

139. Inamoto, Y. *et al.* The effect of bolus viscosity on laryngeal closure in swallowing: Kinematic analysis using 320-row area detector CT.

Dysphagia **28**, 33–42 (2013).

140. Matsuo, K. *et al.* Effect of viscosity on food transport and swallow initiation during eating of two-phase food in normal young adults: A pilot study. *Dysphagia* **28**, 63–68 (2013).

141. Wu, S. *et al.* Effect of Changes in Bolus Viscosity on Swallowing Muscles in Patients with Dysphagia after Stroke. *Chinese Medical Journal* vol. 131 2868–2870 (2018).

142. Qazi, W. M., Ekberg, O., Wiklund, J., Kotze, R. & Stading, M. Assessment of the Food-Swallowing Process Using Bolus Visualisation and Manometry Simultaneously in a Device that Models Human Swallowing. *Dysphagia* vol. 34 821–833 (2019).

143. Krishnan, G., Goswami, S. P. & Rangarathnam, B. A Systematic Review of the Influence of Bolus Characteristics on Respiratory Measures in Healthy Swallowing. *Dysphagia* 1–15 (2020) doi:10.1007/s00455-020-10103-4.

144. Choi, K. H., Ryu, J. S., Kim, M. Y., Kang, J. Y. & Yoo, S. D. Kinematic analysis of dysphagia: Significant parameters of aspiration related to bolus viscosity. *Dysphagia* **26**, 392–398 (2011).

145. Andersen, U. T., Beck, A. M., Kjaersgaard, A., Hansen, T. & Poulsen, I. Systematic review and evidence based recommendations on texture modified foods and thickened fluids for adults (≥18 years) with oropharyngeal dysphagia. *ESPEN. J.* **8**, e127–e134 (2013).

146. Burbidge, A. S., Cichero, J. A. Y., Engmann, J. & Steele, C. M. "A Day in the life of the Fluid Bolus": An Introduction to Fluid Mechanics of the Oropharyngeal Phase of Swallowing with Particular Focus on Dysphagia. *Appl. Rheol.* **26**, 8–17 (2016).

147. Wendin, K. *et al.* Objective and quantitative definitions of modified food textures based on sensory and rheological methodology. *Food Nutr. Res.* **54**, 5134 (2010).

148. Penman, J. P. & Thomson, M. A review of the textured diets developed for the management of dysphagia. *J. Hum. Nutr. Diet.* **11**, 51–60 (1998).

149. Hanson, B. A review of diet standardization and bolus rheology in the management of dysphagia. *Curr. Opin. Otolaryngol. Head Neck Surg.* **24**, 183–190 (2016).

150. American Dietetic Association. *National Dysphagia Diet: Standardization for Optimal Care*. (American Dietetic Association, 2002).

151. Partal, P. & Franco, J. M. Non-newtonian fluids. in *Rheology: encyclopaedia of life support systems (EOLSS)* (ed. Gallegos, C.) 96–119 (UNESCO-EOLSS, 2010).

152. Quinchia, L. A. *et al.* Linear and non-linear viscoelasticity of puddings for nutritional management of dysphagia. *Food Hydrocoll.* **25**, 586–593 (2011).

153. O'Leary, M., Hanson, B. & Smith, C. Viscosity and Non-Newtonian Features of Thickened Fluids Used for Dysphagia Therapy. *J. Food Sci.* **75**, E330–E338 (2010).

154. Mackley, M. R. *et al.* The rheology and processing behavior of starch and gum-based dysphagia thickeners. *J. Rheol. (N. Y. N. Y).* **57**, 1533–1553 (2013).

155. September, C., Nicholson, T. M. & Cichero, J. A. Y. Implications of changing the amount of thickener in thickened infant formula for infants with dysphagia. *Dysphagia* **29**, 432–437 (2014).

156. Brito-de la Fuente, E., Turcanu, M., Ekberg, O. & Gallegos, C. Rheological Aspects of Swallowing and Dysphagia: Shear and Elongational Flows BT - Dysphagia: Diagnosis and Treatment. in (ed. Ekberg, O.) 687–716 (Springer International Publishing, 2019). doi:10.1007/174_2017_119.

157. Adeleye, B. & Rachal, C. Comparison of the Rheological Properties of Ready-to-Serve and Powdered Instant Food-Thickened Beverages at Different Temperatures for Dysphagic Patients. *J. Am. Diet. Assoc.* **107**, 1176–1182 (2007).

158. Hadde, E. K., Nicholson, T. M. & Cichero, J. A. Y. Rheological characterisation of thickened fluids under different temperature, pH and fat contents. *Nutr. Food Sci.* **45**, 270–285 (2015).

159. Howard, M. M., Nissenson, P. M., Meeks, L. & Rosario, E. R. Use of Textured Thin Liquids in Patients With Dysphagia. *Am. J. Speech-Language Pathol.* **27**, 827–835 (2018).

160. Shama, F. & Sherman, P. Identification of stimuli controlling the sensory evaluation of viscosity II. Oral Methods. *J. Texture Stud.* **4**, 111–118 (1973).

161. Nishinari, K. *et al.* Effect of shear thinning on aspiration - Toward making solutions for judging the risk of aspiration. *Food Hydrocoll.* **25**, 1737–1743 (2011).

162. Vickers, Z. *et al.* Relationships Among Rheological, Sensory Texture, and Swallowing Pressure Measurements of Hydrocolloid-Thickened Fluids. *Dysphagia* **30**, 702–713 (2015).

163. Brito-de la Fuente, E. *et al.* Design of a New Spoon-Thick Consistency Oral Nutrition Supplement Using Rheological Similarity with a Swallow Barium Test Feed. *Appl. Rheol.* **22**, 53365 (2012).

164. Cho, H. M., Yoo, W. & Yoo, B. Steady and dynamic rheological properties of thickened beverages used for dysphagia diets. *Food Sci. Biotechnol.* **21**, 1775–1779 (2012).

165. Ishihara, S., Nakauma, M., Funami, T., Odake, S. & Nishinari, K. Swallowing profiles of food polysaccharide gels in relation to bolus rheology. *Food Hydrocoll.* **25**, 1016–1024 (2011).

166. Casanovas, A., Hernández, M. J., Martí-Bonmatí, E. & Dolz, M. Cluster classification of dysphagia-oriented products considering flow, thixotropy and oscillatory testing. *Food Hydrocoll.* **25**, 851–859 (2011).

167. Chen, J. Food oral processing-A review. *Food Hydrocolloids* vol. 23 1–25 (2009).

168. Ekberg, O. *et al.* Effect of barium sulfate contrast medium on rheology and sensory texture attributes in a model food. *Acta radiol.* **50**, 131–138 (2009).

169. Chen, J. & Lolivret, L. The determining role of bolus rheology in triggering a swallowing. *Food Hydrocoll.* **25**, 325–332 (2011).

170. Nyström, M., Qazi, W. M., Bülow, M., Ekberg, O. & Stading, M. Effects of Rheological Factors on Perceived Ease of Swallowing. *Appl. Rheol.* **25**, 9–17 (2015).

171. Hadde, E. K., Cichero, J. A. Y., Zhao, S., Chen, W. & Chen, J. The Importance of Extensional Rheology in Bolus Control during Swallowing. *Sci. Rep.* **9**, 1–10 (2019).

172. Marconati, M. & Ramaioli, M. The role of extensional rheology in the oral phase of swallowing: an in vitro study. *Food Funct.* (2020) doi:10.1039/C9FO02327E.

173. Turcanu, M. *et al.* The role of human saliva on the elongational properties of a starch-based food product. in *2015 E-Health and Bioengineering Conference, EHB 2015* (Institute of Electrical and Electronics Engineers Inc., 2016). doi:10.1109/EHB.2015.7391589.

174. Qazi, W. M., Wiklund, J., Altskär, A., Ekberg, O. & Stading, M. Shear and extensional rheology of commercial thickeners used for dysphagia management. *J. Texture Stud.* **48**, 507–517 (2017).

175. Turcanu, M. *et al.* An alternative elongational method to study the effect of saliva on thickened fluids for dysphagia nutritional support. *J. Food Eng.* **228**, 79–83 (2018).

176. Hadde, E. K. & Chen, J. Shear and extensional rheological characterization of thickened fluid for dysphagia management. *J. Food Eng.* **245**, 18–23 (2019).

177. Stokes, J. R., Boehm, M. W. & Baier, S. K. Oral processing, texture and mouthfeel: From rheology to tribology and beyond. *Current Opinion in Colloid and Interface Science* vol. 18 349–359 (2013).

178. Shewan, H. M., Pradal, C. & Stokes, J. R. Tribology and its growing use toward the study of food oral processing and sensory perception. *Journal of Texture Studies* vol. 51 7–22 (2020).

179. Munialo, C. D., Kontogiorgos, V., Euston, S. R. & Nyambayo, I. Rheological, tribological and sensory attributes of texture-modified foods for dysphagia patients and the elderly: A review. *Int. J. Food Sci. Technol.* **55**, 1862–1871 (2020).

180. Vieira, J. M. *et al.* Rheology and soft tribology of thickened dispersions aiming the development of oropharyngeal dysphagia-oriented products. *Curr. Res. Food Sci.* **3**, 19–29 (2020).

181. Barbon, C. E. A. & Steele, C. M. Thickened Liquids for Dysphagia Management: a Current Review of the Measurement of Liquid Flow. *Curr. Phys. Med. Rehabil. Reports* **6**, 220–226 (2018).

182. IDDSI – International Dysphagia Diet Standardisation Initiative. https://iddsi.org/.

183. Cichero, J. A. Y. *et al.* Development of International Terminology and Definitions for Texture-Modified Foods and Thickened Fluids Used in Dysphagia Management: The IDDSI Framework. *Dysphagia* **32**, 293–314

(2017).

184. Hanson, B., Jamshidi, R., Redfearn, A., Begley, R. & Steele, C. M. Experimental and Computational Investigation of the IDDSI Flow Test of Liquids Used in Dysphagia Management. *Ann. Biomed. Eng.* **47**, 2296–2307 (2019).

185. Kim, Y.-H., Jeong, G. Y. & Yoo, B. Comparative study of IDDSI flow test and line-spread test of thickened water prepared with different dysphagia thickeners. *J. Texture Stud.* **49**, 653–658 (2018).

186. Côté, C., Germain, I., Dufresne, T. & Gagnon, C. Comparison of two methods to categorize thickened liquids for dysphagia management in a clinical care setting context: The Bostwick consistometer and the IDDSI Flow Test. Are we talking about the same concept? *J. Texture Stud.* **50**, 95–103 (2019).

187. Su, M. *et al.* Clinical applications of IDDSI framework for texture recommendation for dysphagia patients. *J. Texture Stud.* **49**, 2–10 (2018).

188. Waito, A. A. *et al.* A Cross-Sectional, Quantitative Videofluoroscopic Analysis of Swallowing Physiology and Function in Individuals With Amyotrophic Lateral Sclerosis. *J. Speech, Lang. Hear. Res.* **63**, 948–962 (2020).

189. Sukkar, S. G., Maggi, N., Travalca Cupillo, B. & Ruggiero, C. Optimizing Texture Modified Foods for Oro-pharyngeal Dysphagia: A Difficult but Possible Target? *Front. Nutr.* **5**, 68 (2018).

190. Reyes-Torres, C. A. *et al.* Design and implementation of modified-texture diet in older adults with oropharyngeal dysphagia: a randomized controlled trial. *Eur. J. Clin. Nutr.* **73**, 989–996 (2019).

191. Crary, M. A., Carnaby, G. D., Shabbir, Y., Miller, L. & Silliman, S. Clinical Variables Associated with Hydration Status in Acute Ischemic Stroke Patients with Dysphagia. *Dysphagia* **31**, 60–65 (2016).

192. Sharpe, K., Ward, L., Cichero, J., Sopade, P. & Halley, P. Thickened fluids and water absorption in rats and humans. *Dysphagia* **22**, 193–203 (2007).

193. Finestone, H. M., Foley, N. C., Woodbury, M. G. & Greene-Finestone, L. Quantifying fluid intake in dysphagic stroke patients: A preliminary comparison of oral and nonoral strategies. *Arch. Phys. Med. Rehabil.* **82**,

1744–1746 (2001).

194. Whelan, K. Inadequate fluid intakes in dysphagic acute stroke. *Clin. Nutr.* **20**, 423–428 (2001).

195. Vivanti, A. P., Campbell, K. L., Suter, M. S., Hannan-Jones, M. T. & Hulcombe, J. A. Contribution of thickened drinks, food and enteral and parenteral fluids to fluid intake in hospitalised patients with dysphagia. *J. Hum. Nutr. Diet.* **22**, 148–155 (2009).

196. Bannerman, E. & McDermott, K. Dietary and Fluid Intakes of Older Adults in Care Homes Requiring a Texture Modified Diet: The Role of Snacks. *J. Am. Med. Dir. Assoc.* **12**, 234–239 (2011).

197. McGrail, A. & Kelchner, L. N. Adequate Oral Fluid Intake in Hospitalized Stroke Patients: Does Viscosity Matter? *Rehabil. Nurs.* **37**, 252–257 (2012).

198. Murray, J., Doeltgen, S., Miller, M. & Scholten, I. A survey of thickened fluid prescribing and monitoring practices of Australian health professionals. *J. Eval. Clin. Pract.* **20**, 596–600 (2014).

199. Murray, J., Miller, M., Doeltgen, S. & Scholten, I. Intake of thickened liquids by hospitalized adults with dysphagia after stroke. *Int. J. Speech. Lang. Pathol.* **16**, 486–494 (2014).

200. Botigué, T. *et al.* Prevalence and Risk Factors Associated With Low Fluid Intake in Institutionalized Older Residents. *J. Am. Med. Dir. Assoc.* **20**, 317–322 (2019).

201. Shim, J. S., Oh, B. M. & Han, T. R. Factors associated with compliance with viscosity-modified diet among dysphagic patients. *Ann. Rehabil. Med.* **37**, 628–632 (2013).

202. Low, J., Wyles, C., Wilkinson, T. & Sainsbury, R. The effect of compliance on clinical outcomes for patients with dysphagia on videofluoroscopy. *Dysphagia* **16**, 123–127 (2001).

203. Lim, D. J. H., Mulkerrin, S. M., Mulkerrin, E. C. & O'Keeffe, S. T. A randomised trial of the effect of different fluid consistencies used in the management of dysphagia on quality of life: a time trade-off study. *Age Ageing* **45**, 309–312 (2016).

204. Frey, K. L. & Ramsberger, G. Comparison of Outcomes Before and After Implementation of a Water Protocol for Patients With Cerebrovascular

Accident and Dysphagia. *J. Neurosci. Nurs.* **43**, 165–171 (2011).

205. Karagiannis, M. & Karagiannis, T. C. Oropharyngeal dysphagia, free water protocol and quality of life: an update from a prospective clinical trial. *Hell. J. Nucl. Med.* **17 Suppl 1**, 26–9.

206. Gillman, A., Winkler, R. & Taylor, N. F. Implementing the Free Water Protocol does not Result in Aspiration Pneumonia in Carefully Selected Patients with Dysphagia: A Systematic Review. *Dysphagia* **32**, 345–361 (2017).

207. Germain, I., Dufresne, T. & Gray-Donald, K. A Novel Dysphagia Diet Improves the Nutrient Intake of Institutionalized Elders. *J. Am. Diet. Assoc.* **106**, 1614–1623 (2006).

208. Adolphe, J. L., Whiting, S. J. & Dahl, W. J. Vitamin Fortification of Puréed Foods For Long-term Care Residents. *Can. J. Diet. Pract. Res.* **70**, 143–150 (2009).

209. Durant, M. A comparison of Energy Provision by Diet Order in a Long-Term Care Facility. *Can. J. Aging / La Rev. Can. du Vieil.* **27**, 225–227 (2008).

210. Vucea, V. *et al.* Nutritional quality of regular and pureed menus in Canadian long term care homes: an analysis of the Making the Most of Mealtimes (M3) project. *BMC Nutr.* **3**, 1–11 (2017).

211. Keller, H. H. *et al.* Prevalence of inadequate micronutrient intakes of Canadian long-term care residents. *Br. J. Nutr.* **119**, 1047–1056 (2018).

212. Dietary Reference Values for nutrients Summary report. *EFSA Support. Publ.* **14**, (2017).

213. Taylor, K. A. & Barr, S. I. Provision of Small, Frequent Meals Does Not Improve Energy Intake of Elderly Residents with Dysphagia Who Live in an Extended-Care Facility. *J. Am. Diet. Assoc.* **106**, 1115–1118 (2006).

214. Wright, L., Cotter, D., Hickson, M. & Frost, G. Comparison of energy and protein intakes of older people consuming a texture modified diet with a normal hospital diet. *J. Hum. Nutr. Diet.* **18**, 213–219 (2005).

215. Rattray, M., Desbrow, B. & Roberts, S. Comparing nutritional requirements, provision and intakes among patients prescribed therapeutic diets in hospital: An observational study. *Nutrition* **39–40**, 50–56 (2017).

216. Scientific Opinion on Dietary Reference Values for energy. *EFSA J.* **11**, 3005 (2013).

217. Marian, M. & Sacks, G. Micronutrients and Older Adults. *Nutr. Clin. Pract.* **24**, 179–195 (2009).

218. Engelhart, M. J. *et al.* Dietary intake of antioxidants and risk of Alzheimer disease. *J. Am. Med. Assoc.* **287**, 3223–3229 (2002).

219. Yang, F., Wolk, A., Håkansson, N., Pedersen, N. L. & Wirdefeldt, K. Dietary antioxidants and risk of Parkinson's disease in two population-based cohorts. *Mov. Disord.* **32**, 1631–1636 (2017).

220. Schirinzi, T. *et al.* Dietary Vitamin E as a protective factor for Parkinson's disease: Clinical and experimental evidence. *Front. Neurol.* **10**, (2019).

221. Sayed, R., El Wakeel, L., Saad, A. S., Kelany, M. & El-Hamamsy, M. Pentoxifylline and vitamin E reduce the severity of radiotherapy-induced oral mucositis and dysphagia in head and neck cancer patients: a randomized, controlled study. *Med. Oncol.* **37**, 1–8 (2020).

222. Groves, N. J., McGrath, J. J. & Burne, T. H. J. Vitamin D as a Neurosteroid Affecting the Developing and Adult Brain. *Annu. Rev. Nutr.* **34**, 117–141 (2014).

223. Di Somma, C. *et al.* Vitamin D and neurological diseases: An endocrine view. *International Journal of Molecular Sciences* vol. 18 2482 (2017).

224. Wimalawansa, S. J. Non-musculoskeletal benefits of vitamin D. *Journal of Steroid Biochemistry and Molecular Biology* vol. 175 60–81 (2018).

225. Lam, I. T. Y. *et al.* Micronutrient Food Fortification for Residential Care: A Scoping Review of Current Interventions. *Journal of the American Medical Directors Association* vol. 17 588–595 (2016).

226. Pownall, S. & Taylor, C. Use of thickening agents and nutritional supplements for patients with dysphagia following stroke. *Br. J. Neurosci. Nurs.* **13**, 260–268 (2017).

227. Dunne, J. L. & Dahl, W. J. A Novel Solution is Needed to Correct Low Nutrient Intakes in Elderly Long-Term Care Residents. *Nutr. Rev.* **65**, 135–138 (2008).

228. Davis, L. A. & Spicer, M. T. Nutrition and Dysphagia in Older Adults. *Top. Geriatr. Rehabil.* **23**, 211–219 (2007).

229. Keller, H., Chambers, L., Niezgoda, H. & Duizer, L. Issues associated with the use of modified texture foods. *J. Nutr. Heal. Aging* **16**, 195–200 (2012).

230. Kemp, S. Restoring pleasure: nutritional management of dysphagia. *Br. J. Community Nurs.* **6**, 284–289 (2001).

231. Hall, G. & Wendin, K. Sensory Design of Foods for the Elderly. *Ann. Nutr. Metab.* **52**, 25–28 (2008).

232. Bourne, M. C. Texture, Viscosity, and Food. in *Food Texture and Viscosity* 1–32 (Academic Press, 2002). doi:10.1016/b978-012119062-0/50001-2.

233. deMan, L. & deMan, J. Texture of Fats. *Phys. Prop. Lipids* 191–217 (2002) doi:10.1201/9780203909171.ch7.

234. *Handbook of Food Structure Development*. (Royal Society of Chemistry, 2019). doi:10.1039/9781788016155.

235. Saha, D. & Bhattacharya, S. Hydrocolloids as thickening and gelling agents in food: A critical review. *Journal of Food Science and Technology* vol. 47 587–597 (2010).

236. Dickinson, E. *An introduction to food colloids*. (Oxford University Press, 1992).

237. Funami, T., Ishihara, S. & Nakauma, M. Texture design of dysphagia foods using polysaccharides. in *Gums and Stabilisers for the Food Industry 16* 407–414 (Royal Society of Chemistry, 2012). doi:10.1039/9781849734554-00407.

238. Shewan, H. M. & Stokes, J. R. Chapter 8: Food Structure Development for Rheological/Tribological Performance. in *Food Chemistry, Function and Analysis* vols 2020-January 175–198 (Royal Society of Chemistry, 2020).

239. Alsanei, W. A. & Chen, J. Chapter 19: Food Structure Development for Specific Population Groups. in *Food Chemistry, Function and Analysis* vols 2020-January 459–479 (Royal Society of Chemistry, 2020).

240. Lapasin, R., Pricl, S., Lapasin, R. & Pricl, S. Industrial applications of polysaccharides. in *Rheology of Industrial Polysaccharides: Theory and Applications* 134–161 (Springer US, 1995). doi:10.1007/978-1-4615-2185-3_2.

241. Goff, H. D. & Guo, Q. Chapter 1: The Role of Hydrocolloids in the Development of Food Structure. in *Food Chemistry, Function and Analysis* vols 2020-Janua 3–28 (Royal Society of Chemistry, 2020).

242. Sworn, G. Natural Thickeners. in *Handbook of Industrial Water Soluble Polymers* 10–31 (Blackwell Publishing Ltd, 2007). doi:10.1002/9780470988701.ch2.

243. Williams, P. A. & Phillips, G. O. Introduction to food hydrocolloids. in *Handbook of Hydrocolloids: Second Edition* 1–22 (Elsevier Inc., 2009). doi:10.1533/9781845695873.1.

244. Sworn, G. Hydrocolloid thickeners and their applications. in *Gums and Stabilisers for the Food Industry 12* 13–22 (The Royal Society of Chemistry, 2004). doi:10.1039/9781847551214-00013.

245. Robinson, G., Ross-Murphy, S. B. & Morris, E. R. Viscosity-molecular weight relationships, intrinsic chain flexibility, and dynamic solution properties of guar galactomannan. *Carbohydr. Res.* **107**, 17–32 (1982).

246. Wyatt, N. B. & Liberatore, M. W. Rheology and viscosity scaling of the polyelectrolyte xanthan gum. *J. Appl. Polym. Sci.* **114**, 4076–4084 (2009).

247. Gupta, P., Elkins, C., Long, T. E. & Wilkes, G. L. Electrospinning of linear homopolymers of poly(methyl methacrylate): Exploring relationships between fiber formation, viscosity, molecular weight and concentration in a good solvent. *Polymer (Guildf).* **46**, 4799–4810 (2005).

248. de Lima, G. G., Lyons, S., Devine, D. M. & Nugent, M. J. D. Electrospinning of Hydrogels for Biomedical Applications BT - Hydrogels: Recent Advances. in (eds. Thakur, V. K. & Thakur, M. K.) 219–258 (Springer Singapore, 2018). doi:10.1007/978-981-10-6077-9_9.

249. Guo, L., Hu, J., Zhang, J. & Du, X. The role of entanglement concentration on the hydrodynamic properties of potato and sweet potato starches. *Int. J. Biol. Macromol.* **93**, 1–8 (2016).

250. Shenoy, S. L., Bates, W. D., Frisch, H. L. & Wnek, G. E. Role of chain entanglements on fiber formation during electrospinning of polymer solutions: Good solvent, non-specific polymer-polymer interaction limit. *Polymer (Guildf).* **46**, 3372–3384 (2005).

251. Bock, N., Dargaville, T. R. & Woodruff, M. A. Electrospraying of polymers with therapeutic molecules: State of the art. *Progress in Polymer Science*

vol. 37 1510–1551 (2012).

252. Felice, B., Prabhakaran, M. P., Zamani, M., Rodríguez, A. P. & Ramakrishna, S. Electrosprayed poly(vinyl alcohol) particles: preparation and evaluation of their drug release profile. *Polym. Int.* **64**, 1722–1732 (2015).

253. Liu, Z., Chen, H., Zheng, B., Xie, F. & Chen, L. Understanding the structure and rheological properties of potato starch induced by hot-extrusion 3D printing. *Food Hydrocoll.* **105**, 105812 (2020).

254. Barnes, H. A. *A Handbook of Elementary Rheology*. *Institute of Non-Newtonian Fluid Mechanics University of Wales* (2000). doi:10.1126/science.1201543.

255. Dunstan, D. E., Chai, E., Lee, M. & Boger, D. V. The rheology of engineered polysaccharides. *Top. Catal.* **9**, 225–228 (1995).

256. Cui, S. & Wang, Q. Understanding the Physical Properties of Food Polysaccharides. in *Food Carbohydrates* (2005). doi:10.1201/9780203485286.ch4.

257. Morris, E. R., Cutler, A. N., Ross-Murphy, S. B., Rees, D. A. & Price, J. Concentration and shear rate dependence of viscosity in random coil polysaccharide solutions. *Carbohydr. Polym.* **1**, 5–21 (1981).

258. Tam, K. C. & Tiu, C. Steady and Dynamic Shear Properties of Aqueous Polymer Solutions. *J. Rheol. (N. Y. N. Y).* **33**, 257–280 (1989).

259. Gorret, N., Renard, C. M. G. C., Famelart, M. H., Maubois, J. L. & Doublier, J. L. Rheological characterization of the EPS produced by P. acidi-propionici on milk microfiltrate. *Carbohydr. Polym.* **51**, 149–158 (2003).

260. Morris, E. R. Shear-thinning of 'random coil' polysaccharides: Characterisation by two parameters from a simple linear plot. *Carbohydr. Polym.* **13**, 85–96 (1990).

261. Taggart, P. & Mitchell, J. R. Starch. in *Handbook of Hydrocolloids: Second Edition* 108–141 (Elsevier Inc., 2009). doi:10.1533/9781845695873.108.

262. Rapaille, A. & Vanhemelrijck, J. Modified starches. in *Thickening and Gelling Agents for Food* 199–229 (Springer US, 1997). doi:10.1007/978-1-4615-2197-6_10.

263. Jane, J. *Current Understanding on Starch Granule Structures*. *J. Appl. Glycosci*

vol. 53 (2006).

264. Zeeman, S. C., Kossmann, J. & Smith, A. M. Starch: Its Metabolism, Evolution, and Biotechnological Modification in Plants. *Annu. Rev. Plant Biol.* **61**, 209–234 (2010).

265. Streb, S. & Zeeman, S. C. Starch Metabolism in Arabidopsis. *Arab. B.* **10**, e0160 (2012).

266. Ferry, A. L. *et al.* Viscosity and flavour perception: Why is starch different from hydrocolloids? *Food Hydrocoll.* **20**, 855–862 (2006).

267. Sheldrake, P. Starch. in *Food Stabilisers, Thickeners and Gelling Agents* 293–324 (Wiley-Blackwell, 2009). doi:10.1002/9781444314724.ch16.

268. Schirmer, M., Jekle, M. & Becker, T. Starch gelatinization and its complexity for analysis. *Starch - Stärke* **67**, 30–41 (2015).

269. Majzoobi, M., Kaveh, Z., Blanchard, C. L. & Farahnaky, A. Physical properties of pregelatinized and granular cold water swelling maize starches in presence of acetic acid. *Food Hydrocoll.* **51**, 375–382 (2015).

270. Tester, R. F., Qi, X. & Karkalas, J. Hydrolysis of native starches with amylases. *Animal Feed Science and Technology* vol. 130 39–54 (2006).

271. Ferry, A. L. S. *et al.* In-mouth amylase activity can reduce perception of saltiness in starch-thickened foods. *J. Agric. Food Chem.* **54**, 8869–8873 (2006).

272. Ferry, A. L., Hort, J., Mltchell, J. R., Lagarrigue, S. & Pamies, B. V. Effect of Amylase Activity on Starch Paste Viscosity and Its Implications for Flavor Perception. *J. Texture Stud.* **35**, 511–524 (2005).

273. Hanson, B., O'Leary, M. T. & Smith, C. H. The effect of saliva on the viscosity of thickened drinks. *Dysphagia* **27**, 10–19 (2012).

274. Morris, E. R. Rheological and Organoleptic Properties of Food Hydrocolloids BT - Food Hydrocolloids: Structures, Properties, and Functions. in (eds. Nishinari, K. & Doi, E.) 201–210 (Springer US, 1993). doi:10.1007/978-1-4615-2486-1_31.

275. Sworn, G. Xanthan Gum. in *Food Stabilisers, Thickeners and Gelling Agents* 325–342 (Wiley-Blackwell, 2009). doi:10.1002/9781444314724.ch17.

276. Habibi, H. & Khosravi-Darani, K. Effective variables on production and structure of xanthan gum and its food applications: A review. *Biocatalysis*

and Agricultural Biotechnology vol. 10 130–140 (2017).

277. Kang, K. S. & Pettitt, D. J. Xanthan, Gellan, Welan, and Rhamsan. in *Industrial Gums: Polysaccharides and Their Derivatives: Third Edition* 341–397 (Elsevier Inc., 2012). doi:10.1016/B978-0-08-092654-4.50017-6.

278. Morris, E. R. Ordered conformation of xanthan in solutions and "weak gels": Single helix, double helix – or both? *Food Hydrocolloids* vol. 86 18–25 (2019).

279. Dobrynin, A. V. Electrostatic persistence length of semiflexible and flexible polyelectrolytes. *Macromolecules* **38**, 9304–9314 (2005).

280. Sopade, P. A., Halley, P. J., Cichero, J. A. Y. & Ward, L. C. Rheological characterisation of food thickeners marketed in Australia in various media for the management of dysphagia. I: Water and cordial. *J. Food Eng.* **79**, 69–82 (2007).

281. Matta, Z., Chambers IV, E., Garcia, J. M. & Helverson, J. M. G. Sensory Characteristics of Beverages Prepared with Commercial Thickeners Used for Dysphagia Diets. *J. Am. Diet. Assoc.* **106**, 1049–1054 (2006).

282. Sasaki, T. & Kohyama, K. Influence of non-starch polysaccharides on the in vitro digestibility and viscosity of starch suspensions. *Food Chem.* **133**, 1420–1426 (2012).

283. Cichero, J. A. Y. Thickening agents used for dysphagia management: Effect on bioavailability of water, medication and feelings of satiety. *Nutr. J.* **12**, 54 (2013).

284. Heyman, B., De Vos, W. H., Van der Meeren, P. & Dewettinck, K. Gums tuning the rheological properties of modified maize starch pastes: Differences between guar and xanthan. *Food Hydrocoll.* **39**, 85–94 (2014).

285. Sikora, M., Kowalski, S. & Tomasik, P. Binary hydrocolloids from starches and xanthan gum. *Food Hydrocoll.* **22**, 943–952 (2008).

286. Moret-Tatay, A., Rodríguez-García, J., Martí-Bonmatí, E., Hernando, I. & Hernández, M. J. Commercial thickeners used by patients with dysphagia: Rheological and structural behaviour in different food matrices. *Food Hydrocoll.* **51**, 318–326 (2015).

287. Sopade, P. A. *et al.* Rheological characterisation of food thickeners marketed in Australia in various media for the management of dysphagia.

II. Milk as a dispersing medium. *J. Food Eng.* **84**, 553–562 (2008).

288. Sopade, P. A. *et al.* Rheological characterization of food thickeners marketed in Australia in various media for the management of dysphagia. III. Fruit juice as a dispersing medium. *J. Food Eng.* **86**, 604–615 (2008).

289. Lotong, V., Chun, S. S., Chambers, E. & Garcia, J. M. Texture and Flavor Characteristics of Beverages Containing Commercial Thickening Agents for Dysphagia Diets. *J. Food Sci.* **68**, 1537–1541 (2003).

290. Hong, S. R., Sun, D. S., Yoo, W. & Yoo, B. Flow behaviors of commercial food thickeners used for the management of dysphagia: Effect of temperature. *Int. J. Food Eng.* **8**, (2012).

291. Cho, H. M. & Yoo, B. Rheological characteristics of cold thickened beverages containing xanthan gum-based food thickeners used for dysphagia diets. *J. Acad. Nutr. Diet.* **115**, 106–111 (2015).

292. Bahram, M., Mohseni, N. & Moghtader, M. An Introduction to Hydrogels and Some Recent Applications. in *Emerging Concepts in Analysis and Applications of Hydrogels* (InTech, 2016). doi:10.5772/64301.

293. Zhang, Y. S. & Khademhosseini, A. Advances in engineering hydrogels. *Science* vol. 356 (2017).

294. Lloyd, D. J. The problem of gel structure. *Colloid Chem.* **1**, 767–782 (1926).

295. Introduction BT - Thermoreversible Networks: Viscoelastic Properties and Structure of Gels. in (ed. te Nijenhuis, K.) 1–12 (Springer Berlin Heidelberg, 1997). doi:10.1007/BFb0008700.

296. Nishinari, K. Some Thoughts on The Definition of a Gel. in *Gels: Structures, Properties, and Functions* 87–94 (Springer Berlin Heidelberg, 2009). doi:10.1007/978-3-642-00865-8_12.

297. Ahmed, E. M. Hydrogel: Preparation, characterization, and applications: A review. *Journal of Advanced Research* vol. 6 105–121 (2015).

298. Thakur, S., Thakur, V. K. & Arotiba, O. A. History, Classification, Properties and Application of Hydrogels: An Overview. in 29–50 (Springer, Singapore, 2018). doi:10.1007/978-981-10-6077-9_2.

299. Chen, Y. Properties and development of hydrogels. in *Hydrogels Based on Natural Polymers* 3–16 (Elsevier, 2019). doi:10.1016/B978-0-12-

816421-1.00001-X.

300. Nishinari, K., Zhang, H. & Ikeda, S. Hydrocolloid gels of polysaccharides and proteins. *Current Opinion in Colloid and Interface Science* vol. 5 195–201 (2000).

301. Brinker, C. J. & Scherer, G. W. Introduction. in *Sol-Gel Science* xvi–18 (Elsevier, 1990). doi:10.1016/b978-0-08-057103-4.50006-4.

302. Morris, V. J. Polysaccharides: Their role in food microstructure. in *Understanding and Controlling the Microstructure of Complex Foods* 3–39 (Elsevier Ltd., 2007). doi:10.1533/9781845693671.1.3.

303. Nakauma, M., Ishihara, S., Funami, T. & Nishinari, K. Swallowing profiles of food polysaccharide solutions with different flow behaviors. *Food Hydrocoll.* **25**, 1165–1173 (2011).

304. Sharma, M., Kristo, E., Corredig, M. & Duizer, L. Effect of hydrocolloid type on texture of pureed carrots: Rheological and sensory measures. *Food Hydrocoll.* **63**, 478–487 (2017).

305. Gabriele, D., De Cindio, B. & D'Antona, P. A weak gel model for foods. *Rheol. Acta* **40**, 120–127 (2001).

306. Maia, J., Covas, J., de Cindio, B. & Gabriele, D. Rheology in materials engineering. *Rheol. II* 111 (2010).

307. Blakemore, W. R. & Harpell, A. R. Carrageenan. in *Food Stabilisers, Thickeners and Gelling Agents* 73–94 (Wiley-Blackwell, 2009). doi:10.1002/9781444314724.ch5.

308. Ninomiya, H., Shimizu, T., Dairaku, M., Komagata, T. & Misawa, M. Jellied medicinal composition for oral administration. (1999).

309. Miyazaki, S. *et al.* Carrageenan Gels for Oral Sustained Delivery of Acetaminophen to Dysphagic Patients. *Biol. Pharm. Bull.* **34**, 164–166 (2011).

310. Zhang, H., Zhang, F. & Yuan, R. Applications of natural polymer-based hydrogels in the food industry. in *Hydrogels Based on Natural Polymers* 357–410 (Elsevier, 2019). doi:10.1016/B978-0-12-816421-1.00015-X.

311. Imeson, A. P. Carrageenan and furcellaran. in *Handbook of Hydrocolloids: Second Edition* (eds. Phillips, G. O. & Williams, P. A.) 164–185 (Elsevier, 2009). doi:10.1533/9781845695873.164.

312. Mangione, M. R., Giacomazza, D., Bulone, D., Martorana, V. & San Biagio, P. L. Thermoreversible gelation of κ-Carrageenan: Relation between conformational transition and aggregation. *Biophys. Chem.* **104**, 95–105 (2003).

313. Ikeda, S. & Nishinari, K. 'Weak gel'-type rheological properties of aqueous dispersions of nonaggregated κ-carrageenan helices. *J. Agric. Food Chem.* **49**, 4436–4441 (2001).

314. Piculell, L., Borgström, J., Chronakis, I. S., Quist, P. O. & Viebke, C. Organisation and association of κ-carrageenan helices under different salt conditions. *Int. J. Biol. Macromol.* **21**, 141–153 (1997).

315. Núñez-Santiago, M. del C. & Tecante, A. Rheological and calorimetric study of the sol-gel transition of κ-carrageenan. *Carbohydr. Polym.* **69**, 763–773 (2007).

316. Jakus, A. E. Chapter 1 - An Introduction to 3D Printing—Past, Present, and Future Promise. in (eds. Dipaola, M. & Wodajo, F. M. B. T.-3D P. in O. S.) 1–15 (Elsevier, 2019). doi:https://doi.org/10.1016/B978-0-323-58118-9.00001-4.

317. Redwood, B., Schöffer, F. & Garret, B. *The 3D Printing Handbook: Technologies, Design and Applications*. (3D Hubs B.V., 2017).

318. Markillie, P. A third industrial revolution. *Economist* **403**, (2012).

319. Jiang, R., Kleer, R. & Piller, F. T. Predicting the future of additive manufacturing: A Delphi study on economic and societal implications of 3D printing for 2030. *Technol. Forecast. Soc. Change* **117**, 84–97 (2017).

320. Gibson, I. *et al.* Introduction and Basic Principles. in *Additive Manufacturing Technologies* 1–18 (Springer New York, 2015). doi:10.1007/978-1-4939-2113-3_1.

321. Wittbrodt, B. T. *et al.* Life-cycle economic analysis of distributed manufacturing with open-source 3-D printers. *Mechatronics* **23**, 713–726 (2013).

322. Portanguen, S., Tournayre, P., Sicard, J., Astruc, T. & Mirade, P. S. Toward the design of functional foods and biobased products by 3D printing: A review. *Trends in Food Science and Technology* vol. 86 188–198 (2019).

323. Choong, Y. Y. C. *et al.* The global rise of 3D printing during the COVID-19 pandemic. *Nature Reviews Materials* (2020) doi:10.1038/s41578-020-

00234-3.

324. The 3D opportunity primer: The basics of additive manufacturing | Deloitte Insights. https://www2.deloitte.com/us/en/insights/focus/3d-opportunity/the-3d-opportunity-primer-the-basics-of-additive-manufacturing.html.

325. Gibson, I. *et al.* Generalized Additive Manufacturing Process Chain. in *Additive Manufacturing Technologies* 43–61 (Springer New York, 2015). doi:10.1007/978-1-4939-2113-3_3.

326. Gibson, I. *et al.* Extrusion-Based Systems. in *Additive Manufacturing Technologies* 147–173 (Springer New York, 2015). doi:10.1007/978-1-4939-2113-3_6.

327. File:RampsStandardPinHeaders.jpg - RepRap. https://reprap.org/wiki/File:RampsStandardPinHeaders.jpg.

328. Como elegir el hotend correcto. https://filament2print.com/es/blog/96_Como-elegir-el-hotend-correcto.html.

329. Derossi, A., Caporizzi, R., Ricci, I. & Severini, C. Critical variables in 3D food printing. in *Fundamentals of 3D Food Printing and Applications* 41–91 (Elsevier, 2018). doi:10.1016/B978-0-12-814564-7.00003-1.

330. Liu, Z. & Zhang, M. 3D Food Printing Technologies and Factors Affecting Printing Precision. in *Fundamentals of 3D Food Printing and Applications* 19–40 (Elsevier, 2019). doi:10.1016/B978-0-12-814564-7.00002-X.

331. Godoi, F. C., Bhandari, B. R., Prakash, S. & Zhang, M. An introduction to the principles of 3D food printing. in *Fundamentals of 3D Food Printing and Applications* 1–18 (Elsevier, 2018). doi:10.1016/B978-0-12-814564-7.00001-8.

332. Zhu, S., Stieger, M. A., van der Goot, A. J. & Schutyser, M. A. I. Extrusion-based 3D printing of food pastes: Correlating rheological properties with printing behaviour. *Innov. Food Sci. Emerg. Technol.* **58**, 102214 (2019).

333. Sun, J. *et al.* A Review on 3D Printing for Customized Food Fabrication. *Procedia Manuf.* **1**, 308–319 (2015).

334. Godoi, F. C., Prakash, S. & Bhandari, B. R. 3d printing technologies applied for food design: Status and prospects. *J. Food Eng.* **179**, 44–54 (2016).

335. Oyinloye, T. M. & Yoon, W. B. Stability of 3D printing using a mixture of pea protein and alginate: Precision and application of additive layer manufacturing simulation approach for stress distribution. *J. Food Eng.* **288**, 110127 (2020).

336. Lipton, J. I. Printable food: the technology and its application in human health. *Current Opinion in Biotechnology* vol. 44 198–201 (2017).

337. Lipton, J. I., Cutler, M., Nigl, F., Cohen, D. & Lipson, H. Additive manufacturing for the food industry. *Trends Food Sci. Technol.* **43**, 114–123 (2015).

338. He, C., Zhang, M. & Fang, Z. 3D printing of food: pretreatment and post-treatment of materials. *Critical Reviews in Food Science and Nutrition* vol. 60 2379–2392 (2020).

339. Burke-Shyne, S., Gallegos, D. & Williams, T. 3D food printing: nutrition opportunities and challenges. *Br. Food J.* (2020) doi:10.1108/BFJ-05-2020-0441.

340. Prakash, S., Bhandari, B. R., Godoi, F. C. & Zhang, M. Future outlook of 3D food printing. in *Fundamentals of 3D Food Printing and Applications* 373–381 (Elsevier, 2018). doi:10.1016/B978-0-12-814564-7.00013-4.

341. Derossi, A., Caporizzi, R., Azzollini, D. & Severini, C. Application of 3D printing for customized food. A case on the development of a fruit-based snack for children. *J. Food Eng.* (2018) doi:10.1016/j.jfoodeng.2017.05.015.

342. Farha, A., Muhtadi, M. & Morshed, R. I. 3D fabrication of food through software implementation for patients of various diseases and dysphagia. *undefined* (2018).

343. Kouzani, A. Z. *et al.* 3D printing of a pavlova. in *IEEE Region 10 Annual International Conference, Proceedings/TENCON* 2281–2285 (Institute of Electrical and Electronics Engineers Inc., 2017). doi:10.1109/TENCON.2016.7848435.

344. Kouzani, A. Z. *et al.* 3D Printing of Food for People with Swallowing Difficulties. *KnE Eng.* **2**, 23 (2017).

345. Dick, A., Bhandari, B. & Prakash, S. 3D printing of meat. *Meat Science* vol. 153 35–44 (2019).

346. Cassens, D., Johnson, E. & Keelan, S. Enhancing Taste, Texture,

Appearance, and Presentation of Pureed Food Improved Resident Quality of Life and Weight Status. *Nutr. Rev.* **54**, S51–S54 (2009).

347. K. Handral, H., Hua Tay, S., Wan Chan, W. & Choudhury, D. 3D Printing of cultured meat products. *Critical Reviews in Food Science and Nutrition* (2020) doi:10.1080/10408398.2020.1815172.

348. Tan, C., Chua, C. K., Li, L. & Wong, G. Enhancing 3D printability of pureed food by addition of hydrocolloids. in *Proceedings of the International Conference on Progress in Additive Manufacturing* vols 2018-May 662–666 (Pro-AM, 2018).

349. Pulatsu, E., Su, J. W., Lin, J. & Lin, M. Factors affecting 3D printing and post-processing capacity of cookie dough. *Innov. Food Sci. Emerg. Technol.* **61**, 102316 (2020).

350. Wilson, A., Anukiruthika, T., Moses, J. A. & Anandharamakrishnan, C. Customized Shapes for Chicken Meat–Based Products: Feasibility Study on 3D-Printed Nuggets. *Food Bioprocess Technol.* **13**, 1968–1983 (2020).

351. Serizawa, R. *et al.* 3D jet printer of edible gels for food creation. in *Behavior and Mechanics of Multifunctional Materials and Composites 2014* (eds. Goulbourne, N. C. & Naguib, H. E.) vol. 9058 90580A (SPIE, 2014).

352. Huang, C. Y. *Extrusion-based 3D Printing and Characterization of Edible Materials*. https://uwspace.uwaterloo.ca/handle/10012/12899 (2018).

353. Dankar, I., Pujolà, M., El Omar, F., Sepulcre, F. & Haddarah, A. Impact of Mechanical and Microstructural Properties of Potato Puree-Food Additive Complexes on Extrusion-Based 3D Printing. *Food Bioprocess Technol.* **11**, 2021–2031 (2018).

354. Dick, A., Bhandari, B., Dong, X. & Prakash, S. Feasibility study of hydrocolloid incorporated 3D printed pork as dysphagia food. *Food Hydrocoll.* **107**, 105940 (2020).

355. Strother, H., Moss, R. & McSweeney, M. B. Comparison of 3D printed and molded carrots produced with gelatin, guar gum and xanthan gum. *J. Texture Stud.* jtxs.12545 (2020) doi:10.1111/jtxs.12545.

356. Smith, C. H., Jebson, E. M. & Hanson, B. Thickened fluids: Investigation of users' experiences and perceptions. *Clin. Nutr.* **33**, 171–174 (2014).

357. Trenfield, S. J., Awad, A., Goyanes, A., Gaisford, S. & Basit, A. W. 3D Printing Pharmaceuticals: Drug Development to Frontline Care. *Trends*

in Pharmacological Sciences vol. 39 440–451 (2018).

358. Sun, J., Zhou, W., Yan, L., Huang, D. & Lin, L. ya. Extrusion-based food printing for digitalized food design and nutrition control. *J. Food Eng.* **220**, 1–11 (2018).

359. ENAC. *Informe de análisis*. http://www.aguashuelva.com/DOC/01-02-2018_Salida_Depsito_N1_2206179.pdf (2017).

360. Ayuntamiento de Huelva. Agua potable y parámetros de calidad del agua semanal. http://www.aguashuelva.com/ESP/191.asp (2015).

361. Fresubin Clear Thickener – Caring for Life. https://www.caringforlife.hk/index.php/en/products/by-indication/fresubin-clear-thickener/.

362. hephestos.jpeg. https://s.3dnatives.com/imprimante/hephestos.jpeg.

363. P3STEEL DUAL por HTA3D - Kit DIY personalizable - HTA3D. https://www.hta3d.com/es/kit-p3steel-dual.

364. Liu, S., Chan, W. L. & Li, L. Rheological Properties and Scaling Laws of κ-Carrageenan in Aqueous Solution. *Macromolecules* **48**, 7649–7657 (2015).

365. Liu, S., Huang, S. & Li, L. Thermoreversible gelation and viscoelasticity of κ-carrageenan hydrogels. *J. Rheol. (N. Y. N. Y).* **60**, 203–214 (2016).

366. Wegrzyn, T. F., Golding, M. & Archer, R. H. Food Layered Manufacture: A new process for constructing solid foods. *Trends Food Sci. Technol.* **27**, 66–72 (2012).

367. Jose, R. R., Rodriguez, M. J., Dixon, T. A., Omenetto, F. & Kaplan, D. L. Evolution of Bioinks and Additive Manufacturing Technologies for 3D Bioprinting. *ACS Biomater. Sci. Eng.* **2**, 1662–1678 (2016).

368. Ren, X., Shao, H., Lin, T. & Zheng, H. 3D gel-printing-An additive manufacturing method for producing complex shape parts. *Mater. Des.* **101**, 80–87 (2016).

369. Pallottino, F. *et al.* Printing on Food or Food Printing: a Review. *Food Bioprocess Technol.* **9**, 725–733 (2016).

370. Sun, J., Zhou, W., Huang, D., Fuh, J. Y. H. & Hong, G. S. An Overview of 3D Printing Technologies for Food Fabrication. *Food Bioprocess Technol.* **8**, 1605–1615 (2015).

371. Izdebska, J. & Zołek-Tryznowska, Z. 3D food printing - Facts and future. *Agro Food Ind. Hi. Tech.* **27**, 33–37 (2016).

372. Severini, C. & Derossi, A. Could the 3D Printing Technology be a Useful Strategy to Obtain Customized Nutrition? *J. Clin. Gastroenterol.* **50**, S175–S178 (2016).

373. Yang, Z., Yang, H. & Yang, H. Effects of sucrose addition on the rheology and microstructure of κ-carrageenan gel. *Food Hydrocoll.* **75**, 164–173 (2017).

374. Piculell, L. Gelling carrageenans. in *Food Polysaccharides and Their Applications* (eds. Stephen, A. M., Phillips, G. O. & Williams, P. A.) 239–287 (CRC Press, 2006).

375. Rochas, C. & Rinaudo, M. Calorimetric determination of the conformational transition of kappa carrageenan. *Carbohydr. Res.* **105**, 227–236 (1982).

376. Iijima, M., Takahashi, M., Hatakeyama, T. & Hatakeyama, H. Detailed investigation of gel-sol transition temperature of κ-carrageenan studied by DSC, TMA and FBM. *J. Therm. Anal. Calorim.* **114**, 895–901 (2013).

377. Funami, T. *et al.* Influence of molecular structure imaged with atomic force microscopy on the rheological behavior of carrageenan aqueous systems in the presence or absence of cations. *Food Hydrocoll.* **21**, 617–629 (2007).

378. Hermansson, A. M., Eriksson, E. & Jordansson, E. Effects of potassium, sodium and calcium on the microstructure and rheological behaviour of kappa-carrageenan gels. *Carbohydr. Polym.* **16**, 297–320 (1991).

379. Thrimawithana, T. R., Young, S., Dunstan, D. E. & Alany, R. G. Texture and rheological characterization of kappa and iota carrageenan in the presence of counter ions. *Carbohydr. Polym.* **82**, 69–77 (2010).

380. Cavallieri, A. L. F., Fialho, N. A. V. & Cunha, R. L. Sodium caseinate and κ-carrageenan interactions in acid gels: Effect of polysaccharide dissolution temperature and sucrose addition. *Int. J. Food Prop.* **14**, 251–263 (2011).

381. Cooke, M. E. *et al.* Structuring of Hydrogels across Multiple Length Scales for Biomedical Applications. *Adv. Mater.* **30**, 1705013 (2018).

382. Norton, I. T., Goodall, D. M., Morris, E. R. & Rees, D. A. Equilibrium and

dynamic studies of the disorder-order transition of kappa carrageenan. *J. Chem. Soc. Faraday Trans. 1 Phys. Chem. Condens. Phases* **79**, 2489–2500 (1983).

383. Tecante, A. & Doublier, J. L. Steady flow and viscoelastic behavior of crosslinked waxy corn starch-κ-carrageenan pastes and gels. *Carbohydr. Polym.* **40**, 221–231 (1999).

384. Wang, L., Zhang, M., Bhandari, B. & Yang, C. Investigation on fish surimi gel as promising food material for 3D printing. *J. Food Eng.* **220**, 101–108 (2018).

385. Chinga-Carrasco, G. *et al.* Pulping and pretreatment affect the characteristics of bagasse inks for 3D printing. *ACS Sustain. Chem. Eng.* **6**, 4068–4075 (2018).

386. Holland, S., Tuck, C. & Foster, T. Fluid Gels: a New Feedstock for High Viscosity Jetting. *Food Biophys.* **13**, 175–185 (2018).

387. Moxon, S. R. *et al.* Suspended Manufacture of Biological Structures. *Adv. Mater.* **29**, 1605594 (2017).

388. Vancauwenberghe, V. *et al.* Pectin based food-ink formulations for 3-D printing of customizable porous food simulants. *Innov. Food Sci. Emerg. Technol.* **42**, 138–150 (2017).

389. Zhu, F. *et al.* 3D Printing of Ultratough Polyion Complex Hydrogels. *ACS Appl. Mater. Interfaces* **8**, 31304–31310 (2016).

390. Kreiger, M. & Pearce, J. M. Environmental life cycle analysis of distributed three-dimensional printing and conventional manufacturing of polymer products. *ACS Sustain. Chem. Eng.* **1**, 1511–1519 (2013).

391. Pearce, J. M. *et al.* 3-D Printing of Open Source Appropriate Technologies for Self-Directed Sustainable Development. *J. Sustain. Dev.* **3**, 17–29 (2010).

392. Ross-Murphy, S. B. & Shatwell, K. P. Polysaccharide strong and weak gels. *Biorheology* **30**, 217–227 (1993).

393. Moresi, M., Bruno, M. & Parente, E. Viscoelastic properties of microbial alginate gels by oscillatory dynamic tests. *J. Food Eng.* **64**, 179–186 (2004).

394. Campo-Deaño, L. & Tovar, C. The effect of egg albumen on the

viscoelasticity of crab sticks made from Alaska Pollock and Pacific Whiting surimi. *Food Hydrocolloids* vol. 23 1641–1646 (2009).

395. Munarin, F. *et al.* Reactive hydroxyapatite fillers for pectin biocomposites. *Mater. Sci. Eng. C* **45**, 154–161 (2014).

396. Mita, T. & Bohlin, L. Shear stress relaxation of chemically modified gluten. *Cereal Chem.* **60**, 93–97 (1983).

397. Antunes, F. E., Coppola, L., Rossi, C. O. & Ranieri, G. A. Gelation of charged bio-nanocompartments induced by associative and non-associative polysaccharides. *Colloids Surfaces B Biointerfaces* **66**, 134–140 (2008).

398. Basu, S., Shivhare, U. S., Singh, T. V. & Beniwal, V. S. Rheological, textural and spectral characteristics of sorbitol substituted mango jam. *J. Food Eng.* **105**, 503–512 (2011).

399. Lupi, F. R. *et al.* Olive oil and hyperthermal water bigels for cosmetic uses. *J. Colloid Interface Sci.* **459**, 70–78 (2015).

400. Tanaka, F. Thermoreversible Gelation Driven by Coil-to-Helix Transition of Polymers. *Macromolecules* **36**, 5392–5405 (2003).

401. Salinas-Vázquez, M. *et al.* Early Numerical Studies on the Peristaltic Flow through the Pharynx. *J. Texture Stud.* **45**, 155–163 (2014).

402. Diañez, I. *et al.* 3D printing in situ gelification of κ-carrageenan solutions: Effect of printing variables on the rheological response. *Food Hydrocoll.* **87**, 321–330 (2019).

403. Ortega, O. *et al.* Therapeutic Effect, Rheological Properties and α-Amylase Resistance of a New Mixed Starch and Xanthan Gum Thickener on Four Different Phenotypes of Patients with Oropharyngeal Dysphagia. *Nutrients* **12**, 1873 (2020).

404. Pollard, M. A. & Fischer, P. Semi-dilute galactomannan solutions: observations on viscosity scaling behavior of guar gum. *J. Phys. Condens. Matter* **26**, 464107 (2014).

405. Zhang, E., Dai, X., Dong, Z., Qiu, X. & Ji, X. Critical concentration and scaling exponents of one soluble polyimide - From dilute to semidilute entangled solutions. *Polymer (Guildf).* **84**, 275–285 (2016).

406. Li, X., Chen, H. & Yang, B. Centrifugally spun starch-based fibers from

amylopectin rich starches. *Carbohydr. Polym.* **137**, 459–465 (2016).

407. Wang, F., Sun, Z. & Wang, Y. J. Study of xanthan gum/waxy corn starch interaction in solution by viscometry. *Food Hydrocoll.* **15**, 575–581 (2001).